The Fate of Phosphorus Along Estuarine Salinity Gradients

A dissertation submitted in partial fulfillment of the requirements for the degree of Doctor of Philosophy at George Mason University

By

Jeanne L. Hartzell
Bachelor of Science
Georgia Southwestern State University, 1991

Co-Director: Thomas E. Jordan, Senior Scientist
Smithsonian Environmental Research Center, Edgewater, MD
Co-Director: Donald P. Kelso, Associate Professor, Emeritus
Environmental Science and Policy Department

Spring Semester 2009
George Mason University
Fairfax, VA

Acknowledgments

One of the most rewarding aspects of my time as a Ph.D. student was the opportunity to work with so many smart and generous people, many of whom received no obvious or tangible benefit from helping me, but nevertheless offered me so much in the form of their time, expertise, lab equipment or lab space.

First and foremost on the list of great people I was fortunate to work with are all of the members of my committee. It is a real pleasure to learn and grow from people you respect, and that was certainly the case with each and every member of my committee. All are rigorous, but patient, teachers who pushed me beyond my comfort level, and I appreciate that. Specifically, I want to thank Chris Jones for helping me out by joining my committee later in the process, and helping to improve the quality of the dissertation. I thank Greg Foster for making me feel at home in the Chemistry Department and providing me with lab space, equipment and many fruitful ideas. I am honored to have been one of Don Kelso's last students at George Mason. Dr. Kelso is a mentor both as a scientist and a human being. And lastly, it was a real honor to study and work under Tom Jordan, who as one anonymous grant proposal reviewer wrote, is "world-renowned" in his field. I have enormous respect for Tom, and benefited tremendously from his patient teachings and rigorous standards.

Besides my committee members, I have reached out to numerous other people for help, and have been rewarded by their generosity. These people include Jeff Cornwell who was instrumental in assisting me with my dissertation, providing lab space, equipment and expertise. A number of mineralogists were also charitable with their time, lab space and ideas, including Bob Hazan of the Carnegie Institution, Jeffrey Post of the Smithsonian Institution, Helen Folger of the U.S. Geological Survey, and Mark Krekeler of Miami University. I also received support from exceptionally bright and motivated undergraduate students including Kim Cone, Jackie Nyguen, Quan Dhin, and Veronica Anderson. Patient and helpful technical assistance also came from Nancy Goff, Joe Miklas, Marc Sigrist, and Mike Owens. Financial support was provided by a National Science Foundation grant (DEB-0235884), the U.S. Environmental Protection Agency (EPA) Science to Achieve Results (STAR) Graduate Fellowship Program, and a grant from the Geological Society of America.

Finally, many thanks to my husband, Will, and sons, Steven and Kyle, for all of your love and support.

Table of Contents

List of Tables

List of Figures

List of Abbreviations

Auth-P	Authigenic carbonate fluorapatite + biogenic apatite + $CaCO_3$ - bound P
CDB	Citrate-dithionite-bicarbonate
CDB-Fe	CDB extractable iron
CFA	Carbonate fluorapatite ($Ca_{10}(PO_4,CO_3)_6F_2$)
Det-P	Detrital apatite of igneous or metamorphic origin
DOP	Degree of pyritization (Fe(pyrite)/[Fe(pyrite) + Fe(acid-soluble)])
DPM	Disintegrations per minute
Fe-P	P extracted with CDB
Org-P	Organic P
P	Phosphorus
PP	Particulate P
Sorb-P	Exchangeable or loosely sorbed phosphorus
WWTP	Waste water treatment plant

Abstract

THE FATE OF PHOSPHORUS ALONG ESTUARINE SALINITY GRADIENTS

Jeanne L. Hartzell, Ph.D.

George Mason University, 2009

Dissertation Co-Directors: Drs. Thomas E. Jordan and Donald P. Kelso

Determining the fate of particulate phosphorus (PP) in estuaries is essential for addressing the widespread problem of estuarine eutrophication, and is key for developing accurate global P budgets. We used a sequential extraction technique and ^{210}Pb dating to determine the form and amount of P that is retained with burial in 1-meter long sediment cores collected along the salinity gradients of four Chesapeake Bay subestuaries with contrasting physiographic provinces: the Patuxent River, the Potomac River, the Choptank River, and Bush River.

We found that citrate-dithionite-bicarbonate (CDB) extractable P was the most important fraction of PP in regulating P bioavailability in the sediments. We refer to this fraction as Fe-P because the CDB extraction targets P bound to iron oxyhydroxides, but CDB may dissolve other P compounds as well. In all four subestuaries, changes in Fe-P

controlled down-core profiles of total PP. Declines in Fe-P also accounted for 90% of observed declines in total PP with increased salinity. In the freshwater sediments of all four subestuaries Fe-P persisted with depth allowing for efficient sequestration of PP. In the Fe-rich Patuxent subestuary, Fe-P was the dominant sink for PP even in the most saline and deepest sediments, in spite of the fact that the Fe was in the form of Fe(II). Solubility calculations indicate that CDB-extractable ferrous phosphate minerals, such as vivianite, may be sequestering P in the Patuxent. In contrast to the Patuxent, Fe-P concentrations declined to near zero with depth in the sediments of the most saline cores in the Potomac and Choptank, indicating that Fe-P is not a long-term sink for P in the saline portions of those subestuaries.

Fe dynamics also controlled an increase in pore water PO_4^{3-} concentrations along the salinity gradient of each subestuary affecting a shift in pore water N:P ratios from greater than 16 (the Redfield ratio) in the freshwater sites to less than 16 in the saline sites. The shift in the Redfield ratio occurred at remarkably similar salinities of 1 – 4 in each subestuary.

Our findings indicate that Fe regulation of P can contribute to the generally observed switch from P limitation of primary production in freshwater to N limitation in mesohaline waters, and can control the long-term burial of PP in estuaries. Thus the amount and form of particulate Fe in estuarine sediments may be a key factor in controlling P bioavailability.

Chapter 1: Introduction

Importance of studying P in estuaries

More than 90 percent of phosphorus transported by rivers to estuaries and coastal waters is in the form of particulates (Froelich 1988, Föllmi 1996); however, the fraction of particulate phosphorus (PP) that can become biologically available is not well known. Since burial in the sediments is the main mechanism for removing P from estuarine waters, understanding P sequestration by estuarine sediments is imperative for understanding global P cycling and for mitigating the worldwide problem of estuarine eutrophication.

One reason it is important to understand global P cycling is that P is an essential nutrient for all life. Therefore P cycling is linked to all of the other biogeochemical cycles, including N, S, C, Fe, and O cycles (Föllmi 1996). P is also thought to limit primary production of the global oceans on a geologic time-scale (Tyrrell 1999). On shorter time-scales, nutrient limitation is more complex and variable, but long-term N deficiencies can be overcome by an increase in fixation of atmospheric N, whereas weathering of continental rocks is the ultimate source for P (Horne and Goldman 1994).

Since P has a role in regulating long-term oceanic primary productivity, P has been instrumental in keeping atmospheric O_2 levels steady throughout the Phanerozoic time period (e.g., Van Cappellen and Ingall 1996, Colman and Holland 2000). During periods of high oxygen levels, aerobic bottom waters increase removal of dissolved P from the water column to sediments through increased bioaccumulation by benthic bacteria and increased uptake by Fe oxides (Ingall and Jahnke 1997). Conversely, during periods of low oxygen, P removal through burial in the sediments is decreased because bioaccumulation and uptake by Fe is decreased (Van Cappellen and Ingall 1997). Decreased uptake by P during periods of low oxygen leads to increased P bioavailability and primary productivity, which in turn produces more O_2. Thus, the interactions of P, Fe and O_2 create a feedback system to maintain stable levels of atmospheric O_2 throughout the Phanerozoic, allowing for the evolution of higher plants and animals (Van Cappellen and Ingall 1996).

P controls on primary production also means that increases in P bioavailability can increase carbon sequestration. For example, it has been estimated that phosphates are already influencing global climate change by compensating for approximately 10 percent of the yearly increase in atmospheric CO_2 from anthropogenic sources (Mackenzie et al. 1993). Therefore, knowledge of the amount of P bioavailability is crucial to developing accurate global change models.

Estuaries also provide excellent opportunities to study P bioavailability in freshwater versus saltwater with the goal of further understanding and mitigating eutrophication of water bodies. In estuaries, where freshwater and saltwater mix, short-term (i.e., non-geologic time) shifts in nutrient limitation can occur. In freshwater, P is generally a limiting nutrient, and N is sufficient for biological uptake (Schindler 1977). However, in saltwater this paradigm switches and P is usually sufficient, and N limits primary production (Howarth and Marino 2006). Changes in P sorption to sediments that occur along the salinity gradient of an estuary may be a key reason for this nutrient limitation transition. Phosphates are more effectively retained in freshwater sediments, while in saline environments phosphates are more efficiently mobilized to the water column (e.g., Caraco et al. 1990, Roden and Edmonds 1997, Jordan et al. 2008). As a result, sedimentary P tends to decrease with increasing salinity (e.g., Lebo and Sharp 1993).

In many estuarine systems, declines in PP with increased salinity are attributed to declines in Fe-bound P with increased salinity (e.g., Upchurch et al. 1974, Strom and Biggs 1982, Lebo and Sharp 1993, Jordan et al. 2008). This indicates that Fe-P interactions along estuarine salinity gradients may play a key role in explaining the general pattern of P limitation in freshwater versus nitrogen limitation in saltwater. The dominant role of iron oxides, hydroxides and oxyhydroxides in scavenging dissolved phosphate anions in many aqueous systems is well documented (Chambers and Odum 1990, Ruttenberg 1992, Slomp et al. 1996b). It is also documented that the mineralogy

and crystallinity of iron species strongly influences ability of sediments to sorb phosphates (Upchurch et al. 1974, Strom and Biggs 1982, Froelich 1988, Fox 1989, Kanungo 1994, Hartzell et al. 2008). Thus knowledge about the nature of iron minerals is important in understanding P cycling.

To further our general understanding of the fate of P in estuaries, we investigated PP burial in the sediments of four Chesapeake Bay subestuaries. The Chesapeake Bay is an impaired water body due to excessive loading of both N and P (e.g., Boesch et al. 2001). For example, phosphorus loads to the Chesapeake Bay and its tributaries have increased by an estimated 13- to 24- fold since European colonization (Boynton et al. 1995). This excessive nutrient loading in the Chesapeake Bay is contributing to heavy growth of phytoplankton, low levels of dissolved oxygen and severe SAV loss (Kemp et al. 2005). The Chesapeake Bay is also the largest estuary in the United States, and as such is a major gateway for P transport from the land to the sea.

Thesis outline

In **Chapter 2**, we present the results of our investigation of the long-term fate of PP entering the Patuxent River subestuary. We found that P bound to citrate-dithionite-bicarbonate extractable Fe (Fe-P) was the dominant form of P at all depths in the sediments and at all salinities, providing a long-term sink for P entering the Patuxent, despite all of the Fe being in the form of Fe(II). We also found that most of the PP input from the watershed was buried in the subtidal sediments in the upper Patuxent subestuary, in the region from tidal freshwater to mesohaline waters.

Chapter 3 details insights gained from comparing PP dynamics in the Patuxent River to three other Chesapeake Bay subestuaries. We chose the Bush River, the Choptank River and the Potomac River as comparison sites because their watersheds differ in land-use and physiographic provinces. We found that the Patuxent sediments had the highest concentrations of Fe-bound P, but in the other rivers, Fe-bound P was still a dominant and dynamic fraction controlling P bioavailability and declines in total PP with increased salinity.

Chapter 4 addresses the question of why primary production is generally phosphorus limited in freshwater but not in coastal marine environments. In this chapter we present findings of distinct shifts in pore water Fe:P ratios that occur along the salinity gradient that in turn promote a shift in pore water N:P ratios of > 16 in the freshwater sediments to > 16 in the saline sediments.

And finally, **Chapter 5** describes our attempts to determine the chemical forms of the Fe that are so important in regulating P bioavailability among our study sites. Our methods included attempts to directly identify Fe mineralogy, measurements of Fe(II) and Fe(III) concentrations in the sediments, analysis of Fe sulfides in the sediments, and calculating the solubility of iron(II) phosphate minerals in saline sediments using a geochemical modeling program (Visual MINTEQ). While attempts to directly identify the Fe minerals were largely unsuccessful, the Fe(II) concentrations, iron sulfide concentrations and geochemical modeling results suggest that ferrous phosphate minerals

may be forming in the saline sediments of the Patuxent, in spite of the commonly held assumption that ferrous phosphate minerals are indicative of freshwater environments.

Chapter 2: Phosphorus burial in sediments along the salinity gradient of the Patuxent River, a subestuary of the Chesapeake Bay (USA)

Abstract

Understanding phosphorus sequestration by estuarine sediments is imperative for quantifying global P cycling and mitigating the worldwide problem of estuarine eutrophication. We used a sequential extraction technique and ^{210}Pb dating to determine the form and amount of particulate phosphorus (PP) that is retained with burial in 1-meter long sediment cores collected along a salinity gradient from tidal freshwater to the mesohaline waters of the Patuxent River, a subestuary of the Chesapeake Bay. PP buried in the freshwater sites was similar in concentration and form to PP entering the Patuxent from the watershed, suggesting efficient sequestration by the freshwater sediments. Fe-bound P (Fe-P) concentrations declined with increased salinity; however Fe-P persisted with depth in the sediments and was the dominant sink for PP at all salinities. The efficient sequestration of PP in both the freshwater and saline sediments allowed for sequestration of the majority of the PP entering from the watershed with the subtidal sediments trapping three times as much PP as the marshes fringing the Patuxent.

Introduction

Understanding the transport of phosphorus from the land to the sea is important for quantifying global P cycling (e.g., Ruttenberg and Berner 1993, Föllmi 1996) and for mitigating the widespread problems associated with eutrophication (e.g., Cloern 2001). Phosphorus is transported to the oceans predominantly by rivers, and up to 95% of phosphorus carried by rivers to estuaries and coastal waters is in the form of particulates (Föllmi 1996). The eventual fate of this particulate P (PP) is uncertain. Some studies have concluded that only a small portion (1-5%) of PP entering the oceans is permanently buried in sediments, making burial of PP in marine systems very ineffective (e.g., Anschutz et al. 1998, Benitez-Nelson 2000). In coastal marine environments, burial can be more efficient, but a substantial amount of PP can still be converted to soluble P that escapes to the water column. For instance, only about 50% of the PP delivered to the Laurentian Trough in the Gulf of St. Lawrence was found to be buried in the sediments (Sundby et al. 1992). Jensen et al. (1995) found that as little as 30% of PP delivered to the shallow Aarhus Bay in Denmark was retained with burial. In a study of sediments from the Atlantic Canadian and Portuguese continental margins and the anoxic region of the Chesapeake Bay, Anschutz et al. (1998) found that 20-30% of total P buried in the sediments was remobilized to the overlying water. In another study of mid-Chesapeake Bay sulfidic sediments, Cornwell et al. (1996) found no major changes in P concentrations with respect to depth in sediments that spanned up to 80-100 years old, indicating that the significant increases in anthropogenic P loading during this time-period were not retained in the sediments. In contrast to marine sediments, phosphates

can be effectively retained in freshwater sediments (Callendar 1982, Fox 1989, Caraco et al. 1990, Chambers and Odum 1990), indicating the importance of salinity in P burial efficiency. In estuaries, where freshwater and saltwater mix, P burial efficiency may vary with salinity. Some estimates indicate that P burial in Chesapeake Bay subestuaries may be unusually efficient compared to other estuaries (Nixon et al. 1996, Boynton et al. 2008); however, these estimates are often based on surficial sediments, and thus long-term fate of P is less certain.

The amount of P sequestered and buried by sediments is affected by the form of PP as well as salinity. Some forms of sediment PP are more labile than others. Quantitatively, organic P has been reported to be one of the most important reservoirs of P in surficial sediments (Froelich et al. 1982, Ruttenberg and Berner 1993, Föllmi 1996). However, with decomposition, organic P can release associated P to the water column; thus organic P may be only a temporary sink for P in some environments (Ruttenberg and Berner 1993, Louchouarn et al. 1997, Cha et al. 2005).

Another quantitatively important form of PP is Fe-bound P, which can account for more than 50% of the chemically weathered-phosphorus river flux to the global oceans (Compton et al. 2000). In the Patuxent River subestuary, Fe-bound P is an especially important fraction of PP, accounting for up to 80% of the PP entering the river from the watershed (Jordan et al. 2008). Although Fe-bound P may be one of the largest and most reactive PP pools in coastal environments, the fate of Fe-bound P entering estuaries and

coastal environments is uncertain (Compton et al. 2000), leading to uncertainties in attempts to quantify the global phosphorus cycle. Iron oxides can strongly sorb P, and may be an important burial sink for PP in some environments (e.g., in the sediment-rich environment of the Mississippi Delta, Ruttenberg and Berner 1993). However, Fe(III) oxides can become reduced to soluble ferrous iron species with sediment burial, releasing associated P. Thus Fe oxides may be only a temporary sink for P in many environments (Krom and Berner 1981, Sundby et al. 1992, Jensen et al. 1995, Föllmi 1996, Anschutz et al. 1998). The fate of Fe-bound P may also change with salinity. The abundance of sulfates in seawater allows for the formation of ferrous sulfide minerals in anaerobic sediments, which in turn diminishes the capacity of Fe to bind with phosphates (e.g., Caraco et al. 1989, Roden and Edmonds 1997). Fe-P-S interactions may explain why a decrease in sediment PP content with increased salinity has been correlated to decreases in Fe-bound P in many estuaries (Upchurch et al. 1974, Strom and Biggs 1982, Jordan et al. 2008).

Phosphates released from organic matter degradation and reductive dissolution of Fe-oxides can be incorporated into carbonate fluorapatite minerals (CFA) which can form authigenically in marine environments. Diagenetic "sink switching," whereby P released from Fe-bound P and organic-P is then incorporated into authigenic CFA, has been found to be a main mechanism for retaining reactive P in marine sediments (Ruttenberg and Berner 1993, Filippelli and Delaney 1996, Slomp et al. 1996a, Louchouarn et al. 1997,

Anderson et al. 2001, van der Zee et al. 2002, Cha et al. 2005). However, the importance of sink-switching in retaining P in estuaries is unknown.

In this study, we examined the long-term fate of PP entering the Patuxent River, a Chesapeake Bay subestuary. Since the Patuxent subestuary is a well-studied ecosystem, we were able to compare our findings regarding the long-term burial of PP burial to the amount and form of PP entering the subestuary (Jordan et al. 2003, Boynton et al. 2008, Jordan et al. 2008). The intent was to address the following questions to further clarify P biogeochemical processes in estuaries: What is the fate of PP entering the Patuxent River subestuary? How much PP is retained in the sediments through long-term burial as opposed to becoming released from the sediments to become potentially bioavailable? What are the predominant chemical forms of PP accumulating in the sediments of the Patuxent subestuary?

Study Location

Our study focused on the upper tidal portion of the Patuxent River, Maryland, USA (Fig. 2-1). The 177 km long Patuxent River is a tributary and subestuary of the Chesapeake Bay. The tidal portion of the river is approximately 80 km long, covers 137 km^2, and averages 5 m deep. The 2,393 km^2 drainage basin of the Patuxent River is located between the cities of Washington, D.C. and Baltimore, MD. The watershed is about 15% cropland, 6% pasture, 44% forest, and 35% other land-types (mostly residential) (U.S. Environmental Protection Agency 1994). Seventy-two percent of the

watershed of the Patuxent lies in the Coastal Plain physiographic province. The remaining 28% of the watershed is in the Piedmont province.

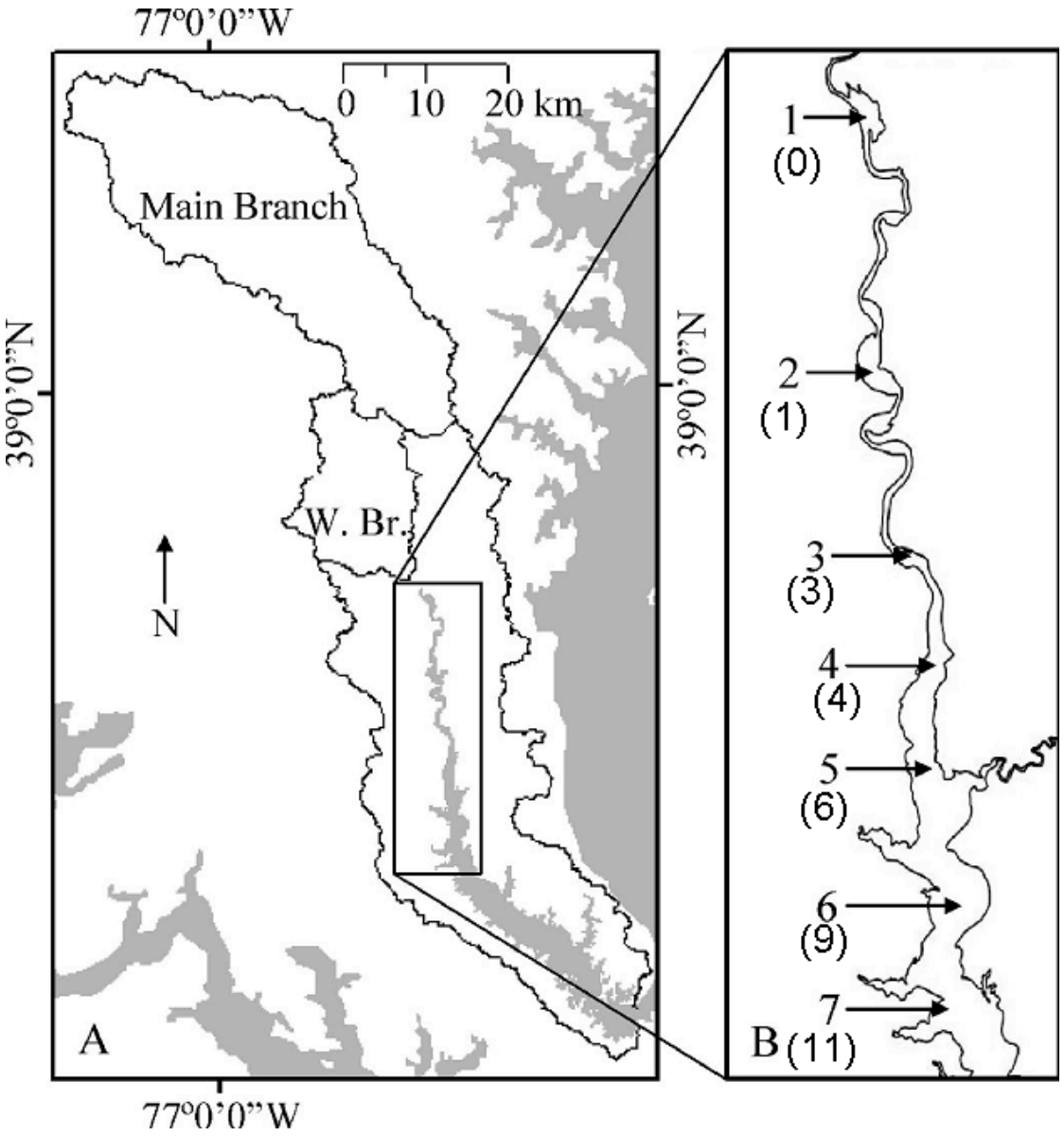

Fig. 2-1 (A) The Patuxent River subestuary and its watershed, (B) An enlargement of the upper Patuxent subestuary, 30-70 km from the mouth of the Patuxent, showing the seven sampling sites. Mean pore water salinity of the cores is shown in parentheses. Adapted from Jordan et al. (2008).

Methods

Sediment and pore water collection

We collected a total of fourteen 1-meter-long sediment cores from 7 different sites along a salinity gradient that ranged from tidal freshwater at site 1, to a salinity of 11 at site 7 (Fig. 2-1). Water depths ranged from 1 m at site 1 to 5 m at site 7. We collected one core from sites 1, 3, 4 and 5, three cores at site 2, five cores at site 6, and two cores at site 7.

We used a piston-corer to collect the sediments. As the piston corer was manually pushed into the sediments, the piston inside of the 8-cm diameter polycarbonate tubing was pulled up, creating a slight vacuum that allowed the sediments to slide into the tube without disturbing any stratification. Immediately after collection, the core tubes were stoppered and placed in core-holders fabricated from 10-cm diameter PVC tubes. The PVC core-holders kept the sediments in the dark and were filled with estuarine water to maintain ambient temperatures. Once back at the lab, the estuarine water in the core holders was bubbled with nitrogen gas to prevent oxygen diffusion through the polycarbonate sediment core tubes. The sediment cores, in their core-holders, were stored at 4^{o}C until they could be sectioned.

All sediment cores were sectioned within 1-5 days of collection. The sediments were extruded from the top of the core into a nitrogen glove bag using a hydraulic jack positioned at the bottom of the core. Two-cm thick samples were collected from the core

at 5 cm intervals (i.e., from 4-6 cm, 9-11 cm, 14-16 cm, etc.). We refer to the samples by their mid-section depth (i.e., the 4-6 cm sample is referred to as 5 cm, 9-11 cm as 10 cm, etc.). For this study, we analyzed the 5 cm section and all of the other sections at 10 cm intervals (i.e., 5, 10, 20, 30 cm, etc.).

The sediment samples were loaded into pre-weighed 50 ml polyethylene centrifuge tubes that were capped while still in the glove bags. The sediments were then weighed, centrifuged at 3000 rpm for 30 minutes to collect pore water (see pore water collection procedure below), frozen and freeze-dried. Freeze-drying was used instead of air drying in an attempt to reduce oxidation, and to make grinding the sediments easier. After freeze-drying, the sediment samples were weighed again to determine total pore water weight. The freeze-dried sediments were then ground with a ceramic mortar and pestle under normal atmospheric conditions.

Pore water was removed from intervals of every 10-20 cm of the sediment samples. The supernatant pore water from the centrifuged sediment samples was extracted with a syringe and filtered with 0.45 µm polycarbonate Millipore syringe filters. The pH of the pore water was measured with a Fisher Scientific Accumet model 910 pH meter. The pore water was transferred into four different containers for analyses. Three ml of filtered pore water was collected in a 7 ml polyethylene scintillation vial, acidified with 30 µl of nitric acid, and stored at 4°C for analysis of dissolved Fe, Al, Ca, Mn, Si and P. One ml of filtered pore water was transferred into a second 7 ml

polyethylene scintillation vial, diluted with 4 ml of distilled water, and frozen until analysis for dissolved phosphate (PO_4^{3-}). Another aliquot was frozen until analysis of dissolved ammonium (NH_4^+) (used in a different study). The remaining pore water was filtered into a 20 ml scintillation vial, and frozen until analysis of dissolved SO_4^{2-}, Cl^-, and F^-.

Chemical Analyses

The freeze-dried and ground sediments were sequentially extracted using the SEDEX method (Ruttenberg 1992). SEDEX is a widely-used extraction scheme that operationally defines five separate chemical fractions of PP which were extracted in the following order: 1) 1 M $MgCl_2$ at pH 8 was used to extract loosely sorbed P (which we will refer to as "sorb-P"); 2) citrate-dithionite-bicarbonate (CDB) was used to dissolve ferric iron-bound P ("Fe-P"); 3) Na-acetate solution at pH 4 was used to dissolve authigenic carbonate fluorapatite + biogenic apatite + $CaCO_3$-associated P ("auth-P"); 4) 1 M HCl was used to dissolve detrital apatite P ("det-P"); and 5) 2 M HCl was used to extract organic P ("org-P") from the residual sediment that had been ashed at 550^{o}C after treatment with $Mg(NO_3)_2$. Although the extractants may dissolve non-targeted forms of PP, we will refer to the extracts by their targeted PP form. All of the SEDEX extractions, except for the organic P step, were performed in sealed 250 ml polycarbonate filter funnels (Nalgene DS0310-4000) fitted with 0.2 μm Nucleopore filters. The filter funnels and Nucleopore filters were cleaned with dilute H_2SO_4 and rinsed twice with deionized

water before 0.4 g of dried and ground sediment was measured and deposited onto the filters.

The sediments and the extractants were shaken for a specified amount of time and then the extracts were filtered through the 0.2 μm membrane filters under a slight vacuum (~15 psi). SEDEX steps 2-4 were followed by rinses of $MgCl_2$ and deionized water to prevent resorption of phosphorus onto solid surfaces during extraction. The extracts were stored at 4º C prior to P analysis.

Except for the CDB extract, the concentrations of dissolved PO_4^{3-} from all of the SEDEX extracts and the filtered pore water were quantified using an ascorbic acid, molybdate colorimetric method (Eaton et al. 1995). Color development for pore water PO_4^{3-} was carried out in the vial used for sample storage to ensure that any PO_4^{3-} that precipitated with Fe(III) during storage would be redissolved during the analysis rather than be lost on the walls of the storage vials. The concentrations of total P, Fe, Mn, Ca, Si and Al in the CDB extracts were measured using a Perkin Elmer Optima model 3000 Inductively Coupled Plasma, Optical Emission Spectrometer. Pore water SO_4^{2-}, Cl^-, and F^- concentrations were measured with a Dionex model 4000 ion chromatograph. Salinity was calculated from Cl^- concentrations.

Sediment characterization

Before sectioning under nitrogen, eight of the cores were characterized by visual examination, using Munsell color charts. Evidence of biotic activity, methane bubbles and hydrogen sulfide smells were also noted for the core descriptions. Fine-grained sediments were required for successful operation of the piston corer; therefore a basic assessment of sediment grain size was assessed tactilely in the field to ensure that the sediments were fine-grained. The sand content from portions of two freshwater cores and one saltwater core was also assessed by sieving wet sediment through a 63 μm sieve after dispersal of the sediments with sodium hexametaphosphate.

^{210}Pb Dating

Sedimentation rates were determined using ^{210}Pb radiometric dating. The activity of ^{210}Pb ($T_{½}$ = 22.3 yrs) in the sediments was determined by measuring the activity of ^{210}Po ($T_{½}$ = 138 days), an alpha-emitting daughter. Samples were stored for several ^{210}Po half-lives to ensure secular equilibrium between the two nucleotides. A ^{208}Po standard tracer was added to the sediments to determine yield efficiency. ^{210}Po in the sediments was extracted using concentrated HCl and HNO_3 at 80 – 90^{o}C. A linear regression model was used to calculate sedimentation rates in cm yr^{-1} and sediment accumulation rates in g m^{-2} yr^{-1} following the procedure described in Cornwell et al. (1996). Surficial sediments that showed little to no change in ^{210}Pb activity with depth were assumed to be in the mixing zone, and were not used in the calculations. Samples with ^{210}Pb activity levels less than 2 disintegrations per minute (dpm) were also not used in the calculations, as

these samples were assumed to be from depths in the sediments where excess ^{210}Pb has completely decayed to background levels.

Results

Spatial variability of PP fractions

Fe-P was the largest fraction of PP at all salinities and all depths in the sediments. Furthermore, Fe-P concentrations persisted with little change in depth in most of our sediments. Although total PP and Fe-P concentrations were lower in the deeper half of the sediments at sites 1 and 3 (Fig. 2-2), and in one of the triplicate cores sampled at site 2, no consistent depth trend was apparent in the other two site 2 cores. Nor were there consistent depth trends in PP below 10 cm at sites 4-7. Total PP and Fe-P declined only in the surficial 10 cm of the sediments from sites 4-7 (Fig. 2-2).

Org-P was the second largest fraction of PP in the sediments of all of the study sites, and depth trends were not apparent in any of the sediment cores. The other three SEDEX fractions were minor in quantity (< 10% of total PP concentrations) and exhibited no consistent depth trends. Depth trends in the concentrations of the sorb-P fraction were not apparent at any of our sites (Fig. 2-2). Concentrations of the auth-P and det-P fractions increased slightly with depth in the sediments of sites 2 and 3, but there was no auth-P or det-P depth trend at site 1, or in the four most saline sites (Fig. 2-2).

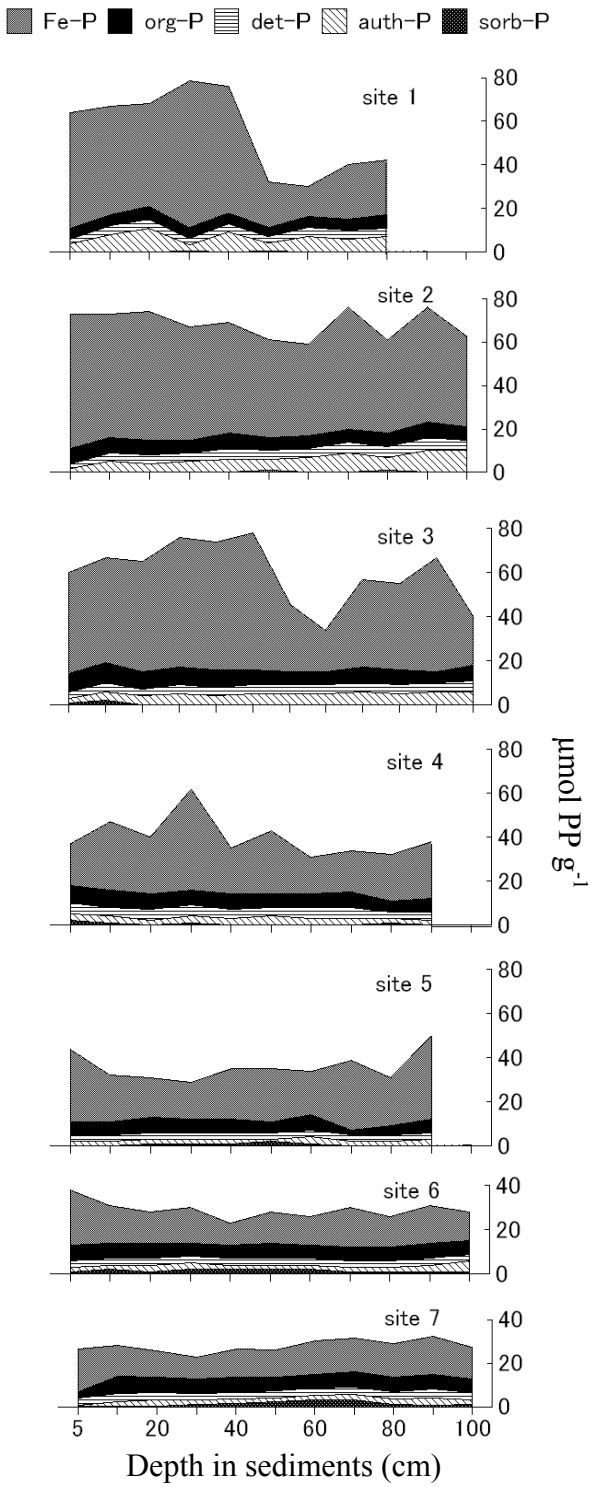

Fig. 2-2 Particulate P pools at the 7 sampling locations. Concentrations across the y-axis are in μmol PP per gram of dry sediment. The x-axis is depth in the sediments in cm.

As well as being the dominant PP fraction in all of our study sites, Fe-P was also the most dynamic fraction, driving any observed spatial changes in total PP. Since there were only minor depth trends in PP in our cores, we were able to average PP concentrations for the entire length of the cores to simplify comparisons of PP retention with changes in salinity. Mean total PP concentrations significantly declined with increased salinity (regression $r^2 = 0.80$, $p < 0.001$), from a high of 69 μmol g^{-1}at site 2 to a low of 28 μmol g^{-1}at site 7 (Fig. 2-3). Therefore, total PP concentrations declined by 41 μmol g^{-1}, or 59% across the salinity gradient. Declines in mean concentrations of Fe-P with increased salinity were also significant (regression $r^2 = 0.82$, $p < 0.001$) and accounted for 37 μmol g^{-1}, or 90%, of the observed decline of 41 μmol g^{-1} in PP (Fig. 2-3). The other 10% decline in total PP with increased salinity was accounted for by declines of 4 μmol g^{-1} in auth-P and 1 μmol g^{-1} in det-P, which were partially offset by an increase of 1 μmol g^{-1} in sorb-P. Org-P showed no clear trends with salinity (Fig. 2-3).

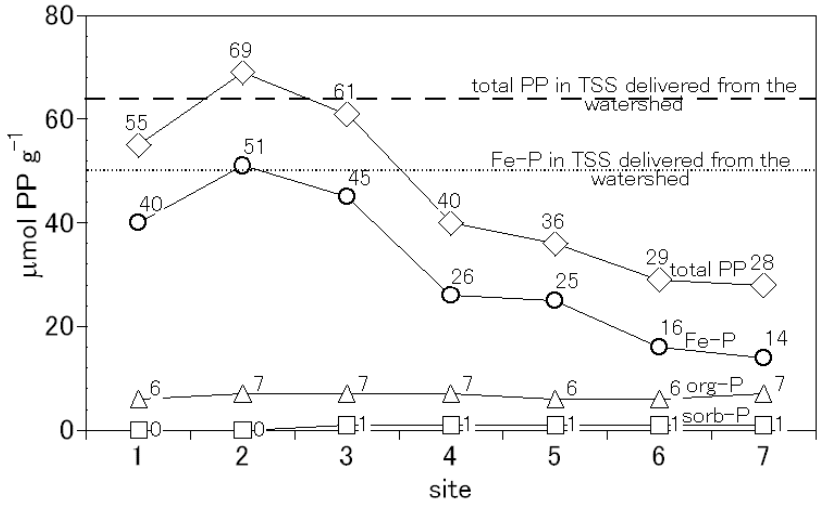

Fig 2-3. Mean concentrations of total PP, Fe-P, org-P and sorb-P in the sediment cores along the salinity gradient (solid lines). The doted lines show concentrations of total P and Fe-P in total suspended solids (TSS) delivered from the watershed (from Jordan et al. 2008).

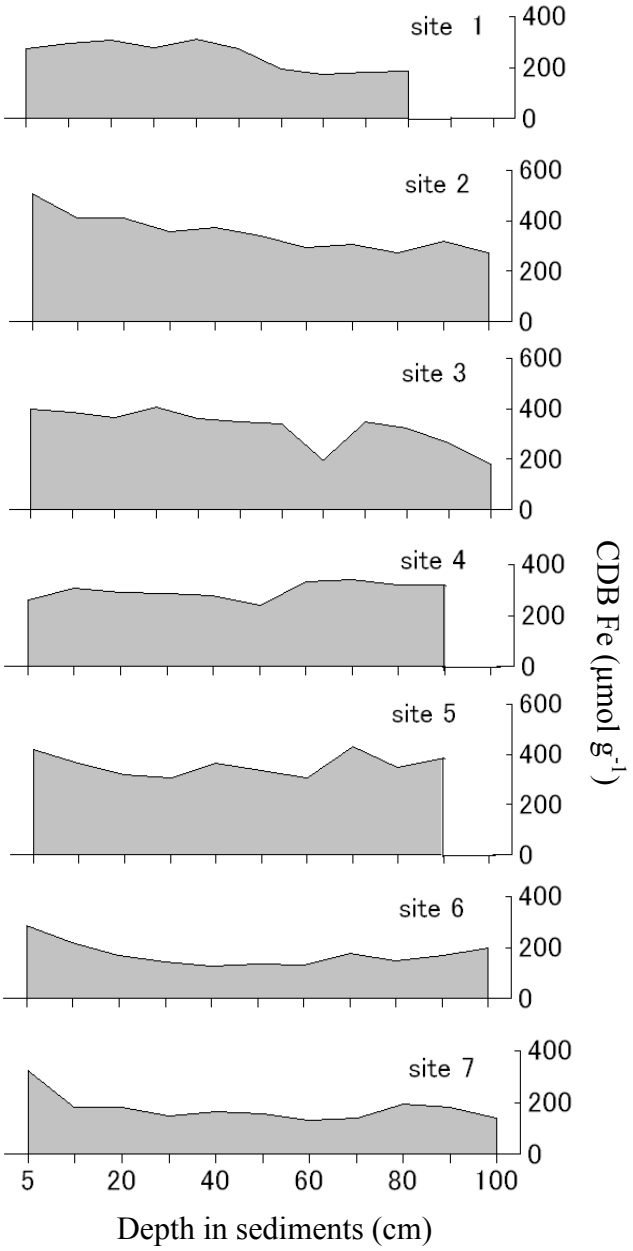

Fig 2-4. CDB extractable Fe (μmol g^{-1}) with depth in sediments (cm).

Spatial trends in CDB extractable Fe (CDB-Fe)

In general, spatial trends in CDB extractable Fe (CDB-Fe) were the same as the spatial trends of PP and Fe-P. Similarly to PP and Fe-P, CDB-Fe decreased in the deeper half of the cores from sites 1 and 3, and in one of the cores collected from site 2, while there was no CDB-Fe trend with depth in the sediments of the other site 2 cores; nor were there consistent depth trends in CDB-Fe in sediments below 10 cm at sites 4-7 (Fig. 2-4). Additionally, there was a general trend of a decline in CDB-Fe with increased salinity (regression $r^2 = 0.38$, $p = 0.02$, Fig. 2-4). However, CDB-Fe did not decline with salinity to the same extent as CDB extractable P (i.e., Fe-P). Thus there appeared to be some decoupling of CDB-Fe and Fe-P downstream of site 3 (Fig. 2-5).

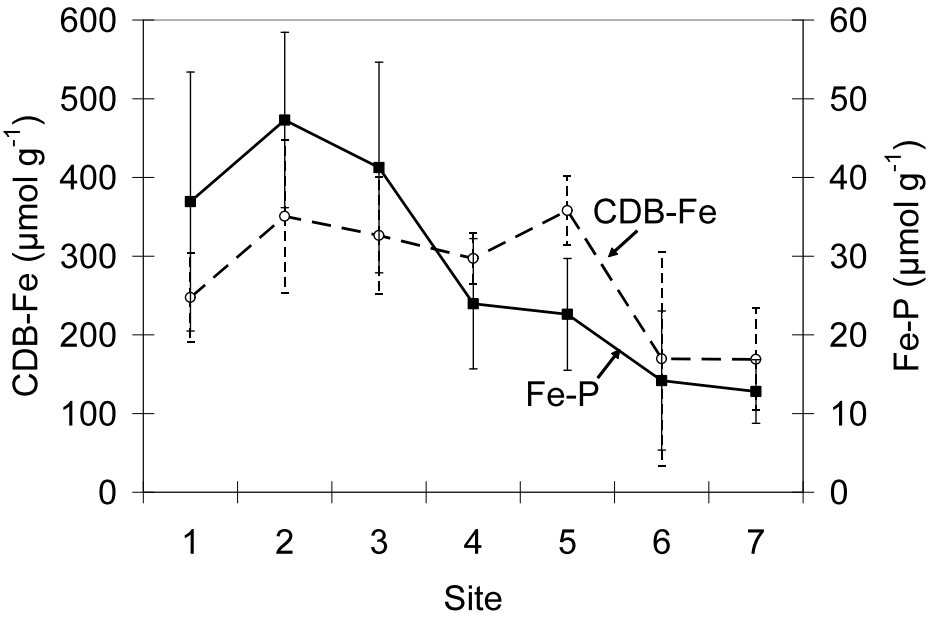

Fig 2-5. CDB extractable Fe (CDB-Fe), shown with white circles, and CDB extractable P (Fe-P), shown with filled squares, along the salinity gradient.

In spite of the apparent decoupling of CDB extractable Fe and P with increased salinity, CDB-Fe was correlated to Fe-P in all of our sediment samples (Spearman's rho correlation coefficient 0.77, $p < 0.001$). Correlations were also found between CDB extractable Al and P (Spearman's rho correlation coefficient 0.43, $p < 0.001$) and Mn and P (Spearman's rho correlation coefficient 0.74, $p < 0.001$). However, the concentrations of CDB extractable Al and Mn were much lower than concentrations of CDB-Fe (mean values for all cores of 37 μmol g^{-1} for Al, 12 μmol g^{-1} for Mn, compared to 257 μmol g^{-1} for Fe), suggesting that most of the CDB extractable P was bound to Fe.

Ratios of CDB extractable Fe and P (i.e., CDB-Fe:Fe-P) in the sediments increased from a mean of 7.6 at sites 1-3, to 14.0 at sites 4 -7, almost a two-fold increase with increased salinity. There was no consistent depth trend in CDB-Fe:Fe-P ratios in most of our cores; although CDB-Fe:Fe-P ratios did decrease with depth in the upper 30 cm of the sediments of some of the site-6 and site-7 cores.

Sediment Characterization

The sediments were fairly uniform in texture with > 92% (wt/wt)of the sediment less than 63 μm in size. No correlation between Fe or P concentrations and sand content was found. All of the cores had a distinctly colored oxidized surficial layer that ranged from 5-10 cm thick in the cores from sites 1-3, and 2-6.5 cm thick in the more saline sites. This visible oxidized surficial layer had correspondingly higher Fe-P concentrations in cores from the saline sites, but did not correspond to trends in any PP

concentrations in the freshwater cores. Worm burrows of depths of up to 5-10 cm in the freshwater cores and 15-30 cm in the mesohaline cores were not found to correlate to any changes in PP fractions with depth.

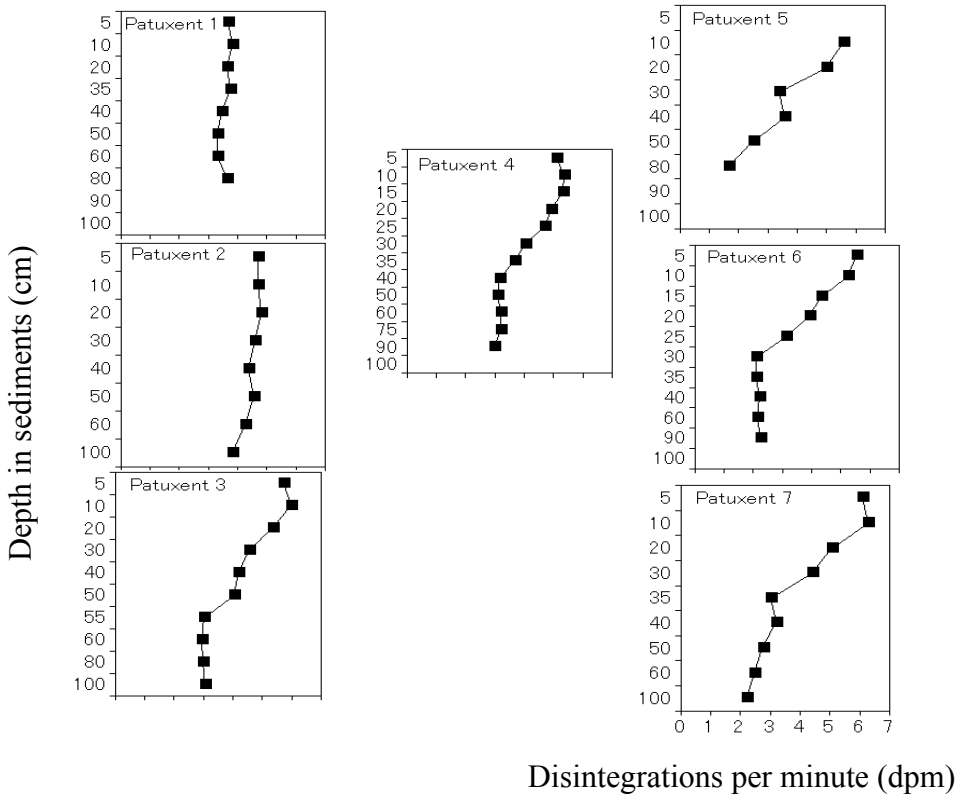

Fig 2-6. ^{210}Pb activity in disintegrations per minute (dpm) with depth in the sediments (cm).

^{210}Pb Dating

The cores in the more saline sites showed lower sedimentation rates than the cores collected from the fresher portions of the rivers based on ^{210}Pb activity. Sedimentation rates for sites 1 and 2 were estimated to be 1.4 and 3.4 cm yr^{-1} respectively, which was up

to 7 times greater than sedimentation rates for sites 3 – 7, which ranged from 0.5 to 1.1 cm yr^{-1}. Sediment accumulation rates at sites 1 and 2 were 7.6 and 14 kg m^{-2} yr^{-1} respectively, and ranged from 2.3 to 4.4 kg m^{-2} yr^{-1} at sites 3 – 7. At sites 1 and 2, there was little change in unsupported ^{210}Pb activity with change in depth in the sediments, and ^{210}Pb activity did not reach background levels in either of these two cores, indicating that the sediments may be relatively young (Fig. 2-6). Additionally, the relationship between excess ^{210}Pb activity and depth in the sediments was not statistically significant ($p > 0.05$) for site 1, indicating that sedimentation may be episodic at that site. The ^{210}Pb activity in the sites 3-7 sediment cores exhibited a larger change in unsupported ^{210}Pb activity with depth in the sediments, allowing more precise estimates of sediment rates at these sites (Fig. 2-6). Linear regression models used to determine sedimentation rates (Cornwell et al. 1996) provided statistically significant results ($p < 0.05$ and r^2 values ≥ 0.90) for sites 3 – 7. At sites 1 and 2, there was little change in unsupported ^{210}Pb activity with change in depth in the sediments (Fig. 2-6). Thus estimates of sedimentation rates were uncertain for these two sites, perhaps indicating nonsteady-state deposition.

Since ^{210}Pb-based measurements involve some inherent uncertainty (e.g., Brush et al. 1982), and are based on relatively small amounts of sediments, we examined bathymetric maps made in the 1800s to get a sense of how historical sediment accretion rates in the Patuxent compare to our ^{210}Pb measurements. Comparison of modern bathymetric maps with archival maps from the U.S. National Oceanic and Atmospheric Administration's Office of Coast Survey indicated that sedimentation has been

heterogeneous, especially in the tidal freshwater reaches of the Patuxent. For example, at some locations near sites 2 and 3, the water depths were 2 – 5 meters deeper in the 1860 than in 1997, while other locations near sites 2 and 3 were several meters shallower in 1860, indicating a complex history of deposition and scouring. However, most water depths in the vicinity of our study sites were 30 to 90 cm deeper in 1860 than in 1997, indicating an overall trend of deposition. Additionally, it has been estimated that relative sea level has been rising by about 3 – 4 mm yr^{-1} in the Chesapeake Bay (Hicks et al. 1983, Douglas 1991), which means sea level has risen by about 50 cm since 1860. Adding together a 30 to 90 cm decrease in water depth since 1860, plus a relative sea level rise of 50 cm since 1860, indicates that most subtidal have experienced from 80 to 140 cm of sediment deposition in the past 140 – 150 years, which equates to sedimentation rates ranging from approximately 0.5 to 1.1 cm yr^{-1}. Thus, the historical maps support the ^{210}Pb-based measurements for sites 3 – 7 (which also ranged from 0.5 to 1.1 cm yr^{-1}). The sedimentation rates obtained from ^{210}Pb measurements for sites 1 and 2 (1.4 to 3.4 cm yr^{-1} respectively) were higher than indicated by comparing most locations on the historical bathymetric maps. However, these sediment rates were not out of the range of a few localized bathymetric depth changes in the tidal freshwater region of the Patuxent.

Pore water solutes

Pore water PO_4^{3-} concentrations increased with increased salinity (Fig. 2-7). There was no clear trend in pore water PO_4^{3-} concentrations with depth in the sediments

of sites 1-4, but PO_4^{3-} concentrations increased with depth in the surficial 40 cm at sites 5-7 (Fig. 2-7). In contrast to PO_4^{3-}, pore water Fe concentrations declined with increased salinity (Fig. 2-7). There was no overall trend with pore water Fe concentrations and depth in the sediments of sites 4-7; however there was a slight increase in pore water Fe in the surficial 40 cm of sites 1-3 (Fig. 2-7).

Pore water sulfate concentrations increased along the salinity gradient, with concentrations of less than 1 mmol L^{-1} at all depths at sites 1-4, and exceeding 6 mmol L^{-1} in the surficial sediments of sites 6-7. Sulfate concentrations greater than 1 mmol L^{-1} persisted to sediment depths of up to 50 cm at site 6. Below 60 cm in sediment depth, sulfate concentrations were below 1 mmol L^{-1} at all of our sites (Fig. 2-7).

Pore water pH increased with salinity with pH values ranging from 6.8 – 7.6 at sites 1 and 2, and 7.3 to 8.3 at sites 6 and 7. pH increased slightly in the surficial 30 – 40 cm of the sediments of sites 5 – 7, but there was no trend with further depth in the sediments (Fig. 2-7).

As expected, salinity and F^- concentrations increased with site number. Trends in salinity with depth in the sediments were not apparent in any of our cores, except for one core from site 6 in which salinity increased from 6 at 20 cm to 11 at 80 cm. There was no clear trend in F^- pore water concentrations with depth in the sediments (Fig. 2-7).

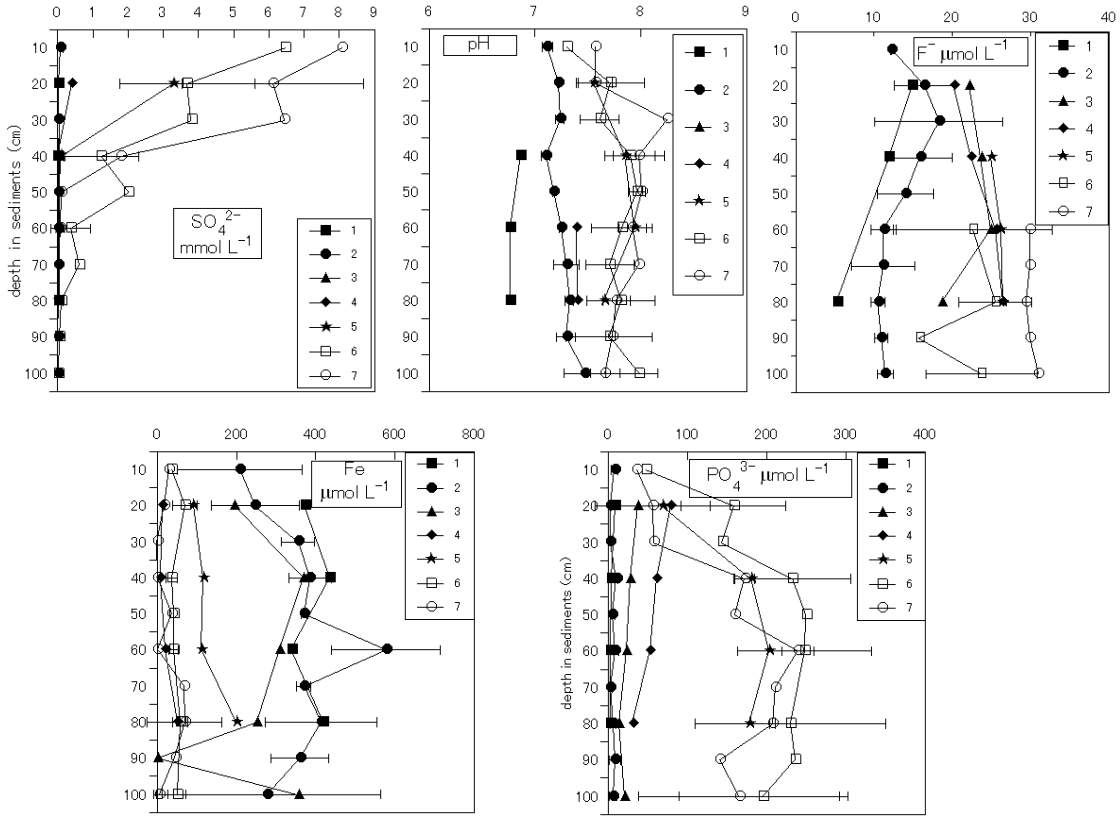

Fig 2-7. Pore water solutes with depth in sediments.

Discussion

The fate of PP entering the upper Patuxent River subestuary

To determine the fate of PP entering the upper Patuxent subestuary we compared our long-term P burial results to PP concentrations entering from the watershed (Jordan et al. 2008), PP concentrations and burial rates in the marshes adjacent to our study sites (Khan and Brush 1994, Merrill 1999, Greene 2005, Boynton et al. 2008), and P inputs from the watershed (Jordan et al. 2003, Boynton et al. 2008). Thus we developed an overall budget detailing the quantity and form of P retained in the entire upper Patuxent River subestuary.

We found that the majority of P entering the Patuxent is sequestered in the sediments of the upper Patuxent. The forms and concentrations of the PP retained with depth in the sediments of the three freshest sites were similar to the forms and concentrations of PP in the suspended solids discharged from the Patuxent watershed (Jordan et al. 2008, Fig. 3) indicating that PP is efficiently preserved in the freshwater sediments of the upper Patuxent River subestuary. While PP concentrations declined with increased salinity, PP concentrations persisted with depth in the sediments of the saline sites after an initial depletion in the surficial 10 cm. Thus P was efficiently preserved in both the freshwater and saline sediments.

P Burial Rates

To determine the quantity of PP that was so efficiently preserved by the sediments, we combined our findings of PP concentrations and sedimentation rates in the upper Patuxent River subestuary. Sedimentation rates for sites 3 – 7 were obtained from our ^{210}Pb-based measurements, which provided statistically significant results, and were corroborated by comparisons of the modern and archival maps, as well as findings of similar sedimentation rates in the Chesapeake Bay mesohaline regions (Cooper and Brush 1983, Cornwell et al. 1996, Zimmerman and Canuel 2000, O'Keefe 2007). The sedimentation rates obtained from ^{210}Pb measurements for sites 1 and 2 (1.4 to 3.4 cm yr^{-1} respectively) were not unusually high compared to other findings for tidal freshwater environments (Brush et al. 1982, Scatena 1987, Darke and Megonigal 2003). However, as indicated by the comparison of the modern and historical bathymetric maps, as well as other researchers, sedimentation rates in the freshwater reaches of estuaries can be especially complex and heterogeneous (e.g., Brush et al. 1982, O'Keefe 2007). Thus our sedimentation rates obtained from the sediment cores for sites 1 and 2 may not be representative of the greater tidal freshwater region of the Patuxent. Therefore, to quantify PP burial rates at sites 1 and 2 we used more conservative values (i.e., lower sedimentation rates) than the sedimentation rates we obtained from our ^{210}Pb dating. For site 1 we used a sedimentation rate of 0.5 cm yr^{-1} and a sediment accumulation value of 2.9 kg m^{-2} yr^{-1}, estimated by pollen analysis of sediment cores collected from the vicinity of our site 1 by Khan and Brush (1994); and for site 2, we averaged the rates for site 1 (from Khan and Brush, 1994) and site 3 (our data) for a mean sedimentation rate of 0.8

cm yr^{-1} and a mean sediment accumulation rate of 3.7 kg m^{-2} yr^{-1}. Even using the conservative sedimentation rates for sites 1 and 2, we found that the sediments of the upper Patuxent subestuary play a major role in sequestering phosphorus entering the river, with estimated PP accumulation rates that ranged from 4.9 to 8.4 g P m^{-2} yr^{-1} at sites 1 – 3, to 2.2 g P m^{-2} yr^{-1} at sites 6 and 7 (Table 2-1).

Our estimated PP burial rates for the subtidal sediments of the upper Patuxent subestuary are comparable, or higher, than estimated rates for tidal freshwater marshes, which are widely regarded as important traps for sediments and nutrients (e.g., Mitsch and Gosselink 2000). Estimates of PP trapping by freshwater marshes along the Patuxent River include rates of 0.4 – 2.4 g P m^{-2} yr^{-1} in marshes adjacent to site 1 (Khan and Brush 1994), and 2.3 – 4.3 g P m^{-2} yr^{-1} in marshes adjacent to sites 1 – 5 (Merrill 1999, Greene 2005, Boynton et al. 2008). Our PP burial rates are also mostly higher than P accumulation rates for continental margins, which have been recognized as keys sites for P burial flux (e.g., Berner 1982, Ruttenberg and Berner 1993), and range from 0.03 to 2.5 g P m^{-2} yr^{-1} (Filippelli 1997).

Table 2-1. P burial rates for subtidal and marsh areas of the upper Patuxent subestuary

Study site(s)	Site 1	Site 2	Site 3	Sites 4 and 5 [a]	Sites 6 and 7 [a]
Subtidal areas					
Sedimentation rate (cm yr^{-1})	0.5 [b]	0.8 [c]	1.1	0.7	0.6
Sediment accumulation rate (kg m^{-2} yr^{-1})	2.9 [b]	3.7 [c]	4.4 $\pm$ 0.9 [d]	2.9 $\pm$ 0.9 [d]	2.4 $\pm$ 0.1 [d]
P concentration (g PP kg^{-1})	1.7	2.1	1.9	1.2	0.9
Subtidal P burial rates (g m^{-2} yr^{-1})	4.9	7.8	8.4 $\pm$ 1.7	3.5 $\pm$ 1.1	2.2 $\pm$ 0.09
Subtidal area (km^2)	2.5	3.2	2.2	13.6	12.5
Subtidal P burial (kg x 10^4 yr^{-1})	1.2	2.5	1.8 $\pm$ 0.4	4.7 $\pm$ 1.5	2.7 $\pm$ 0.1
Marsh areas					
Sediment accumulation [e] rate (kg m^{-2} yr^{-1})	2.1	2.1	2.1	2.1	2.1
P concentration (g PP kg^{-1})	1.1 [e]	1.1 [e]	1.1 [e]	1.1 [e]	1.1 [e]
Marsh P burial rates (g m^{-2} yr^{-1})	2.3 [e]	2.3 [e]	2.3 [e]	2.3 [e]	1.3 [e]
Marsh area (km^2)	4.7	4.4	4.6	2.6	2
Marsh P burial (kg x 10^4 yr^{-1})	1.1	1.0	1.1	0.6	0.3

[a] Values for sites 4 and 5 as well as 6 and 7 are grouped together by arithmetic means;
[b] Sedimentation rates and mass accumulation rates for site 1 are from Khan and Brush (1994);
[c] Sedimentation rates and mass accumulation rates for site 2 are mean values of sites 1 and 3;
[d] Standard errors given are from regression coefficients from the ^{210}Pb calculations;
[e] Marsh data are from Boynton et al. (2008)

P burial by the subtidal and marsh sediments

We compared our results of PP burial in the subtidal sediments to PP burial rates in the marshes adjacent to our sites. Our findings suggest that 12.9 x 10^4 kg P yr^{-1} is being retained by the subtidal sediments in the upper Patuxent subestuary (Table 2-1). Using PP burial rates compiled for the marshes of the Patuxent by Boynton et al. (2008), we estimated that the marshes adjacent to our study sites retained an estimated 4.1 x 10^4 kg P yr^{-1} (Table 2-1). Thus an estimated total of 17 x 10^4 kg P yr^{-1} is retained by burial in the upper Patuxent subestuary (Table 2-1 and Fig. 2-8). Of this total, the subtidal sediments played a dominant role in sequestering P, retaining 76% of the total P buried in the upper Patuxent subestuary. Our estimates support those of Boynton et al. (2008), who found that 30% of the long term P burial in the upper Patuxent subestuary is retained by marshes and 70% by the surficial subtidal areas. It is interesting to note that even in the fresher regions of our study (sites 1 – 3), where the marshes are almost twice as extensive as the subtidal areas, subtidal P burial exceeds marsh P burial (Fig. 2-8). In the more saline reaches (sites 4 – 7), the amount of P sequestered by burial is more than 8 times the amount sequestered by marshes; this is mainly because the subtidal area is more extensive than the marshes fringing this area. However, we also found P burial rates to be higher in the more saline subtidal areas than in the saline tidal marshes.

P budget for the Patuxent

Total P inputs to the Patuxent have been estimated to be 21 – 31 x 10^4 kg P yr^{-1} (Jordan et al. 2003, Boynton et al. 2008). These estimates are not substantially larger

than our estimates of 17 x 10^4 kg P yr^{-1} retained in the upper Patuxent subestuary, indicating that most of the P delivered from the watershed is retained through long-term burial in the sediments of the upper Patuxent subestuary. Thus we estimate that only 4 – 14 x 10^4 kg P yr^{-1} is exported further down the subestuary. Furthermore, the majority of the P sequestration is occurring in the subtidal sediments as opposed to the marsh sediments (Fig. 2-8). Therefore it seems clear that subtidal sediments provide an important role for sequestering the majority of P entering the Patuxent.

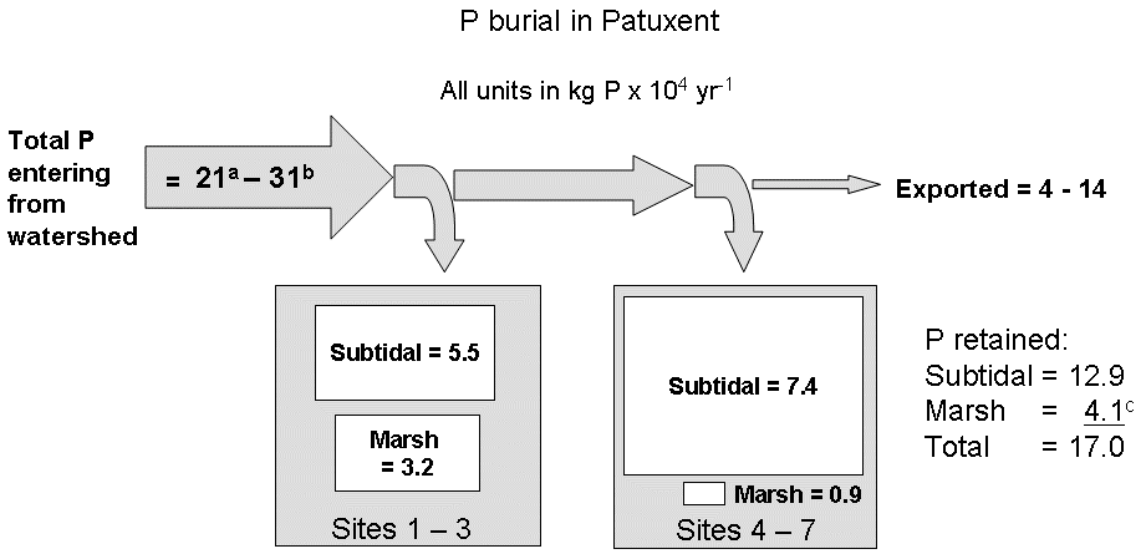

Fig 2-8. Schematic of P burial in the Patuxent.
[a] TP entering watershed from Boynton et al. (2008);
[b] TP entering watershed from Jordan et al. (2003);
[c] Marsh burial rates are from Boynton et al. (2008).

Other studies have also found that subtidal sediments in estuaries play a larger role in trapping PP than tidal marshes (Jordan et al. 1986, Correll et al. 1992, Boynton et al. 2008). There may be several reasons that subtidal sediments can play a dominant role in sequestering P. For one, sediment accumulation rates may be constrained in marshes because they are under water for less time than the subtidal areas. Additionally, in order for marshes to be sustained for long periods of time, sediment accretion rates cannot vary substantially from local relative sea-rise (Mitsch and Gosselink 2000). The organic-rich soils of the Patuxent marshes may also have less phosphorus per gram of sediment than the subtidal sediments. For example, reported PP concentrations in Patuxent freshwater marshes range from 10 to 42 μmol g^{-1} of dry sediment (Khan and Brush 1994, Merrill 1999, Greene 2005, Boynton et al. 2008) compared to our findings of 55 – 69 μmol g^{-1} of dry sediment in the freshwater subtidal sediments.

In spite of the efficient sequestration of PP by the sediments, we were unable to relate the downcore patterns of PP in our sediments to historical land-use patterns in the Patuxent watershed. Land clearing for agricultural and timber uses in the Patuxent watershed began in the 1600s and 1700s. By the mid-1800s land clearing had intensified to the point that 85% of the forest had been cut down and the majority of the land was used for farming (D'Elia et al. 2003). Erosion caused by the land-clearing and agriculture activities can increase sediment input (Brush and Davis 1984), but not necessarily alter PP concentrations in the sediments. While land-use changes that increase sedimentation may not alter PP concentrations in the sediments, there has been a 20-fold increase in the

population of the Patuxent River watershed since the 1960s, resulting in increased nutrient loadings from sewage (D'Elia et al. 2003). Maryland banned phosphate detergents in 1984, resulting in a 50% reduction of P loading to the Patuxent by 1985-1986, coupled with another 50% reduction in P loads to the estuary through continuing improvements to wastewater treatment methods in the 1990s (Lung and Bai 2003). These two public policy actions helped reduce point sources of phosphorus loading to the Patuxent in the 1980s and 1990s. Although non-point sources of P are now the largest inputs of P to the Patuxent, reductions in point sources have reduced total P loading to the Patuxent since the mid-1980s (Boynton et al. 2008). We could speculate that the high P loading from sewage effluent in the later half of the 20th century may be reflected in the high concentrations of PP in our three freshest sites. However, the peaks and fluctuations of historical loadings do not correspond to downcore PP patterns in our sediments. For example, the lower concentrations of PP and Fe-P in the lower half of sites 1, 3 and one of the site 2 cores (Fig. 2-2) can not be explained by fluctuations in historical P loading patterns. Low concentrations of PP were observed at sediment depths of 50-60 cm in the site 1 core, which would correspond to about 1958-1968 (if our dating estimates are reliable), not a time of reduced nutrient loading to the Patuxent (D'Elia et al. 2003). The lower concentrations of PP in lower half of the site 2 core correspond to approximately 1979, also not a time of reduced P input. Historical trends of P loading were also not apparent in the cores from sites 3-7, even though the chronology of these cores was preserved (Fig. 2-6). Other researchers have reported that historical patterns of P enrichment were not detectable in mesohaline sediment profiles (Cornwell et al. 1996,

O'Keefe 2007). It appears that the sediment P record is not very reflective of watershed loading at our sites. Instead, the depth patterns of PP and Fe-P in our cores are more similar to the depth patterns of CDB extractable Fe (Figs. 2-2 and 2-5), indicating that the amount of CDB-Fe in the sediments had a greater control over the depth profiles of PP in our cores. Perhaps high P loading from wastewater treatment plants, which is mostly in the form of dissolved inorganic P, may be rapidly sorbed onto sediments or taken up by algae, and thus detectable only in the immediate vicinity of the discharge. Localized high PP concentrations in suspended and surficial sediments near sewage outfalls have been observed near municipal outputs in Philadelphia (Lebo 1991) and Washington D.C. (Callendar 1982). Alternatively, since WWTP discharges are mainly in the bioavailable form of dissolved PO_4^{3-}, perhaps the PO_4^{3-} is repeatedly cycled in the water column and is carried away and dispersed downstream.

The chemical forms of PP retained in the sediments

Although Fe-P and org-P are considered potentially bioavailable forms of PP (Ruttenberg and Berner 1993, Jensen et al. 1995, Anschutz et al. 1998), both were quantitatively important and persistent sinks for P in the sediments of the Patuxent subestuary. CDB extractable Fe is normally attributed to Fe-oxides (Ruttenberg 1992, Kostka and Luther 1994, Slomp et al. 1996b), but we have no direct evidence that the Fe-P in our sediments is bound to Fe oxides. The Fe-P persisted well below the oxic surficial sediments, as evidenced by the presence of methane bubbles in the freshwater cores, sulfate depletion in the saltwater cores, and the absence of Fe(III) extractable in

our sediments below 20 cm (Chapter 5). CDB can extract non-targeted compounds such as labile polyphosphates (Jensen and Thamdrup 1993), pyrite (Slomp et al. 1996b), acid volatile sulfides and mixed valence Fe minerals such as magnetite (Kostka and Luther 1994), and ferrous phosphate minerals such as vivianite (Williams et al. 1980). Thus it is possible that the Fe-P in our sediments is bound to something other than Fe oxides, such as ferrous Fe minerals.

Although the presence of ferrous phosphate minerals, such as vivianite, is normally interpreted as evidence of freshwater environments (Postma 1982, Hearn et al. 1983), vivianite precipitation has been suggested in a few marine environments. For example, vivianite precipitation may occur deep enough in sediments that pore water sulfide has been depleted (Martens et al. 1978). In iron-rich marine environments, such as the Amazon delta, ferrous Fe produced by Fe oxide reduction can exceed the supply of sulfides, leaving excess Fe(II) available for ferrous phosphate mineral precipitation below depths of ferrous sulfide mineral formation (Aller et al. 1986, Burns 1997). While pyrite formation has been reported in the sediments of our study sites in the Patuxent, relatively low degree of pyritization (DOP) values have been found (mean DOP values of <0.40, even in the most saline sites) (O'Keefe 2007, Chapter 5). These DOP values imply that pyrite formation is not iron-limited in our sediments (Raiswell et al. 1988). Therefore, most of the Fe(II) is not associated with sulfides and may be available to form ferrous phosphates after sulfide depletion with depth in the sediments.

Org-P concentrations did not decline with depth in the sediments and were quantitatively the second most important sink for PP in the Patuxent. While some researchers have found that org-P declines with depth in sediments (e.g., Ruttenberg and Berner 1993, Louchouarn et al. 1997, Cha et al. 2005), other studies have observed no declines with depth or declines only in the surficial oxidized layer of sediments (Slomp et al. 1996a, van der Zee et al. 2002). It is possible that the org-P fraction in our sediments is in a form that is biologically unavailable, such as in the form of diesters or phosphonates, that have been shown to accumulate as P sinks in anaerobic sediments (Carman et al. 2000, Reitzel et al. 2007). The burial efficiency of organic carbon has been correlated to the length of time exposed to oxygen in sediment pore waters (Hartnett et al. 1998). Perhaps the high sedimentation rates in the Patuxent limit the time which organic matter is exposed to the oxidized surface layers of the sediments, thus enhancing the preservation of org-P. Additional research is required to determine the form of the buried org-P, as well as the buried Fe-P, in our sediments.

Although many researchers have found evidence of authigenic CFA formation in marine sediments (e.g., Ruttenberg and Berner 1993, Slomp et al. 1996a, Louchouarn et al. 1997), we did not find evidence of diagenetic redistribution or "sink switching" from org-P or Fe-P to CFA in the Patuxent subestuary. There are several lines of evidence that indicate that CFA is not forming at the expense of org-P and Fe-P in our sediments. For one, Fe-P and org-P are persistent with depth in the sediments and thus it does not appear that org-P and Fe-P are releasing associated P with depth in the sediments to allow for

diagenetic sink switching. Additionally, concentrations of auth-P did not increase in our cores, except for at two of the fresher sites (i.e., sites 2 and 3) where there was a concurrent increase in the det-P fraction, suggesting that a change in the sediment source may be the cause of the increase in the apatite fractions at these sites.

Additionally, trends in pore water F^- and PO_4^{3-} did not provide support for the hypothesis of authigenic CFA formation in our sediments. If authigenic CFA is forming in our sediments, we should see an initial build-up of F^- and PO_4^{3-} in our pore waters at or below the redox boundary, as these solutes are released from Fe oxides, followed by a decrease in these solutes with further burial below the redox boundary as CFA precipitates (e.g., Ruttenberg and Berner 1993). While there was an increase in PO_4^{3-} in the surficial 40 cm of the three most saline sites, depth trends below 40 cm were not apparent (Fig. 2-7). Furthermore, we did not see a trend in Fl^- pore water depth profiles.

Conclusions

The preservation of PP with depth in the sediments leads to efficient sequestration of P entering the Patuxent River subestuary. The sediments of the upper Patuxent subestuary sequester approximately 55 – 80% of the total phosphorus entering from the watershed, 76% of which is trapped by the subtidal sediments, with the remaining 24% buried in the marshes. Thus, the subtidal sediments of the Patuxent subestuary provide a quantitatively more important sink for P than the tidal marshes.

Despite the burial efficiency of PP in the subtidal sediments, historical trends of anthropogenic P loading to the Patuxent subestuary were not discernable. Depth profiles of PP in our cores are more closely correlated with the amount of CDB Fe in the sediments than to anthropogenic loading trends.

Fe-P was the largest sink for PP at all salinities and all depths. Fe-P concentrations declined along the salinity gradient, but nevertheless constituted the dominant fraction of PP at all depths in our saltwater sites. In spite of the importance of the Fe-P fraction in retaining PP in the Patuxent River sediments, the exact form of Fe-P remains unidentified. It is possible that limited availability of sulfides in our sediments is allowing the formation of ferrous phosphate minerals, even in our most saline sites. Thus, while we did not find evidence of sink switching from Fe-P or org-P to CFA, diagenetic redistribution from Fe-oxide bound P to ferrous phosphate minerals, or some other unidentified CDB extractable PP form, may be occurring in the Patuxent subestuary.

Additional research also needs to be conducted to compare phosphate retention among different estuaries and subestuaries. Subestuaries of the Chesapeake Bay may have unusually high P burial rates (e.g., see Nixon et al. 1996). Also, the Patuxent River subestuary may be exceptionally rich in Fe-P compared to other estuaries around the world, and the importance of Fe-P as a long-term sink for P may vary with location. Even within the Chesapeake Bay, the Patuxent may stand out as unusual; Jordan et al.

(1997) found Coastal Plain sediment inputs to be richer in P than those discharged from Piedmont watersheds within the Chesapeake Bay. Therefore, P retention may vary with regional watershed geology adding to the complexity and challenge of developing accurate global P budgets.

Chapter 3. The role of Fe in sequestering P in the sediments of four Chesapeake Bay subestuaries

Abstract

Determining the long-term fate of particulate phosphorus (PP) entering estuaries is essential for quantifying the global P cycle and mitigating the wide-spread problem of eutrophication. We used a sequential extraction technique to compare the form and amount of PP that is retained with burial in 1-meter long sediment cores collected from four Chesapeake Bay subestuaries with contrasting watershed land-use patterns and physiographic provinces: the Patuxent, Potomac, Choptank and Bush Rivers. Sediment cores were collected along a salinity gradient from tidal freshwater to a salinity of 1 in the Bush River, and from tidal freshwater to the mesohaline waters of the other three subestuaries. We found that citrate-dithionite-bicarbonate (CDB) extractable P was the most important fraction of PP in regulating P bioavailability in the sediments. We refer to this fraction as Fe-P because the CDB extraction targets P bound to iron oxyhydroxides, but CDB may dissolve other P compounds as well. In each subestuary Fe-P provided long-term P sinks in the freshwater sediments and 90% of the declines we observed in total PP concentrations with increased salinity were caused by declines in the Fe-P fraction. Fe-P concentrations also declined to near zero with depth in the most saline cores of the Potomac and Choptank indicating that Fe-P is not a long-term sink for P in the saline reaches of those rivers. However, in the Patuxent Fe-P persisted as the

largest PP fraction at all salinities and all depths in the sediments. Also in the Patuxent, CDB extractable Fe (CDB-Fe) concentrations were higher, and CDB-Fe:Fe-P ratios were lower, than in the other three subestuaries, indicating that CDB-Fe is more available to provide a long-term sink for P in the Patuxent. We did not find evidence that authigenic apatite-P was an important sink for P in any of the four subestuaries. Nor did we find compelling evidence that watershed physiographic province determined PP burial. With the exception of one site that receives wastewater effluent, historical trends of anthropogenic P loading were not discernable in the sediments. Instead, PP burial patterns followed patterns of CDB-Fe and Fe-P concentrations in the sediments. In spite of the apparent importance of Fe-P in controlling P sequestration in Chesapeake Bay sediments, its exact form remains unknown.

Introduction

Phosphorus (P) bioavailability can regulate primary production of the global oceans on a geologic time-scale (Tyrrell 1999) and contribute to eutrophication of estuaries and other water bodies around the world (e.g., Nixon 1995). As such, it is important to investigate processes that regulate P bioavailability. More than 90 percent of phosphorus transported by rivers to estuaries and coastal waters is in the form of particulates (Froelich 1988, Föllmi 1996); however, the fraction of particulate phosphorus (PP) that can become biologically available is not well known. Since burial in the sediments is the main mechanism for removing P from estuarine waters, understanding P sequestration by estuarine sediments is key to understanding global P cycling and for mitigating eutrophication.

The amount of P sequestered and buried by sediments is affected by the form of PP. PP can be loosely adsorbed as PO_4^{3-} to clay particles, or to Fe or Al hydroxides; bound as complexes to Fe or Al oxides; incorporated into calcareous or metallic minerals; or incorporated into organic compounds (Froelich 1988). Determining the form of PP requires a time-consuming serial digestion and extraction scheme (e.g., Ruttenberg 1992) that has rarely been applied in estuaries (exceptions include Jordan et al. 2008, Chapter 2); as a consequence there are uncertainties in estuarine P burial.

Adding to the complexity of estimating estuarine P burial is the fact that the amount and form of PP buried in estuarine sediments changes along the salinity gradient of estuaries. Freshwater sediments tend to be more efficient at sequestering P than saltwater sediments (Upchurch et al. 1974, Strom and Biggs 1982, Lebo and Sharp 1993, Sundareshwar and Morris 1999, Jordan et al. 2008). Decreases in sediment PP content with increased salinity may be related to observed decreases in Fe-bound P with increased salinity (e.g., Lebo and Sharp 1993, Jordan et al. 2008). In both freshwater and saltwater sediments, P bound to Fe oxides can be released during the process of sediment burial and the associated reductive dissolution of the Fe oxides. However, in freshwater sediments, the Fe(II) can diffuse upward to the aerobic surficial sediments, become re-oxidized, and bind PO_4^{3-}, thus preventing PO_4^{3-} from being released to the water column (Caraco et al. 1990, Chambers and Odum 1990). Fe(II) can also precipitate with PO_4^{3-} in freshwater sediments, forming ferrous phosphate minerals, such as vivianite (Postma 1982, Gächter and Müller 2003). In contrast to freshwater sediments, sulfides present in

saline sediments effectively decouple Fe-P interactions. Fe(II) readily binds with sulfides to form ferrous sulfides, making Fe less available to bind P in saline sediments. Therefore, the importance of Fe in sequestering P may be diminished in saltwater sediments. However, PO_4^{3-} released from reduced Fe oxides, or from the decomposition of organic matter, can set up the conditions suitable for the formation of authigenic carbonate fluorapatite (CFA) minerals, which are important sinks for P in marine environments (Ruttenberg and Berner 1993, Filippelli and Delaney 1996, Slomp et al. 1996a, Louchouarn et al. 1997, Cha et al. 2005). Thus, since salinity can affect P binding, the amount and chemical form of PP sequestered in the sediments for long-term burial may vary along the salinity gradient of estuaries.

In addition to changes along the salinity gradient, PP burial may also vary with the geology and land-use patterns of the estuarine watersheds. For example, the form of PP burial in rivers with carbonate-rich watersheds can differ from PP burial in noncarbonate environments (Paludan and Morris 1999, House 2003). Therefore, we may expect the form of P buried in the Potomac subestuary of the Chesapeake Bay, with a watershed which includes some carbonate-rich formations, to differ from the form of P buried in Chesapeake subestuaries that do not include carbonate rocks in their drainage basins. PP concentrations may also differ with physiographic province. In the Chesapeake Bay, sediment inputs from the Coastal Plain physiographic province were found to be richer in P than sediments discharged from the Piedmont (Jordan et al. 1997); thus P burial may differ between subestuaries in the Coastal Plain and Piedmont.

Agricultural and urban activities can also enrich waterways in N and P (Carpenter et al. 1998); thus P burial patterns may reflect P loading from anthropogenic activities.

In a previous study, we investigated the long-term fate of P entering the Patuxent River, a subestuary of the Chesapeake Bay. We used a sequential extraction method to quantify five different pools of PP, including organic-P, authigenic apatite P, and P extracted with citrate-dithionite bicarbonate (CDB) (Ruttenberg 1992). We refer to CDB extractable P as Fe-P because the CDB extraction targets P bound to iron oxyhydroxides, although CDB may dissolve other P compounds as well. We found that P cycling in the Patuxent River subestuary was dominated by Fe-P at all salinities and all depths in the sediments (Chapter 2). We also found no evidence that Fe-P or organic P were releasing associated PO_4^{3-} with depth to allow for the formation of authigenic apatite in the Patuxent. Additionally, despite the burial efficiency of PP in the sediments, historical trends of anthropogenic P loading to the Patuxent subestuary were not discernable. Instead, depth profiles of PP in our cores were more closely correlated with the amount of CDB extractable Fe (CDB-Fe) in the sediments than to anthropogenic loading trends, underscoring the potential importance of CDB-Fe in controlling P bioavailability in the Patuxent.

In contrast to our findings in the Patuxent, other researchers have found marine and coastal sediments to have limited capacity for Fe-bound P retention with burial (Sundby et al. 1992, Jensen et al. 1995, Anschutz et al. 1998). The persistence of Fe-P in

the Patuxent River motivated us to compare Chesapeake Bay subestuaries with differing watersheds to find out whether the Patuxent is unusual. As such, the objective of this study was to address the following questions: How does P retention in the sediments compare among Chesapeake Bay subestuaries? Does Fe-P provide a long-term sink for P in other Chesapeake Bay subestuaries besides the Patuxent? Is authigenic apatite formation an important mechanism for P removal in other Chesapeake Bay subestuaries? Does PP burial vary by physiographic province and land-use within the Chesapeake Bay?

Study Sites

We compared spatial and temporal patterns of phosphorus burial along the salinity gradient of four Chesapeake Bay subestuaries selected for contrasting watershed geology and land-use patterns, including the Patuxent River, the Potomac River, the Choptank River, and the Bush River. All rivers are in Maryland, USA with the locations shown in Fig. 3-1. A summary of the watershed characteristics, from the Chesapeake Bay Program Office's website (www.chesapeakebay.net) is given in Table 3-1.

The Patuxent watershed is located in a rapidly developing outer suburb of the metropolitan Washington, DC and Baltimore region. Land-use patterns include 11% urban development and 36% agricultural (Chesapeake Bay Program Office). The Patuxent watershed is predominantly in the Coastal Plain physiographic province of the western shore of the Chesapeake Bay, with a smaller percentage (28%) located in the Piedmont region.

The majority (55%) of the Potomac watershed is in the Appalachian physiographic province, which includes the carbonate-rich Valley and Ridge sub-province. The carbonate subunit covers a total of 15% of the Potomac River basin (Denis and Blomquist 1995). The Potomac has the most forested land of any of the watersheds we studied (60%) and the overall watershed is rural, with 5% urban development and 33% agricultural activities (Chesapeake Bay Program Office). However, the Potomac watershed also includes Washington, DC and the surrounding suburbs, contributing to a high population density in the tidal freshwater portion of this watershed.

The Choptank River watershed is located entirely within the Coastal Plain physiographic province on the eastern shore of the Chesapeake Bay, and is the most rural (3% urban) and agricultural watershed (54%) of our study sites (Chesapeake Bay Program Office).

The Bush River, located in the northwestern portion of the Bay, is south of the largest tributary to the Bay, the Susquehanna River. The majority (75 %) of the Bush watershed is located in the Piedmont, with a smaller portion (25 %) in the Coastal Plain (Pasternack et al. 2001). Similarly to the Patuxent, the Bush River watershed is undergoing rapid development as a suburb of the Washington DC and Baltimore metropolitan area; 10% of the watershed is urban and 31% is agricultural (Chesapeake Bay Program Office).

Table 3-1. Characteristics of the watersheds of the four subestuaries (Chesapeake Bay Program Office): watershed area (10^3 km^2); percentages of developed land; agricultural land, forested land, and wetlands; human population density per km^2; and % physiographic province (A = Appalachian, P = Piedmont, C = Coastal Plain).

Subestuary	Area 10^3 km^2	% urban	% agric.	% forested	% wetland	Pop. km^{-2}	Physio.
Patuxent	2.4	11	36	45	6	246	C (72%) P (28%)
Potomac	36.5	5	33	60	1	142	A (55%) P (19%) C (26%)
Choptank	2	3	54	25	19	42	C (100%)
Bush	0.2	10	31	45	12	187	P (~75 %) C (~25 %)

Methods

Sediment and pore water collection

During multiple cruises in 2005 and 2006, we collected a total of 26 sediment cores from the four different rivers. A summary of the coordinates of the sampling locations is given in Appendix A, and the approximate locations are shown in Fig. 2-1. We used a piston-corer to collect sediment cores of approximately one-meter in depth. Refer to Chapter 2 for details on the coring process. All cores were sampled in tidal waters. Cores were collected along salinity ranges of 0 – 11 in the Patuxent, 0 – 10 in the Choptank, 0 – 6 in the Potomac, and 0 – 1 in the Bush; and from water depths ranging from 1 – 5 m in the Patuxent, 3 – 7 m in the Choptank, 1 – 4 m in the Potomac and 0.5 to 2 m in the Bush. We were unable to access the more saline reaches of the Bush River because of U.S. military restrictions.

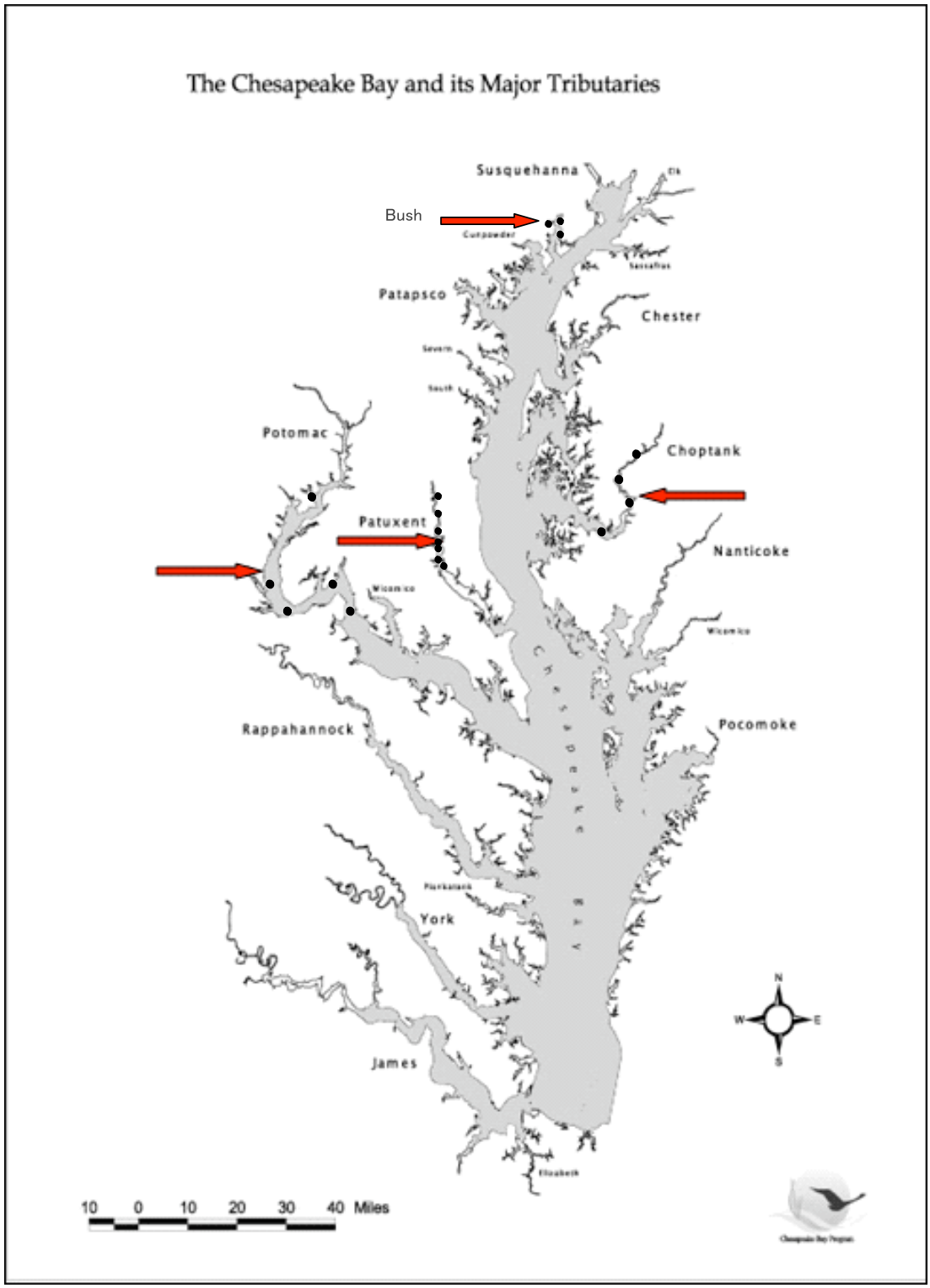

Fig. 3-1. Map of the Chesapeake Bay and the four subestuaries and approximate sampling locations

All sediment cores were sectioned at 5-cm intervals under a nitrogen glove bag within 1-5 days of collection. Refer to Chapter 2 for details of the sectioning process.

Pore water was collected from intervals of every 10-20 cm of the sediment samples using the procedure outlined in Chapter 2. The pH of the pore water sample was measured with a Fisher Scientific Accumet model 910 pH meter and subsequently divided into four separate aliquots for analyses. One aliquot was acidified and stored at 4°C for analysis of dissolved Fe, Al, Ca, Mn, Si and P. One aliquot was frozen until analysis for dissolved phosphate (PO_4^{3-}). Another aliquot was frozen until analysis of dissolved ammonium (NH_4^+) (used in a different study). The remaining pore water was frozen until analysis of dissolved anions (SO_4^{2-}, Cl^-, and F^-).

Extraction of particulate P

The freeze-dried and ground sediments were sequentially extracted using the SEDEX method (Ruttenberg 1992). SEDEX is a widely used extraction scheme that operationally defines five separate fractions of PP that were sequentially extracted in the following order: 1) 1 M $MgCl_2$ at pH 8 was used to extract loosely sorbed P (which we will refer to as "sorb-P"); 2) citrate-dithionite-bicarbonate (CDB) was used to dissolve metal oxide bound P, such as Fe and Mn oxide bound-P (which we will refer to as "Fe-P"); 3) Na-acetate solution at pH 4 was used to dissolve authigenic carbonate fluorapatite (CFA) + biogenic apatite + $CaCO_3$-associated P ("auth-P"); 4) 1 M HCl was used to dissolve detrital apatite P ("det-P"); and 5) 2 M HCl was used to extract organic P ("org-

P") from the residual sediment that had been ashed at 550°C after treatment with $Mg(NO_3)_2$. Although the extractants may dissolve non-targeted forms of PP, we will refer to the extracts by abbreviations based on their targeted PP form. All of the SEDEX extractions, except for the organic P step, were performed in sealed 250 ml polycarbonate filter funnels (Nalgene DS0310-4000) fitted with 0.2 μm Nucleopore filters. The filter funnels and Nucleopore filters were cleaned with dilute H_2SO_4 and rinsed twice with deionized water before 0.4 g of dried and ground sediment was measured onto the filters.

Analytical methods

Except for the CDB extract, the concentrations of dissolved PO_4^{3-} from all of the SEDEX extracts and the filtered pore water were quantified using an ascorbic acid, molybdate colorimetric method (Eaton et al. 1995). The concentrations of total P, Fe, Mn, Ca, Si and Al in the CDB extracts and the pore water were measured using a Perkin Elmer Optima model 3000 Inductively Coupled Plasma, Optical Emission Spectrometer. Pore water SO_4^{2-}, Cl^-, and F^- concentrations were measured with a Dionex model 4000 ion chromatograph.

Sediment characterization

Before sectioning under nitrogen, the cores were characterized by visual examinations of color, using Munsell color charts. Evidence of biotic activity, methane bubbles and hydrogen sulfide odors were also noted. Fine-grained sediments were required for successful operation of the piston corer; therefore a basic assessment of

sediment grain size was assessed tactilely in the field to ensure that the sediments were fine-grained. The sand content from one freshwater core and one saline core from each river was also assessed by sieving wet sediment through a 63 μm sieve after dispersal of the sediments with sodium hexametaphosphate.

^{210}Pb Dating

Sedimentation rates were determined using ^{210}Pb radiometric dating. We measured ^{210}Pb activity in 17 of our cores, one for each site except for site 4 on the Potomac, and site 2 on the Bush River. The activity of ^{210}Pb ($T_{½}$ = 22.3 yrs) in the sediments was determined by measuring the activity of ^{210}Po ($T_{½}$ = 138 days), an alpha-emitting daughter. Samples were stored for several ^{210}Po half-lives to ensure secular equilibrium between the two nucleotides. A ^{208}Po standard tracer was added to the sediments to determine yield efficiency. ^{210}Po in the sediments was extracted using concentrated HCl and HNO_3 at 80 – 90^{o}C. Sedimentation rates in cm yr^{-1} and sediment accumulation rates in g m^{-2} yr^{-1} were calculated following the procedure described in Cornwell et al. (1996). Surficial sediments that showed little to no change in unsupported ^{210}Pb activity (i.e., ^{210}Pb activity above background levels) with depth were assumed to be in the mixing zone and were not used in the calculations. Samples with ^{210}Pb activity levels less than 2 disintegrations per minute (dpm) were also not used in the calculations, as these samples were assumed to be from depths in the sediments where excess ^{210}Pb has completely decayed.

Results

Variability of PP fractions

Total PP

Total PP declined with increased salinity in all three subestuaries where we were able to sample into mesohaline waters (Fig. 3-2). In the Patuxent, mean values of total PP concentrations for the entire length of the core(s) were highest at site 2 at 69 μmol g^{-1}, and declined to a low of 28 μmol g^{-1} at site 7, for a decline of 41 μmol g^{-1} or 59% with increased salinity. The Patuxent stands out as having the highest concentrations of PP at all salinities (Fig. 3-2). Mean total PP concentrations were lower in the freshwater sites of the Potomac and Choptank Rivers than the freshwater Patuxent sites; and the percentage of decline in total PP along the salinity gradient was also more pronounced in the Potomac and Choptank Rivers than in the Patuxent. In the Potomac River, mean total PP concentrations declined from a high of 41 μmol g^{-1} at site 1, to a low of 12 μmol g^{-1} at site 4, for a decline of 29 μmol g^{-1} or 71%. In the Choptank River, mean total PP concentrations declined from a high of 38 μmol g^{-1} at site 1, to a low of 10 μmol g^{-1} at site 3, for a decline of 28 μmol g^{-1} or 74%. In the Bush River, we were not able to sample across the salinity gradient; however, the Bush River is notable for having the lowest concentrations of total PP in the freshwater sites of any of the four rivers (Fig. 3-2).

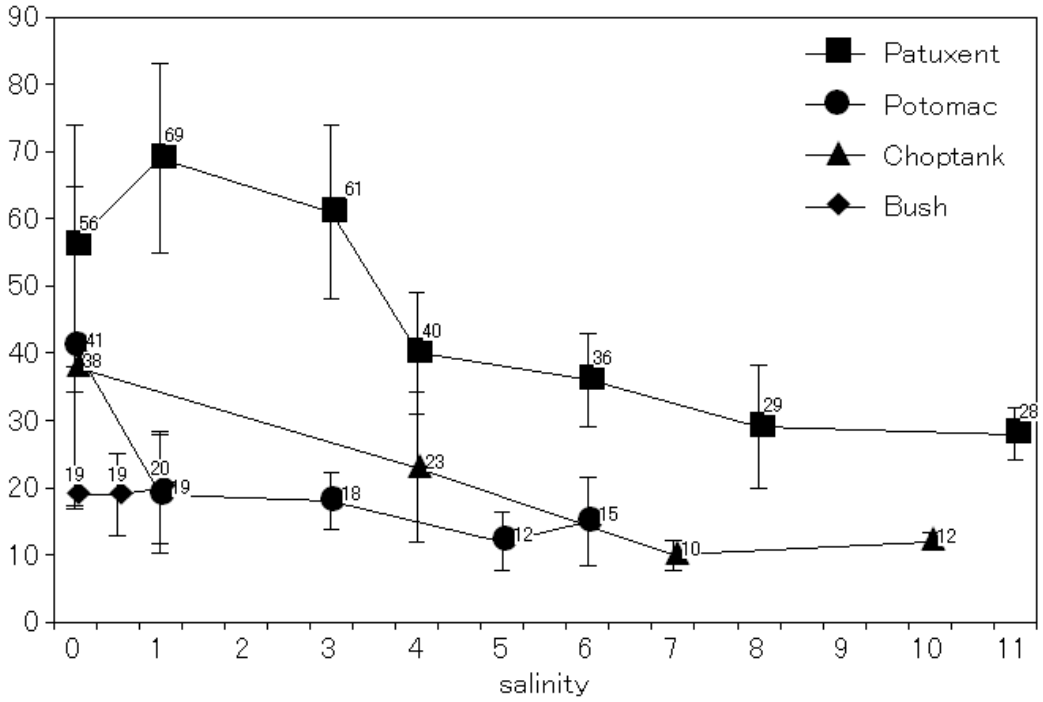

Fig. 3-2. Mean values of PP concentrations for the entire core length along the salinity gradient of the four subestuaries.

Fe-P trends

Fe-P was the most dynamic PP fraction in all four subestuaries. Declines in Fe-P with increased salinity accounted for 90% of the declines observed in total PP along the salinity gradient. Trends in the Fe-P fraction also drove the trends in total PP with the depths in the sediments of all four subestuaries. In the freshwater reaches of all four subestuaries, Fe-P was the dominant fraction for the upper half, or entire length, of the sediment cores (Chapter 2 and Fig. 3-3). In contrast to the freshwater sediments, Fe-P retention with depth in the saline sediments differed among the subestuaries. In the Patuxent, Fe-P was the dominant fraction at all sediment depths and all salinities.

However, Fe-P concentrations declined to near zero with depth in the most saline cores of the Choptank and the Potomac (Fig. 3-3).

Org-P trends

Org-P was quantitatively the largest fraction in the deeper sections of the more saline cores of the Potomac and Choptank as well as in the deeper halves of the Bush sites 2 and 3 cores (Fig. 3-3). In contrast, org-P was the second most abundant PP fraction at almost all depths and all salinities in the Patuxent (Chapter 2). Org-P declined with depth in the sediments of the Potomac, Choptank and Bush subestuaries, especially in the upper 10 cm of the sediments (Fig. 3-4). Depth trends in org-P were not clear in the Patuxent (Fig. 3-4). Org-P showed no clear trends with salinity changes in any of the four subestuaries.

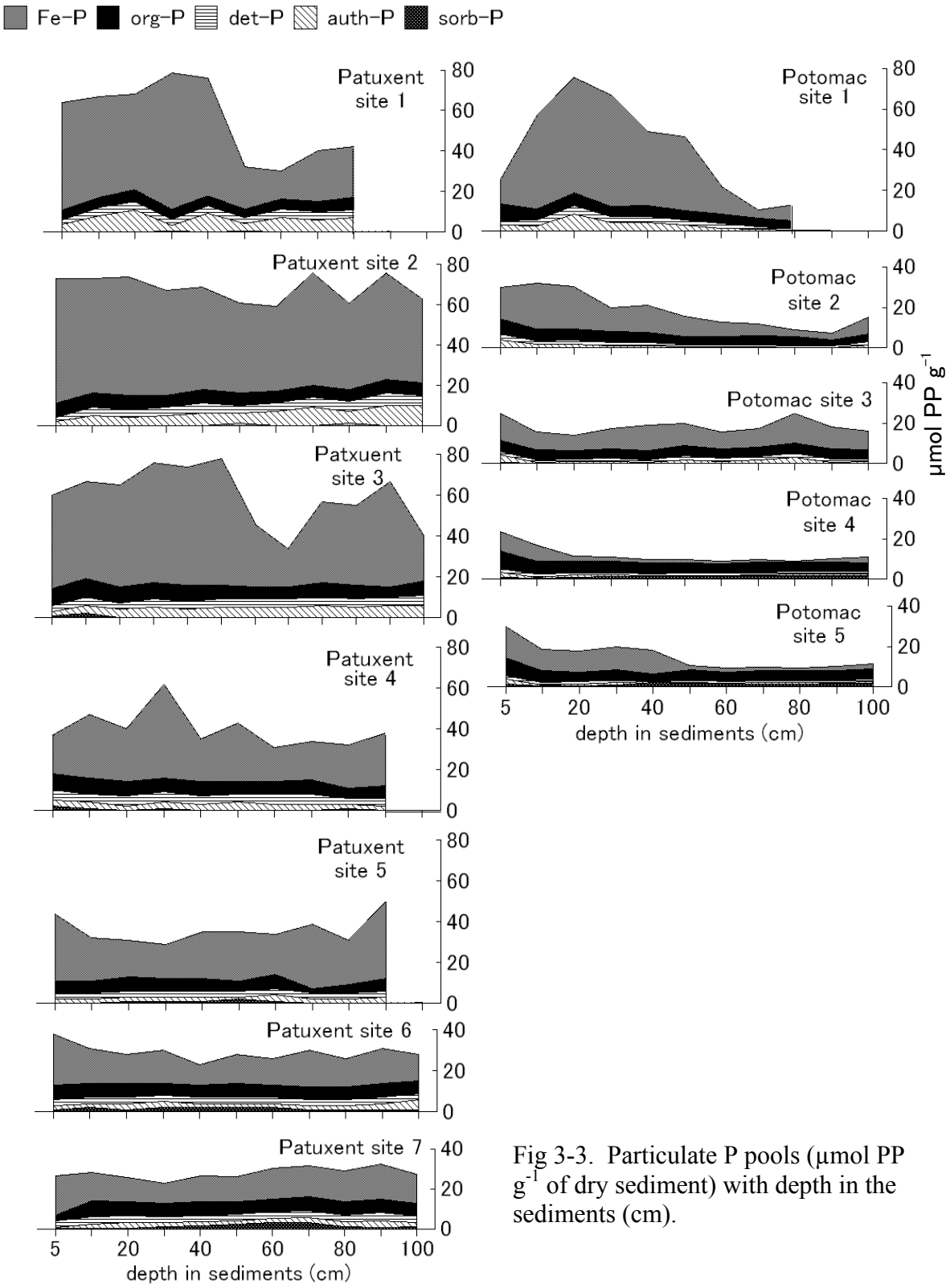

Fig 3-3. Particulate P pools (μmol PP g^{-1} of dry sediment) with depth in the sediments (cm).

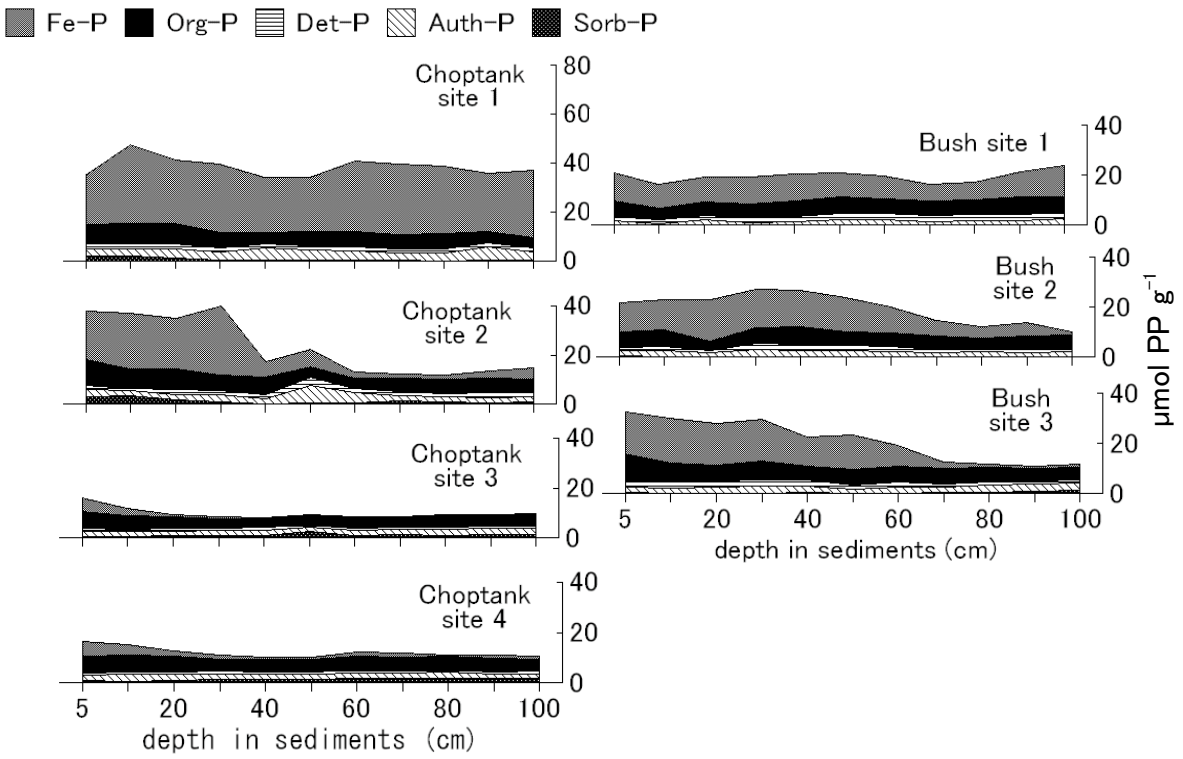

Fig 3-3. Particulate P pools (μmol PP g^{-1} of dry sediment) with depth in the sediments (cm).

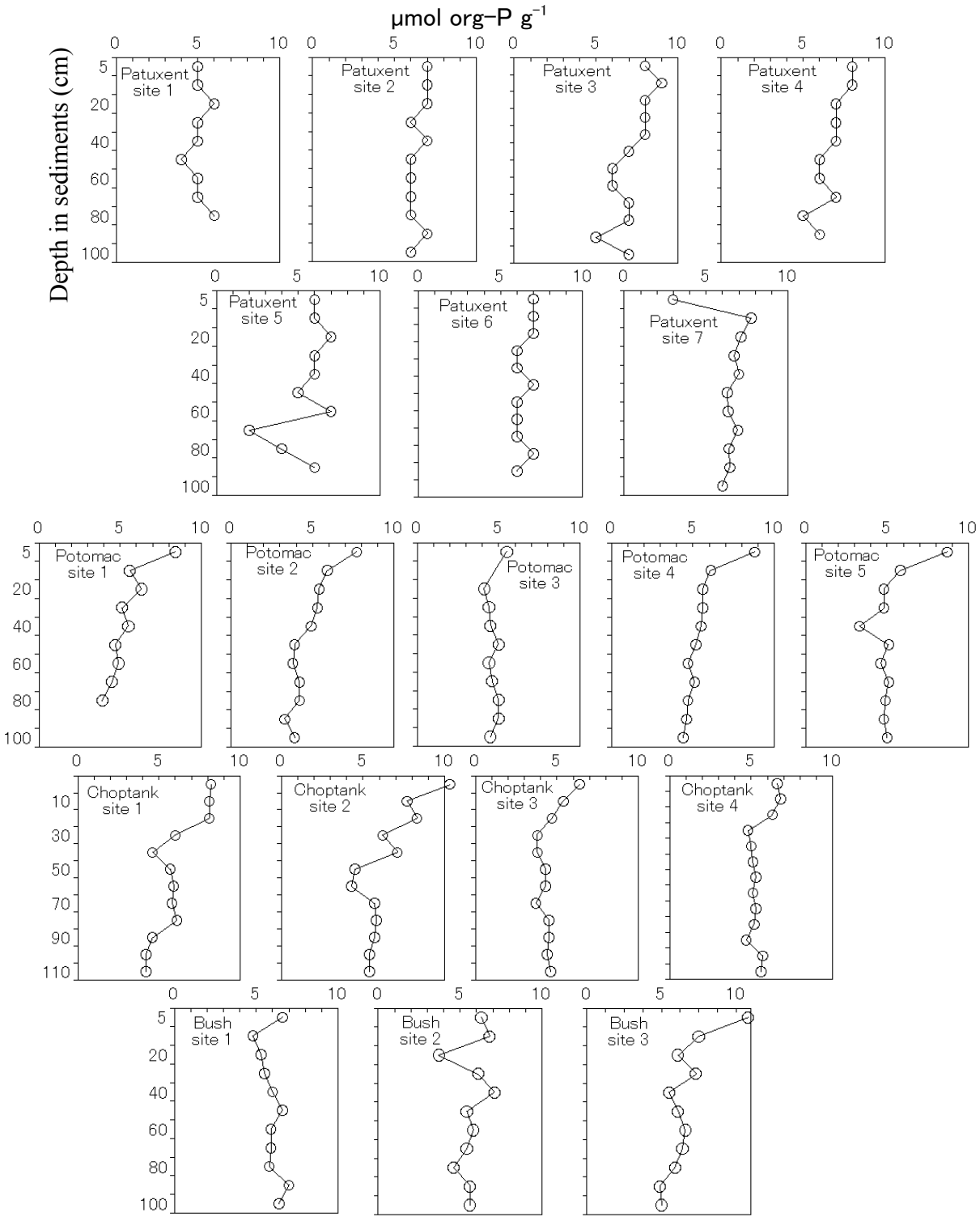

Fig. 3-4. Organic P with depth in sediments

Auth-P and Det-P trends

Auth-P and det-P declined with increased salinity in the sediments of the Patuxent, Potomac and Choptank subestuaries. Trends in auth-P and det-P with depth in the sediments were not consistent. Auth-P and det-P increased slightly with depth in the sediments of some of the freshwater cores, but in most of the cores, no depth trend was found. In all four subestuaries, depth trend patterns in auth-P and det-P were similar to each other (Fig. 3-3).

Sorb-P trends

Sorb-P increased in concentration with salinity in all three rivers with salinity gradients. However, the concentrations remained low even in the most saline sites ($\leq$ 4 μmol P g^{-1} dry sediment) and there were no clear trends in sorb-P concentrations with depth in the sediments (Fig. 3-3).

CDB extractable Fe (CDB-Fe) trends

Although CDB can extract other compounds besides ferric Fe minerals, trends in Fe extracted by the CDB (i.e., CDB-Fe) mirrored trends in the total PP and Fe-P fractions in the sediments of all four subestuaries. CDB-Fe was correlated to Fe-P in the sediments of all four subestuaries ($R^2 \geq 0.72$, $p < 0.001$). One notable exception is site 1 of the Potomac, which receives effluent from a wastewater treatment plant; at that site a peak in PP was not correlated to a peak in CDB-Fe (Figs. 3-3 and 3-5).

Similarly to trends in total PP and Fe-P, there was a general trend of decreased CDB-Fe with increased salinity in all three subestuaries where we were able to sample across the salinity gradient (Fig. 3-5). In general, CDB-Fe concentrations in the Patuxent were higher at all salinity levels than CDB-Fe concentrations in the other three rivers (Fig. 3-5). CDB-Fe decreased in the deeper half of some of the freshwater cores (i.e., Patuxent sites 1 and 3, and one of the site 2 cores, Potomac sites 1 and 2, and Bush sites 2 and 3) following similar trends in total PP and Fe-P in those cores. CDB-Fe was also more persistent with depth in the saline sediments of the Patuxent, whereas CDB-Fe declined with depth in the saline sediments of the Choptank and the Potomac subestuaries (Fig. 3-5).

Ratios of CDB-Fe:Fe-P were directly proportional to salinity in all four subestuaries, establishing a trend between these variables. CDB-Fe:Fe-P ratios increased with depth in the sediments in all of the subestuaries except for the Patuxent. The magnitudes of the CDB-Fe:Fe-P ratios were the smallest in the Patuxent River relative to the other rivers (Fig. 3-6). CDB-Fe:Fe-P ratios ranged from 5.3 - 22.8 in the Patuxent; 5.5 – 195.8 in the Potomac; 7.2 – 195.8 in the Choptank; and 11.1 – 70.3 in the Bush.

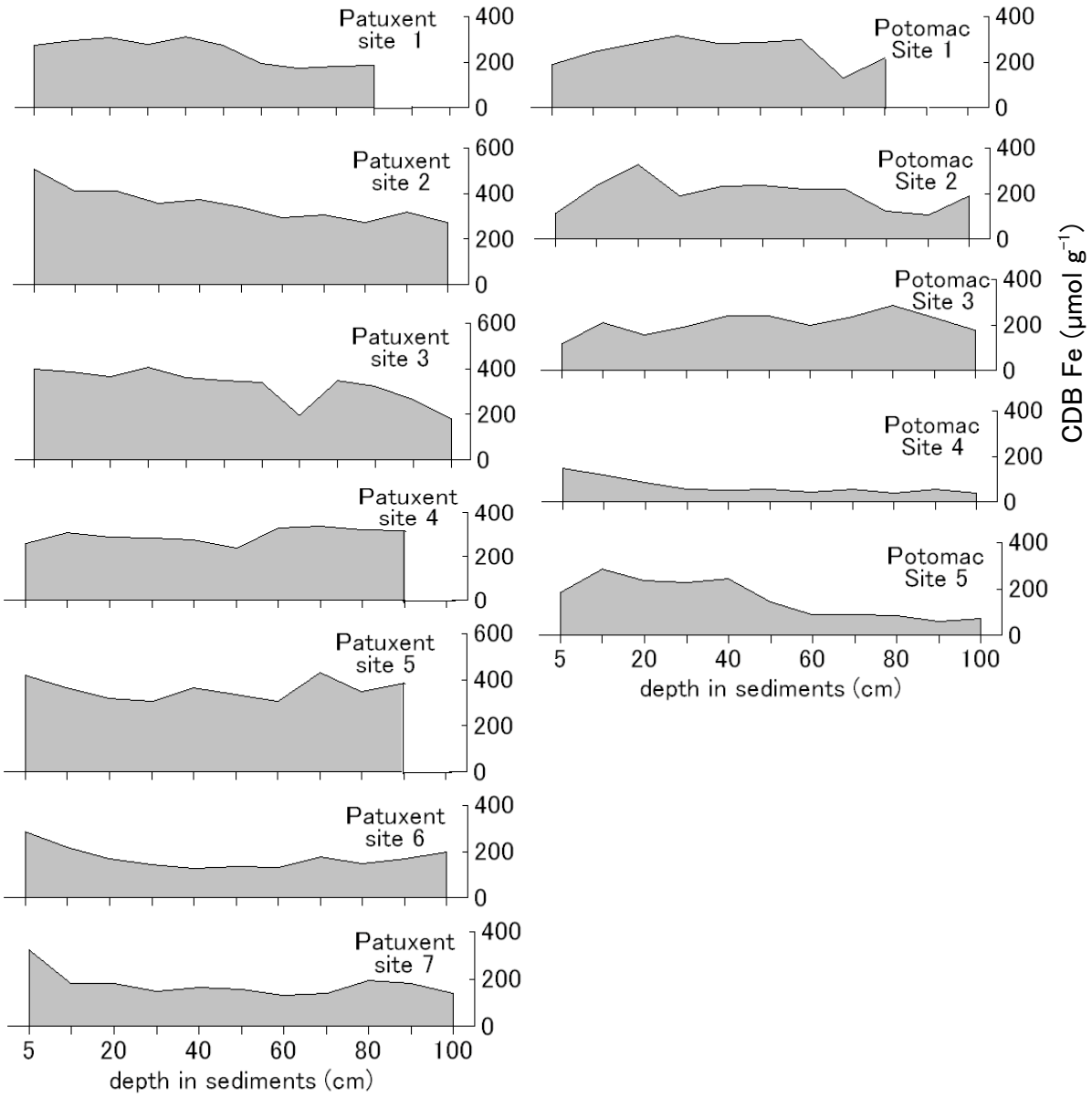

Fig 3-5. CDB extractable Fe (µmol g^{-1}) with depth in sediments (cm).

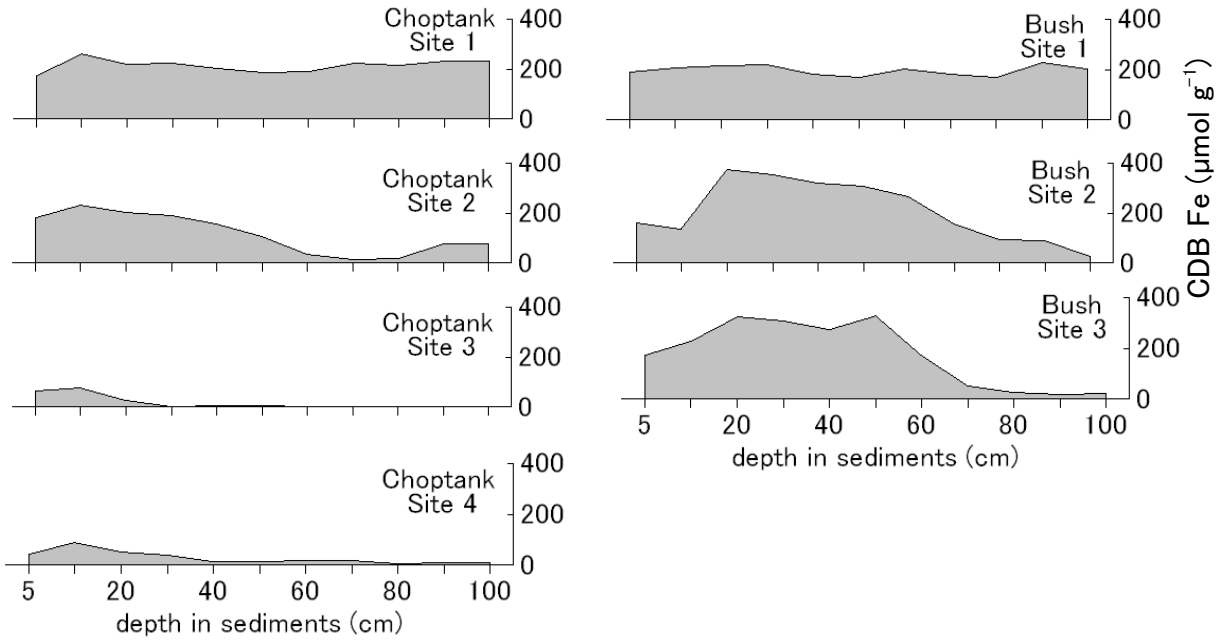

Fig 3-5 (continued). CDB extractable Fe (µmol g^{-1}) with depth in sediments (cm).

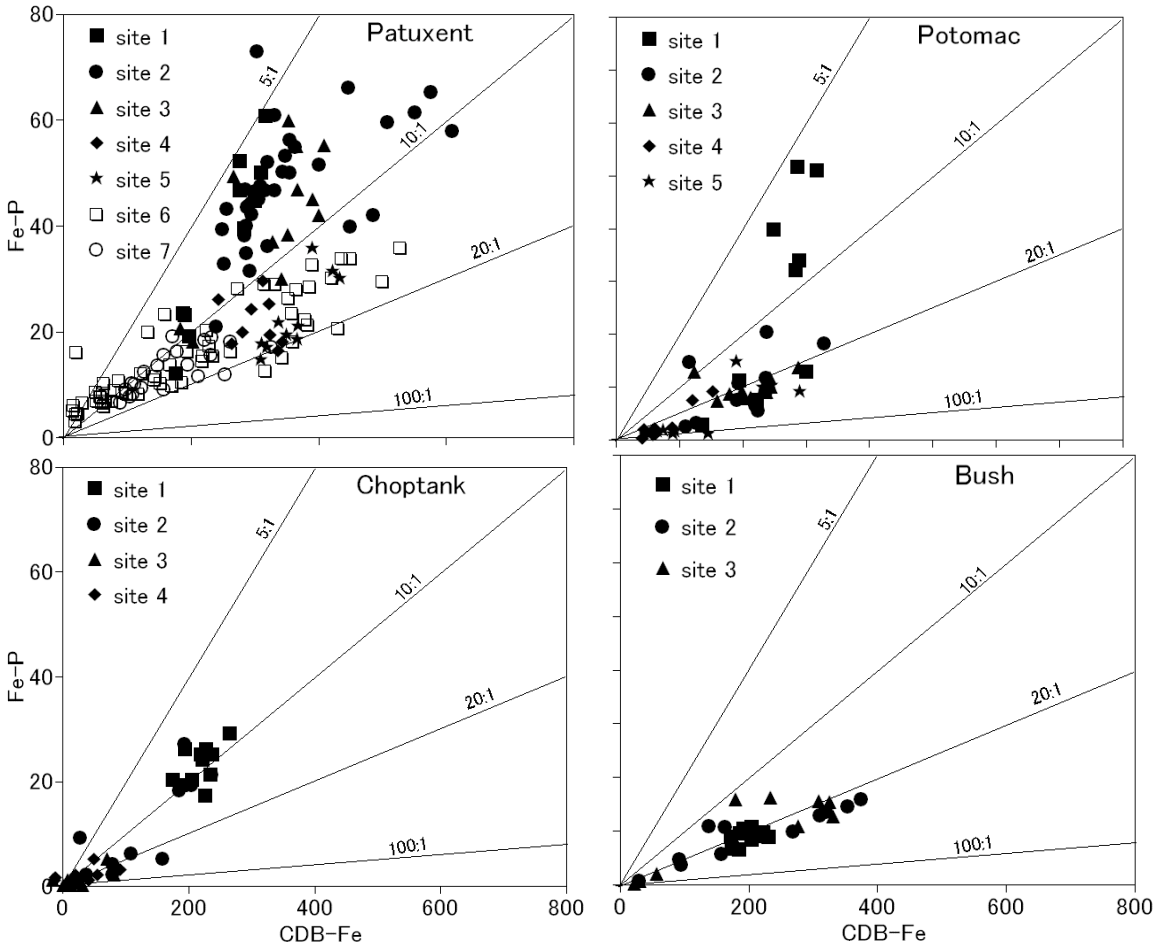

Fig. 3-6. CDB extractable P (Fe-P) and Fe (CDB-Fe) by site

Sediment characterization

The sediments were fairly uniform in grain size, with ≥ 92% of the sediment < 63 μm in size, except for one sample (Bush River site 1, 10 cm in depth) in which 85% of the sediment grains were < 63 μm in size. Trends in sediment texture with depth or salinity were not noted, and no correlation between phosphorus concentrations the proportion of fine-grained sediment was found. All of the cores had a distinctly colored oxidized surficial layer of sediment on the top which generally extended from 0 to 5-10 cm in depth in the sediments. This oxidized surficial layer matched an increase in total PP and Fe-P concentrations in the saline sites, but did not correspond to changes in Fe-P or PP concentrations in the freshwater cores. Worm burrows of depths of up to 5-10 cm in the freshwater cores and 15-30 cm in the saline sediments were not found to correlate to any changes in PP fractions with depth.

^{210}Pb Dating

In general, the cores in the more saline reaches of each river had lower sedimentation rates than the cores collected from the fresher portions of the rivers (Table 3-3). The relationship between excess ^{210}Pb activity and depth in the sediments was not statistically significant ($p > 0.05$) at five of our sites (Patuxent site 1, Potomac sites 3 and 5, Choptank site 3, and Bush site 1), indicating non-steady-state sediment deposition or vertical mixing at those sites (Fig. 3-7). Taking into consideration just the cores with statistically significant results, the apparent sedimentation rates ranged from 0.6 to 3.4 cm yr^{-1} in the freshwater (salinities of 0-1) sites and 0.5 to 1.1 cm yr^{-1} in the more saline sites

(Table 3-2). Sediment accumulation rates ranged from 2.6 to 14.0 kg m^{-2} yr^{-1} in the freshwater sites and 2.0 to 4.4 kg m^{-2} yr^{-1} in the more saline sites.

Table 3-2. A summary of the ^{210}Pb results and the data used to calculate P burial rates in the four subestuaries.

Location	Estimated Sedimentation rate (cm yr^{-1}) (range of values)	Estimated sediment accumulation rate (kg m^{-2} yr^{-1}) (range of values)	P concentration in sediments (g kg^{-1})	P burial rates (g m^{-2} yr^{-1})	Linear regression model
Patuxent					
Site 1	1.3 (1.0 – 2.0)	7.4 (5.5 – 11.1)	1.7	12.6	$R^2 = 0.75$ p = 0.06 n = 5
Site 2	3.4 (3.0 – 3.9)	14.0 (12.7 – 16.2)	2.1	29.4	$R^2 = 0.95$ p = 0.001 n = 6
Site 3	1.1 (0.9 – 1.3)	4.4 (3.7 – 5.5)	1.9	8.4	$R^2 = 0.93$ p = 0.03 n = 4
Site 4	0.45 (0.4 – 0.5)	2.0 (1.7 – 2.3)	1.2	2.4	$R^2 = 0.94$ p = 0.006 n = 5
Site 5	0.85 (0.7 – 1.1)	3.8 (3.2 – 4.7)	1.1	4.2	$R^2 = 0.90$ p = 0.01 n = 5
Site 6	0.5 (0.5 – 0.6)	2.3 (2.0 – 2.7)	0.9	2.1	$R^2 = 0.94$ p = 0.006 n = 5
Site 7	0.6 (0.5 – 0.8)	2.5 (2.0 – 3.3)	0.9	2.3	$R^2 = 0.91$ p = 0.003 n = 6

Location	Estimated Sedimentation rate (cm yr^{-1}) (range of values)	Estimated sediment accumulation rate (kg m^{-2} yr^{-1}) (range of values)	P concentration in sediments (g kg^{-1})	P burial rates (g m^{-2} yr^{-1})	Linear regression model
Potomac					
Site 1	1.6 (1.3 – 2.1)	9.1 (7.4 – 11.9)	1.3	11.8	$R^2 = 0.71$ p = 0.007 n = 6
Site 2	0.6 (0.5 – 0.8)	3.5 (2.9 – 4.6)	0.6	2.1	$R^2 = 0.91$ p = 0.05 n = 4
Site 3	1.5 (0.5 – 1.8)	8.2 (2.9 – 10.1)	0.6	4.9	$R^2 = 0.23$ p = 0.68 n = 3
Site 4	Not analyzed	Not analyzed	0.4	----	----
Site 5	0.8 (0.5 – 1.2)	4.2 (3.1 – 6.9)	0.5	2.1	$R^2 = 0.77$ p = 0.12 n = 4
Choptank					
Site 1	1.8 (1.6 – 2.0)	7.4 (6.7 – 8.2)	1.2	8.9	$R^2 = 0.93$ p < 0.001 n = 9
Site 2	1.1 (0.8 – 1.6)	4.2 (3.2 – 6.1)	0.7	2.9	$R^2 = 0.84$ p = 0.08 n = 4
Site 3	0.4 (0.3 – 0.7)	2.1 (1.5 – 3.3)	0.3	0.6	$R^2 = 0.88$ p = 0.22 n = 3
Site 4	0.6 (0.5 – 0.8)	3.2 (2.6 – 4.1)	0.4	1.3	$R^2 = 0.91$ p = 0.04 n = 4
Bush					
Site 1	0.6 (0.3 – 4.0?)	3.8 (1.8 – 24.5)	0.6	2.3	$R^2 = 0.27$ p = 0.48 n = 4
Site 2	Not analyzed	Not analyzed	0.7	-----	-----
Site 3	0.6 (0.5 – 0.6)	2.6 (2.4 – 2.9)	0.7	1.8	$R^2 = 0.98$ p = 0.01 n = 4

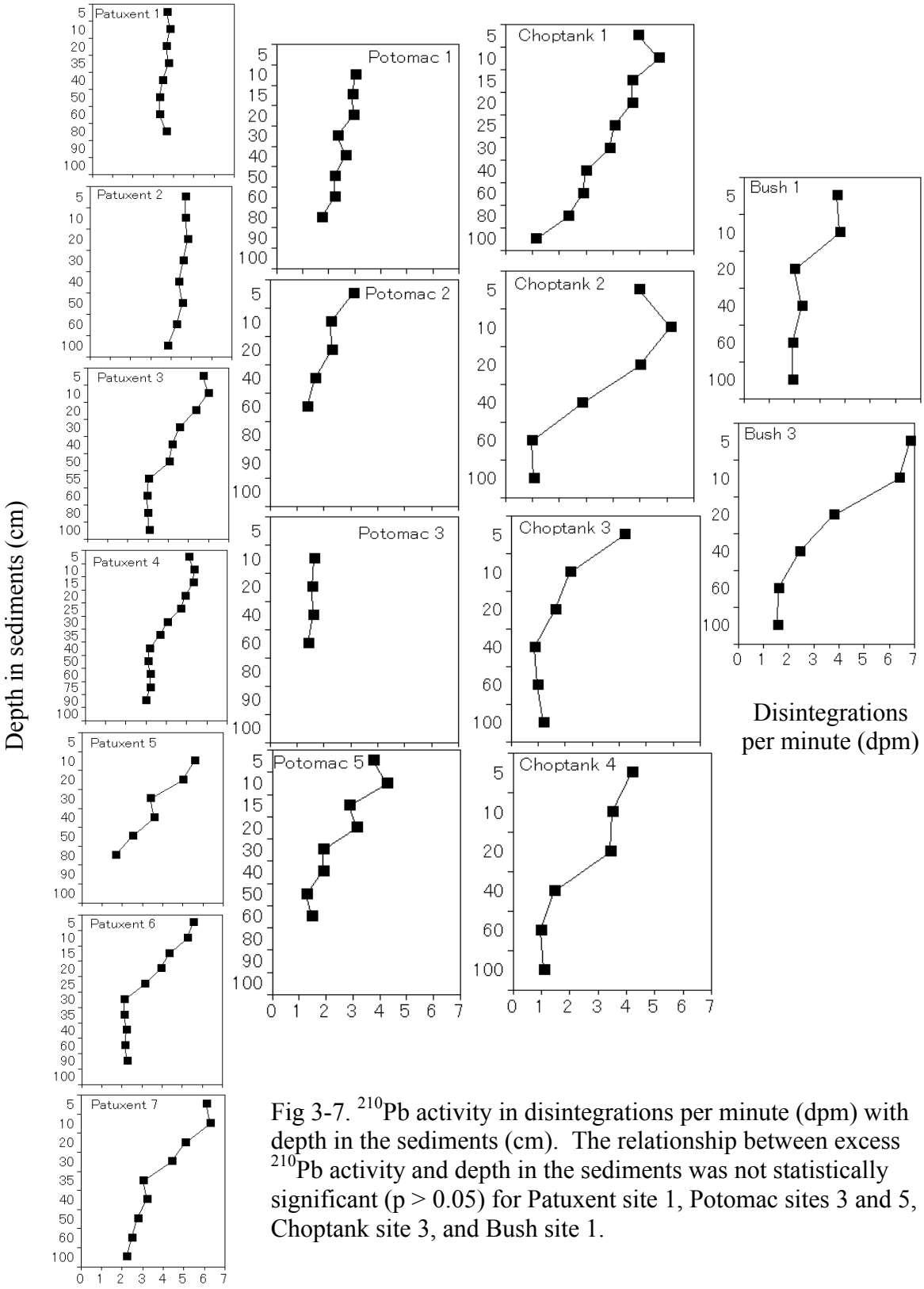

Fig 3-7. ^{210}Pb activity in disintegrations per minute (dpm) with depth in the sediments (cm). The relationship between excess ^{210}Pb activity and depth in the sediments was not statistically significant ($p > 0.05$) for Patuxent site 1, Potomac sites 3 and 5, Choptank site 3, and Bush site 1.

Discussion

The role of Fe-P in sequestering P

Our data suggest that Fe played a dominant role in regulating P sequestration in the sediments of all four subestuaries. Fe-P trends with depth in the sediments controlled total PP depth trends, and in all three subestuaries where we were able to sample across the salinity gradient, declines in the Fe-P fraction accounted for 90% of the decline in total PP with increased salinity.

Other researchers have also found declines in Fe-P concentrations with increased salinity (Strom and Biggs 1982, Froelich 1988, Sundareshwar and Morris 1999, Jordan et al. 2008) that may be related to Fe-P-S interactions that can occur in more saline sediments, rendering iron unavailable for P sequestration (Caraco et al. 1989, Roden and Edmonds 1997, Rozan et al. 2002, Gächter and Müller 2003). Additionally, it has been shown that sulfides enhance the reduction of Fe(III) to Fe(II) (e.g., Afonso and Stumm 1992). Thus, one would expect that Fe-P would not be as important in providing a long-term sink for PP in saline sediments, which is consistent with our findings for the Potomac and Choptank subestuaries, where Fe-P concentrations declined to near zero in the deepest portions of the cores (Fig. 3-3). The Patuxent subestuary stands out as exceptionally rich in total PP and Fe-P among the rivers investigated in this study, and possibly among estuarine and marine sediments around the world (Table 3-3). While it should be noted that few studies of estuarine PP include sediments from the freshwater segments, which is where we found the highest concentrations of Fe-P and total P, the

Patuxent is also exceptionally rich in Fe-P in the saline sediments. High Fe-P concentrations have been found in a few saline sediments such as in the Northern Baltic Sea where oxygen conditions fluctuated and salinity ranged from 4 – 7 (Virtasalo et al. 2005) and marine sediments with extensive bioturbation (Louchouarn et al. 1997); however, compared to most other marine and estuarine sediments, Fe-P concentrations in the saline sediments of the Patuxent stand out as exceptionally high (Table 3-3).

Table 3-3. Approximate mid-range concentrations of SEDEX P forms (μmol g^{-1}) in sediments from various locations. Sorb-P and Fe-P are combined because several studies used methods that combined the two forms. The five highest concentrations for each P form are shown in bold. Concentrations that represent >50% of total P are underlined. Table adapted from T. Jordan, unpublished.

	Fe-P sorb-P	auth-P	det-P	org-P	total
Patuxent River Estuary, this study					
Freshwater, sites 1-3	**<u>49.00</u>**	6.00	4.00	6.00	**65.00**
Saline water, sites 4-7	**<u>19.50</u>**	2.00	3.50	6.00	31.00
Potomac River Estuary, this study					
Freshwater, sites 1-2	**<u>23.00</u>**	2.00	2.00	5.00	31.00
Saline water, sites 3-5	6.00	1.00	1.00	5.00	13.00
Choptank River Estuary, this study					
Freshwater, site 1	**<u>27.00</u>**	4.00	2.00	6.00	38.00
Saline water, sites 2-4	4.00	2.00	1.00	5.00	13.00
Bush River Estuary, this study					
Freshwater, sites 1-3	<u>11.00</u>	2.00	2.00	6.00	21.00
Northern Baltic Sea, Virtasalo et al. (2005) (salinity ranged from 4-7)					
oxic	6.60	3.50	**16.00**	**19.00**	**45.00**
suboxic	**21.00**	9.10	**20.00**	**24.00**	**74.00**
anoxic	5.50	3.70	**16.00**	**24.00**	**49.00**
Gulf of St. Lawrence, Louchouarn et al. (1997)					
sta 19	4.00	11.50	6.50	3.00	25.00
sta 36	2.50	**13.50**	7.50	4.00	27.50
sta 1	5.50	**11.00**	4.50	4.00	25.00
sta 16	15.00	**14.00**	**10.50**	4.50	**44.00**
sta 106	5.00	9.50	5.00	3.00	22.50

Sacramento-San Joaquin Delta, Nilsen and Delaney (2005) (mostly freshwater)					
Sherman Is.	2.58	2.64	1.00	0.78	7.00
Frack's Track	6.40	2.40	6.00	1.20	16.00
Mandelville Slough	14.26	4.60	2.00	4.14	25.00
Potato Slough	14.00	6.50	**9.00**	4.50	34.00
Consumnes River	13.76	10.24	8.00	8.00	40.00
Arabian Sea, Schenau and DeLange (2001)					
500-100m Oxygen minimum	6.95	**13.50**	3.70	7.85	32.00
1200-2000m	5.65	7.00	4.00	5.40	22.05
3000-4000m	5.75	8.00	4.40	4.60	22.75
Berner et al. (1993)					
Mississipppi Delta	6.06	6.06	3.24	6.27	21.63
Amazon Delta	8.02	3.84	1.05	4.53	17.43
Long Island Sound	0.76	5.52	8.95	3.81	19.05
Equatorial Atlantic	5.54	**12.34**	0.25	6.80	25.18
Black Sea	5.12	3.94	2.17	8.47	19.69
NE Atlantic margin, van der Zee et al. (2002)					
depositional shelf 113m	5.00	1.75	4.60	8.00	19.35
slope 1387m	5.50	3.00	3.75	7.00	19.25
shelf 396m	3.00	3.25	4.50	6.50	17.25
depositional canyon 3097m	7.50	2.30	3.50	**9.50**	22.80
SW Japan Sea, Cha et al. (2005)					
basin	2.00	5.00	2.00	**10.00**	19.00
lower margin	4.50	4.00	2.00	8.50	19.00
upper margin	3.50	4.00	1.50	6.00	15.00
Faul et al. (2005)					
N. California (10BC)	1.10	6.80	6.80	5.00	19.60
N. California (01BC)	2.80	6.90	7.40	6.70	23.70
Equatorial Pacific (TT)	0.67	6.60	0.13	0.95	8.40
Equatorial Pacific (BN)	0.88	8.40	0.32	1.40	10.90
Filippelli and Delaney (1996)					
E. Equatorial Pacific	2.13	9.00	0.12	0.98	12.23
W. Equatorial Pacific	1.11	7.08	0.06	0.55	8.80
E. Mediterranean Sea, Slomp et al. (2004)					
above sapropel layer	6.95	5.54	1.75	3.81	18.05
within sapropel layer	7.89	12.06	1.54	5.43	26.91
Liu et al. (2004)					
Bohai sea	1.25	2.50	8.50	3.95	16.20
Yellow sea	0.85	0.75	7.50	3.35	12.45
Tamburini et al. (2002)					
N. Atlantic	5.00	6.10	0.97	2.10	14.20
Slomp et al. (1996)					
N. Atlantic	3.25	3.25	3.00	3.25	12.75

Since concentrations of CBD-Fe were higher in the Patuxent than in the other rivers (Fig. 3-5), it is possible that the amount of Fe(II) in the reduced sediments exceeded the supply of sulfides in the Patuxent subestuary, leaving excess Fe(II) available for ferrous phosphate mineral precipitation. Ferrous phosphate formation has been found in the iron-rich marine environment of the Amazon Delta below depths in the sediments where sulfate has been exhausted (Aller et al. 1986, Burns 1997). It is also possible that the Fe in the Patuxent is in a form that is more readily available to bind P than in the other rivers. For example, Fe minerals that persist in saltwater sediments can be more crystalline and less able to sorb P than more poorly crystalline, and more easily reducible, iron species that can be found in freshwater sediments (Slomp et al. 1996b, Hyacinthe and Van Cappellen 2004, Hartzell et al. 2008). The lower ratios of CDB-Fe and Fe-P in the Patuxent than the other rivers (Fig. 3-6) indicate that the Fe in the sediments of the Potomac, Choptank and Bush subestuaries is less available for binding P. Perhaps a greater proportion of the CDB-Fe in the Potomac, Choptank and Bush Rivers is in a form unavailable to bind P, such as in the form of FeS, than in the Patuxent (Slomp et al. 1996b). Fe-P burial may be function of the relative abundance of Fe and S in the sediments. Additional research would be required to determine how Fe and sulfide minerals may differ between the rivers and how this affects P burial.

The role of org-P in sequestering P

Org-P declined with depth in the sediments of the Potomac, Choptank and Bush subestuaries, but not in the Patuxent. In spite of this decline in most of the sediment

cores, enough org-P persisted to provide one of the largest sinks for PP in the sediments of all four of the subestuaries, especially in the deeper sediments of the more saline sites, indicating that the majority of the org-P is refractory. While some researchers have reported declines in org-P that continued to depths of up to 300 cm in the sediments (Ruttenberg and Berner 1993), other studies have noted that org-P either decreases only in the surficial sediments (Slomp et al. 1996a) or declines only slightly with depth (van der Zee et al. 2002, Cha et al. 2005). The variability in org-P preservation with depth in the different subestuaries may be an indication of different forms of organic P at different locations. For example, organic polyphosphates are a labile form of organic P that can become enriched in P during oxic conditions and depleted in P with the onset of anoxic conditions that may occur with sediment burial or oxygen-depleted bottom waters (Khoshmanesh et al. 2002). In contrast, some forms of organic P such as diesters and phosphonates may be biologically unavailable and accumulate as P sinks in anaerobic sediments (Carman et al. 2000, Reitzel et al. 2007).

Lack of evidence of carbonate fluorapatite (CFA) formation

Despite the decline in Fe-P and org-P with depth in the sediments of the Potomac, Choptank, and Bush subestuaries, we did not find compelling evidence for the diagenetic redistribution of Fe-P and org-P to authigenic CFA in any of the subestuaries. In some of our freshwater cores, auth-P did increase slightly with depth in the sediments (e.g., Patuxent site 2, Bush site 1 and Choptank site 1), which could indicate authigenic CFA formation. However, the pore water solute profiles at these sites did not provide support

for the hypothesis of CFA formation. That is, we did not see an initial build-up of F^- and PO_4^{3-} at or below the redox boundary, followed by a decrease in these solutes with further burial below the redox boundary, which would indicate CFA precipitation. The auth-P fraction does extract biogenic apatite (e.g., apatite in the form of fish bones, scales or teeth), and P associated with $CaCO_3$, thus an increase in auth-P in some of our freshwater sites does not necessarily indicate the diagenetic formation of CFA. Since the geochemically refractory det-P fraction also increased with depth in the freshwater sediments where we saw auth-P increases, a change in sediment source is likely responsible for downcore changes in both apatite fractions.

PP burial patterns with land-use and physiographic province

Land-Use

One core, collected at Potomac site 1, seemed to reflect historical trends in P loading. Potomac site 1 is located in an embayment (Gunston Cove) that has been receiving effluent from a wastewater treatment plant (WWTP) since 1970. There was a peak in P loading in the mid-1970s followed by a sharp decrease in P loading in the late 1970s and early 1980s as the WWTP was upgraded to remove phosphates (Fig. 3-8). PP patterns in the sediment core collected from this site also depict a sharp peak in PP concentrations followed by a decline in PP concentrations with the more recent sediments (Fig. 3-3). Our dating calculations indicate that the PP peak at 20 cm would correspond to approximately 1989, which is later than the mid-1970s period of peak loading (Fig. 3-8). Still, the similarities in the down-core PP patterns and the WWTP loading data are

intriguing (Fig. 3-8). Given the inherent uncertainty in radiometric dating data (Brush et al. 1982), it is possible that our ^{210}Pb calculations have overestimated the dates of the sediments in Gunston Cove. Alternatively, bioturbation or physical mixing may have altered the position of the peak P loading in the sediment core, or the high P loading in the 1970s may have diffused up in the sediments and accumulated around 20 cm in depth. Another possibility for the time difference in peak loading profiles is that algae and submerged aquatic vegetation within Gunston Cove may have recycled the wastewater P for several years before it was deposited in the sediments. This possibility is supported by the observation that there was a 10-15 year lag period between a reduction in phosphorus loading from the WWTP and a phytoplankton decline in Gunston Cove (Jones et al. 2007).

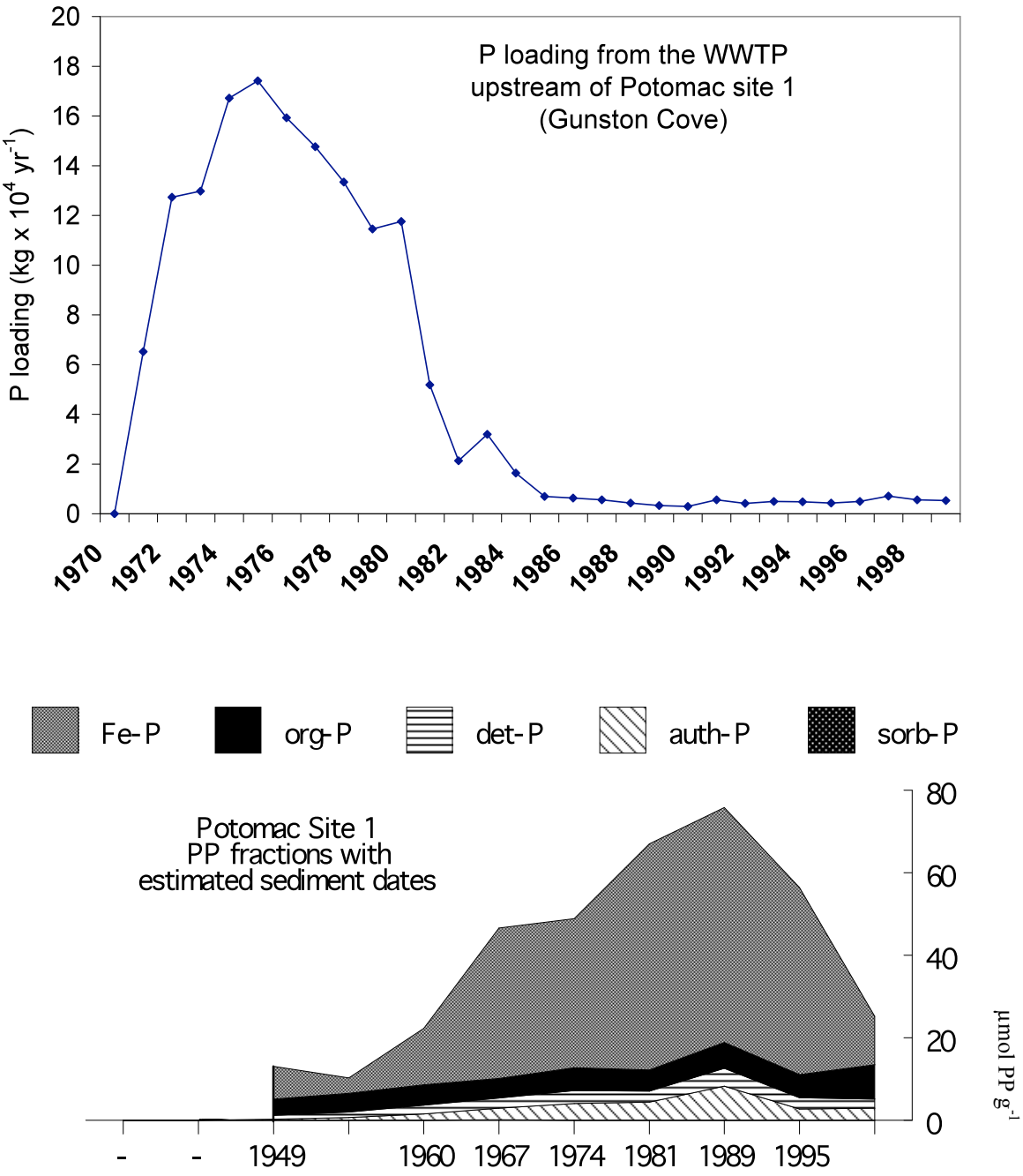

Fig. 3-8. Top figure: P loading (kg x 10^4 yr^{-1}) from the Noman Cole wastewater treatment plant, which is located upstream from Potomac site 1. Loading data are from the year the plant began operations (1970) until 1998. Bottom figure: PP fractions in sediment core collected at Potomac site 1. Dates estimated from ^{210}Pb activity are given on the x-axis; concentrations of PP are given on the y-axis in units of μmol g^{-1} of dry sediment

Besides Potomac 1, we were unable to clearly relate depth patterns of PP in our cores to historical P loading patterns in any of the other sites. Instead, in the other sediment cores we saw either patterns of little change in PP concentrations with depth, or depth patterns that reflected CDB-Fe concentration patterns. Other researchers have also reported that historical patterns of P enrichment were not detectable in sediment profiles (Cornwell et al. 1996, O'Keefe 2007). There may be several reasons that historical P loading patterns may not be discernable in the sediment record. Although increased development and agriculture have been shown to increase P loading to estuaries (e.g., Jordan et al. 2003), much of this increased P loading may be in the form of PP caused by increased sediment loading. For example, Jordan et al. (1997a, b, c) found variations in P discharge among different watersheds was related to concentrations of suspended particles. While increased sedimentation may increase PP loading, this would not necessarily alter PP concentrations patterns in the sediment cores.

In contrast to PP loading from sedimentation, P loading from WWTPs is mainly in the form of bioavailable dissolved PO_4^{3-}. Perhaps historical patterns of WWTP P loading were detectable only in the immediate vicinity of a sewage outfall in our sediments because the dissolved PO_4^{3-} is rapidly sorbed onto sediments or taken up by algae. Localized high PP concentrations in sediments near sewage outfalls have been observed by other researchers. For example, PP concentrations of 140-250 μmol g^{-1} have been found in the suspended sediments near municipal inputs from Philadelphia (Lebo 1991); whereas 20-60 km downriver from Philadelphia, sediment phosphorus levels

declined to 70 μmol g^{-1}. In the surficial sediments of the Potomac River, P concentrations of 150 μmol g^{-1} were found in the sediments near the Blue Plains WWTP of Washington D.C., while 10-20 km downstream PP concentrations ranged from 15 – 60 μmol g^{-1} (Callendar 1982). The sediment record from the Potomac 1 core suggests that excess WWTP P was retained in the sediments (Fig. 3-8). However, it appears that not all of the excess WWTP P was retained by the sediments of Gunston Cove. PP concentrations in the sediments of the Potomac 1 core reached a high of 76 μmol g^{-1} (or 2.35 mg g^{-1}) at 20 cm, which may reflect the peak loading from the WWTP (Fig. 3-8). If we consider that the sedimentation rate in the approximately 4 km^{-2} area of Gunston Cove was 9.1 kg m^{-2} yr^{-1} (Table 3-2), then the sediments of Gunston Cove could have been retaining up to 8.6 x 10^4 kg P yr^{-1} during the time of maximum P loading. However, during each of the years from 1971 through 1979 the WWTP discharge exceeded 8.6 x 10^4 kg P yr^{-1}, with a maximum discharge of 17.4 x 10^4 kg P yr^{-1} in 1974. Thus, much of the P discharged from the WWTP is not recorded in the sediments. Perhaps this excess dissolved PO_4^{3-} was repeatedly cycled in the water column and was carried away and dispersed downstream and hence not easily discernable in the sediment record outside of the immediate vicinity of the WWTP.

Physiographic Province

The PP concentrations in the estuarine sediments seem to reflect some characteristics of the physiographic provinces of the watershed. For example, if we exclude the sediments of Potomac 1, which may be anomalously high in PP because of

WWTP loading, then the freshwater sediments from the two subestuaries with Coastal Plain watersheds (the Patuxent and the Choptank) are enriched with PP compared to the Bush and Potomac subestuaries (Fig. 3-2). Indeed, even though the Piedmont Bush watershed has similar land-use patterns as the predominantly Coastal Plain Patuxent River watershed (Table 3-1), the Bush River sediments have much lower concentrations of PP than the Patuxent River sediments (Fig.3-2). Previous researchers have found that Coastal Plain sediments discharged to the Chesapeake Bay are enriched in P compared to Piedmont sediments (Jordan et al. 1997). However, we also found that the sediments from Choptank subestuary, with a watershed entirely within the Coastal Plain, were not as enriched in PP as the sediments from the predominantly Coastal Plain Patuxent (Fig. 3-2). Therefore, it appears that other factors besides physiographic province are determining PP concentrations and PP burial. The Patuxent and the Choptank differ in land-use patterns (Table 3-1) which may affect PP concentrations. Additionally, the Patuxent is also enriched in CDB-Fe compared to the Choptank and the other subestuaries (Fig. 3-5), suggesting the importance of local geology in controlling PP burial.

One might have expected that the auth-P fraction would have been quantitatively more important in the Potomac subestuary, which has carbonate rocks in its watershed. Carbonate sediments can be an important sink for P in freshwater (e.g., House 2003) and saltwater environments (e.g., McGlathery et al. 1994). However, Louchouarn et al. (1997) reported that $CaCO_3$ may have inhibited CFA formation in the sediments of the

Gulf of St. Lawrence. Louchouarn et al. (1997) also found that bioirrigation may limit CFA formation by allowing solute exchange with the overlying water, thus prohibiting the build-up of pore water supersaturation. Perhaps even though soluble phosphate was released by Fe-P and org-P with depth in the sediments of the Potomac, Choptank, and Bush subestuaries, bioirrigation, or in the case of the Potomac, the presence of $CaCO_3$ may have inhibited the formation of CFA in our sediments.

Conclusions

In the Patuxent subestuary, PP concentrations in the three freshest sites were similar to the concentrations of PP in the suspended solids discharged from the Patuxent watershed (Jordan et al. 2008, Chapter 2), suggesting that PP is preserved in the freshwater sediments after deposition. In the other three subestuaries, the freshwater sediments also exhibited little to no downcore trends in PP concentrations, indicating that PP was not lost to factors such as reductive dissolution or microbial degradation with sediment burial. Thus, PP retention appeared to be very efficient with burial in the freshwater sediments of all four subestuaries.

Fe-P concentrations declined with increased salinity in the Patuxent, Potomac and Choptank. Fe-P did not provide a long-term sink for P in the saline reaches of the Potomac and Choptank, where Fe-P concentrations declined to near zero in the deepest sediments. However, the Patuxent River sediments were exceptional in retaining Fe-P even in the most saline and deepest depths in the sediments. CDB-Fe:Fe-P ratios were

also lower in the Patuxent than in the other three subestuaries, indicating that CDB-Fe is in a form that is more available to bind P in the Patuxent.

In addition to declines in Fe-P with depth in the saline sediments of the Potomac and Choptank, we also observed some decline in organic P concentrations with depth in the sediments of the Potomac, Choptank and Bush Rivers. However, the majority of the org-P was refractory and persisted with depth. We did not find evidence that phosphates released from Fe-P or organic P were being diagenetically redistributed to form authigenic apatite-P in any of the four subestuaries.

With the exception of one site that receives wastewater effluent, changes in historical land-use patterns were not discernable in the PP sediment profiles. Additionally, there were no compelling differences in PP burial with watershed physiographic province. While the Coastal Plain Patuxent was enriched in PP compared to the Piedmont Bush and Appalachian Potomac, the Patuxent was also enriched compared to the Coastal Plain Choptank. The enrichment of PP in the Patuxent was largely reflective of the comparatively high amounts of CDB-Fe in the sediments.

The differences in the form and amount of PP buried in the sediments of the four Chesapeake Bay subestuaries we studied underscore the challenges in attempts to quantify P sequestration in estuarine sediments. Our results indicate that attempts to develop accurate global P budgets and address the worldwide problem of estuarine

eutrophication can be complicated by large differences in PP burial that can occur within a single estuary and with fairly small changes in salinity. Additionally, we have shown that Fe-P, which is normally assumed to be a reactive form of P, can be either a sink or source of bioavailable P. Fe-P burial rates may also depend on the amount or form of Fe mineralogy available to bind P. Considering the large role that Fe plays in controlling PP burial in the Chesapeake Bay, as well as other locations world-wide, additional research to determine the exact form of this Fe-P seems warranted.

Chapter 4: Pore water biogeochemistry and the nutrient limitation switch along the salinity gradient of four Chesapeake Bay subestuaries.

Abstract

Phosphorus is generally a limiting nutrient in freshwater ecosystems, whereas in coastal marine waters P is usually sufficient and N becomes a limiting nutrient. Changes in Fe sequestration of P along the salinity gradient may partly account for this nutrient limitation switch. To investigate this hypothesis, we analyzed pore water from 1-meter-long cores collected from four Chesapeake Bay subestuaries: the Potomac, Patuxent, Choptank and Bush Rivers. We collected cores along a salinity gradient from tidal freshwater to a salinity of 1 in the Bush River, and to the mesohaline regions of the other three subestuaries. In all four subestuaries pore water concentrations of Fe declined and pore water PO_4^{3-} concentrations increased with increased salinity, indicating that soluble Fe may be less available to precipitate with PO_4^{3-} in saline environments. Concentrations of NH_4^+ also declined along the salinity gradient in each subestuary, but NH_4^+ trends with salinity were not as pronounced as those of PO_4^{3-} and Fe. The opposing trends of pore water PO_4^{3-} and NH_4^+ led to distinct shifts in N:P ratios from greater than 16 (the Redfield ratio) in the freshwater cores to less than 16 in the more saline cores. Pore water PO_4^{3-} concentration increases with increased salinity were the dominant mechanism affecting the shift in the N:P ratio, indicating that Fe regulation of P can contribute to a

switch from P limitation in freshwater to N limitation in mesohaline waters. Furthermore, the shift from N:P > 16 to N:P < 16 occurred at remarkably similar salinities of 1 – 4 in each subestuary.

Introduction

Mitigating the widespread problems associated with eutrophication of estuarine and coastal waters requires understanding the factors that determine which nutrients limit primary production. Phosphorus generally limits primary production of phytoplankton in freshwater ecosystems (e.g., Schindler 1977, House 2003). In contrast, in the saline waters of most temperate estuaries and coastal marine waters, N often limits primary production (Nixon 1995, Howarth and Marino 2006). In estuaries, where freshwater and saltwater mix, the limiting nutrient can switch from P in tidal freshwater and low salinity waters to N in saltier waters, presenting challenges for watershed managers attempting to mitigate estuarine eutrophication. Estuaries also present excellent natural laboratories in which to explore the possible reasons for the general paradigm of P limitation in freshwater and N limitation in coastal saltwater.

A switch from P limitation to N limitation of primary production with increasing salinity in estuaries could be caused by a decrease in N availability, an increase in P availability, or some combination or both. A decrease in N availability with increased salinity could be caused by processes in the water column. For example, in a review of N distributions in 44 estuaries, NO_2^- and NO_3^- concentrations were highest in the freshwater and oligohaline portions because of the proximity to the riverine sources, and limited

uptake by phytoplankton in this turbid portion of the system (Boynton and Kemp 2008). As these bioavailable N species are transported downstream into more saline waters, they are taken up by phytoplankton and diluted with N depleted marine water; thus water column reserves of bioavailable N become depleted in the more saline waters. Differences in planktonic nitrogen fixation rates in freshwater versus saltwater may also lead to less N availability for primary production in coastal saltwater ecosystems (Howarth 1988, NRC 2000). In freshwater systems, a nitrogen deficiency can be overcome by nitrogen fixation by planktonic cyanobacteria, which is one reason that N limitation is relatively rare in freshwater systems (Smith 1983). In contrast, nitrogen fixation rates in coastal marine and saline estuarine waters are very low, even when the molar ratio of bioavailable N:P is well below the optimum Redfield ratio of 16:1 (Howarth et al. 1988). Nitrogen fixation rates may be low in saltwater because two trace metals required for nitrogen fixation, Mo and Fe, are less available to cyanobacteria in seawater, leading to low growth rates of planktonic nitrogen fixers and increased vulnerability to grazing (Marino et al. 2002). Although N fixation by planktonic cyanobacteria appears to be rare or absent in saline estuaries and coastal waters, rates of N fixation similar to those observed in freshwater have been reported in a few coastal and estuarine ecosystems with salinities less than 10 to 12 (Howarth et al. 1999, Marino et al. 2002, Howarth and Marino 2006). Thus, in the low salinity reaches of estuaries, nitrogen fixation may still be an important process for compensating for N deficits. Therefore, observations that a nutrient limitation switch from P to N can occur at salinities < 10-12

(e.g., Caraco et al. 1987, Fisher et al. 1992) might not be caused by differences in N fixation rates.

Although the N processes in the water column may contribute to the generally observed switch from P to N limitation with increased salinity, the focus of this paper is on biogeochemical processes in the sediments, which can be a dominant force that affects the relative availability of both N and P. For instance, N losses through denitrification can be an important process in removing bioavailable N in aquatic systems. However, there appears to be little to no difference in N loss through denitrification between freshwater and coastal marine sediments (Seitzinger 1988). Therefore, biogeochemical N losses in sediments might not explain why N is generally a limiting nutrient in coastal marine environments.

In contrast to N, the differences in P biogeochemistry in the sediments of freshwater and saltwater ecosystems can promote a greater supply of bioavailable P in coastal saltwater ecosystems compared to freshwater ecosystems. Therefore changes in P sediment biogeochemistry may be instrumental in promoting the generally observed nutrient limitation switch. It has been documented that P is more effectively retained in freshwater sediments, while in saline environments P is more efficiently released from the sediments to the water column (e.g., Roden and Edmonds 1997); as a result, sedimentary P concentrations tend to decrease with increasing salinity (e.g., Lebo and Sharp 1993, Jordan et al. 2008). In many estuarine systems, a decline in particulate P

(PP) concentrations has been closely correlated with declines in Fe-bound P with increased salinity (e.g., Chapters 2 and 3, Upchurch et al. 1974, Strom and Biggs 1982, Lebo and Sharp 1993, Jordan et al. 2008). The reason that Fe-bound P declines with salinity is because the ubiquitous presence of sulfates in saltwater allows for the formation of ferrous sulfide minerals in the sediments, which in turn diminish the capacity of Fe to bind with phosphates (e.g., Caraco et al. 1989, Roden and Edmonds 1997).

We hypothesized that phosphates released from Fe minerals because of Fe-P-S interactions in saline environments build up in the sediment pore waters and diffuse to the overlying water, increasing PO_4^{3-} availability to phytoplankton, and promoting the nutrient limitation switch. To explore this hypothesis we examined pore water solutes of PO_4^{3-}, NH_4^+, and Fe along the salinity gradient of four Chesapeake Bay subestuaries with contrasting watershed land-use patterns and physiographic provinces. We examined whether increases in P availability with increased salinity can contribute to a shift from P limitation in freshwater to N limitation in saltwater. We also examined the role of Fe in regulating P availability along the salinity gradient. Finally, we identified the location along the salinity gradient where pore water N:P ratios switch from > 16 to < 16.

Study sites

We investigated phosphorus sequestration and pore water chemistry of the sediments in the tidal portions of the Patuxent River, the Potomac River, the Choptank

River, and the Bush River. All four rivers are subestuaries of the Chesapeake Bay, are located in Maryland, USA, and experience mean tidal fluctuations of < 1 m. A summary of the watershed characteristics of each subestuary is given in Chapter 3.

Methods

Sediment core collection and processing

We used a hand-operated piston-corer to collect 1 meter long sediment cores in water that ranged from 1 – 7 m in depth. Refer to Chapter 2 for details on the coring process. We collected sediment cores at seven different locations in the Patuxent, five in the Potomac, four in the Choptank, and three in the Bush River. The coring locations spanned pore water salinity gradients of 0 – 11 in the Patuxent, 0 – 6 in the Potomac, 0 – 10 in the Choptank, and 0.4 – 1.2 in the Bush River (Fig. 3-1 and Chapter 3). In the Bush River, military restrictions on access and proximity to the freshwater head of the Chesapeake Bay limited the range of salinities that could be sampled. All sediment cores were sectioned at 5-cm intervals under a nitrogen glove bag within 1-5 days of collection. (See Chapter 2 for details.)

Pore water was collected from intervals of every 10-20 cm depth in the sediment using procedures outlined in Chapter 2. The filtered pore water was transferred into four different aliquots for analyses. One aliquot was acidified and stored at 4°C for analysis of dissolved Fe. One aliquot was frozen until analysis for dissolved phosphate (PO_4^{3-}).

Another aliquot was frozen until analysis of dissolved ammonium (NH_4^+). The remaining pore water was frozen until analysis of dissolved Cl^-.

Analytical methods

Concentrations of dissolved PO_4^{3-} in the filtered pore water were quantified using an ascorbic acid, molybdate colorimetric method (Eaton et al. 1995). Total Fe in the pore water was measured using a Perkin Elmer Optima model 3000 Inductively Coupled Plasma, Optical Emission Spectrometer. Dissolved NH_4^+ was analyzed with an Astoria Pacific automated analyzer (Method A303-S02). Pore water Cl^- concentrations were measured with a Dionex model 4000 ion chromatograph. Pore water salinity was calculated from Cl^- concentrations.

Results

Pore water solute trends with salinity and depth in the sediments

Pore water Fe and NH_4^+ concentrations declined, and PO_4^{3-} concentrations increased along the salinity gradient of each of the four subestuaries, even in the Bush River where the salinity gradient was very slight (Fig. 4-1). In contrast to salinity trends, pore water solute trends with depth in the sediments were not as clear. While pore water NH_4^+ concentrations increased with depth in the sediments at most sites, pore water Fe and PO_4^{3-} concentration trends with depth were less consistent. There was no trend in pore water PO_4^{3-} concentrations with depth in the sediments of the freshest sites; however, PO_4^{3-} concentrations increased with depth in some of the sediments of the more

saline sites (Fig. 4-1). In contrast to PO_4^{3-}, there was no trend in Fe concentration with depth in the saline sediments; however pore water Fe concentrations increased with depth in the sediments of some of the fresher sites (Fig. 4-1).

Since pore water solute trends with depth were not consistent, to characterize trends with salinity we compared the mean values of the solutes for all depths at a given site. Mean pore water Fe concentrations declined by 88 to 100% along the salinity gradient of each river. In contrast, mean pore water PO_4^{3-} concentrations increased by 90 to 97% with increased salinity in each subestuary, approximately the same extent as Fe declined with increased salinity (Fig. 4-2). Declines in pore water NH_4^+ along the salinity gradient were not as pronounced as the observed declines in pore water Fe concentrations, ranging from declines of 43 – 69% (Fig. 4-2). Trends in pore water NH_4^+ concentrations with salinity were also not as consistent as the trends in pore water Fe and PO_4^{3-} concentrations with salinity. For example, in both the Patuxent and Bush subestuaries the highest mean concentrations of NH_4^+ in the Patuxent subestuary did not occur in the pore waters of the freshest site (Fig. 4-2)

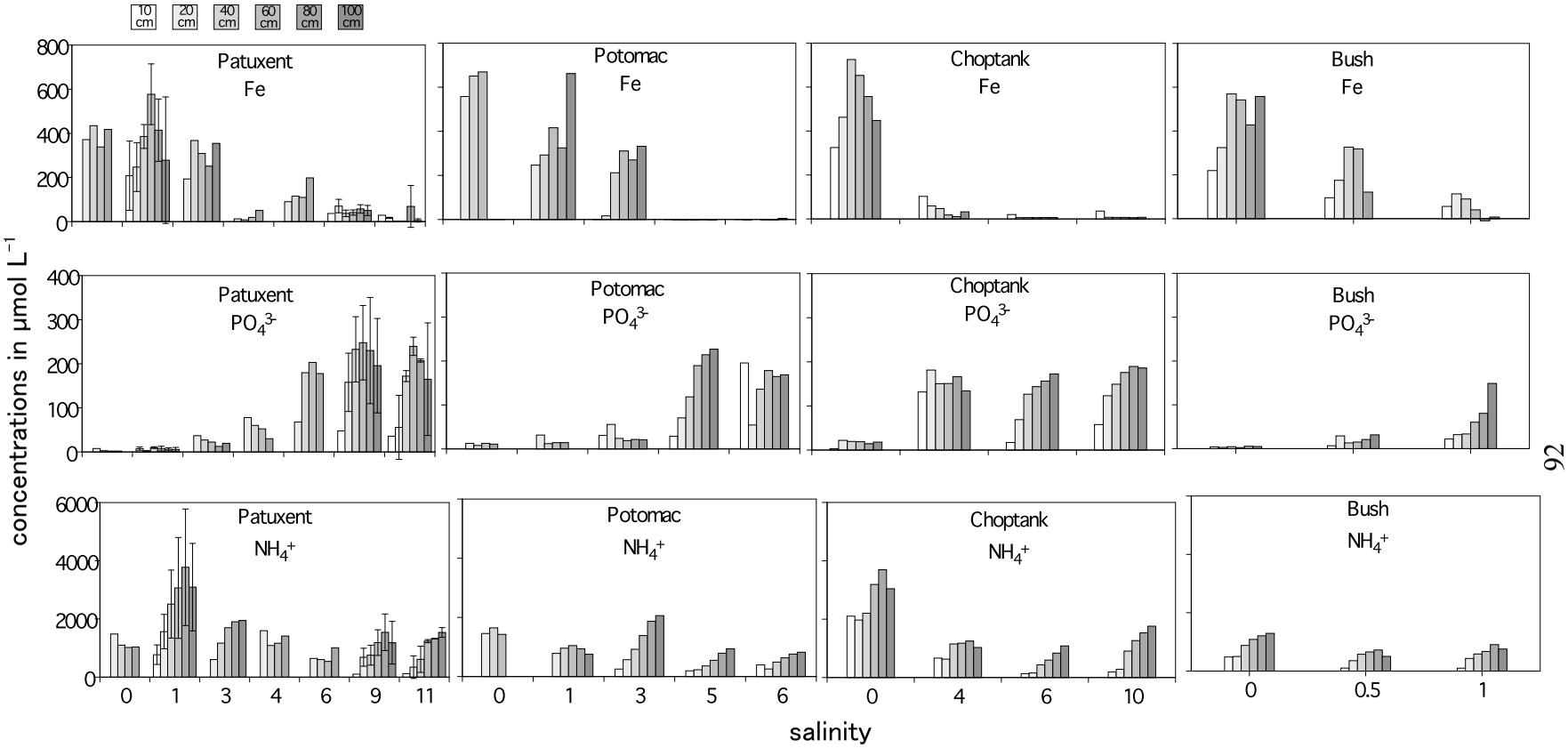

Fig. 4-1. Pore water Fe, PO_4^{3-}, and NH_4^+ concentrations in µmol L^{-1} with depth in the sediments

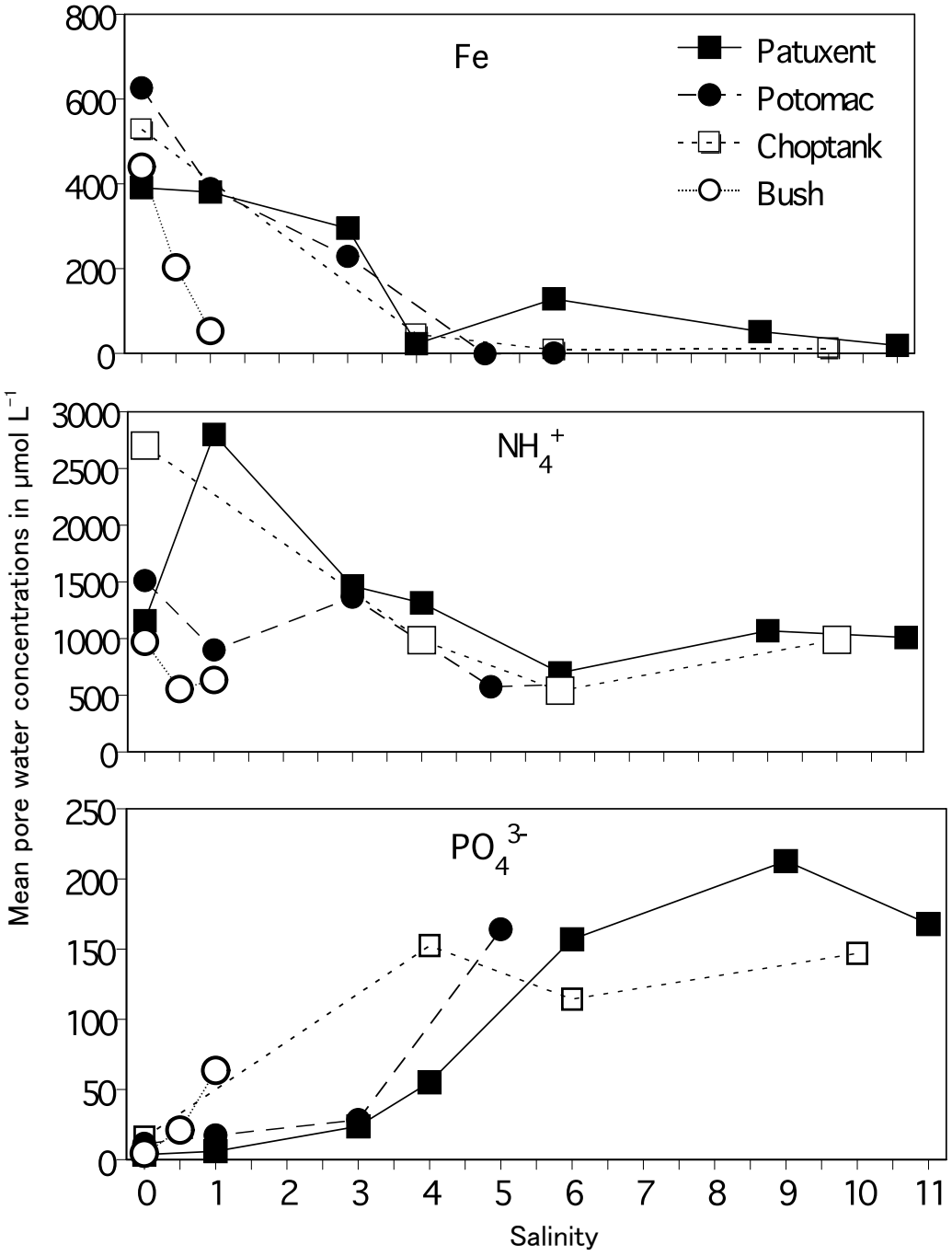

Fig. 4-2. Pore water concentrations of Fe, NH_4^+ and PO_4^{3-} along the salinity gradient of the four subestuaries. Concentrations are means of all depths for the entire length of the core(s) collected at a site.

Trends in pore water Fe:P and N:P ratios with salinity

The contrasting salinity trends of pore water PO_4^{3-} and Fe concentrations led to distinct shifts in pore water Fe:P ratios along the salinity gradient. Fe:P ratios were higher in the freshwater sediments than in the more saline sediments (Fig. 4-3). Trends in Fe:P ratios with depth in the sediments were not apparent.

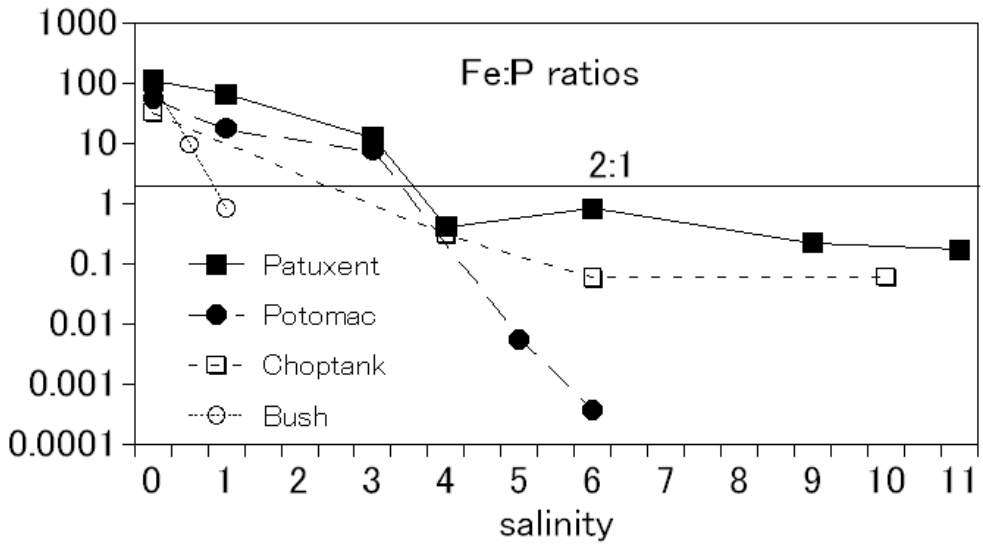

Fig. 4-3. Mean pore water Fe:P ratios along the salinity gradients of the four subestuaries. Ratios are mean values of all depths for the entire length of the core(s) collected at a site.

The contrasting trends of NH_4^+ and PO_4^{3-} led to distinct declines in N:P ratios with increased salinity in all four subestuaries (Fig. 4-4). In general, pore water N:P ratios were all >16 (the Redfield ratio) in the fresher sites, and <16 in the sites in the more saline sites, with the switch occurring at salinities of 1 – 4. Trends in pore water N:P ratios with depth in the sediments were not apparent.

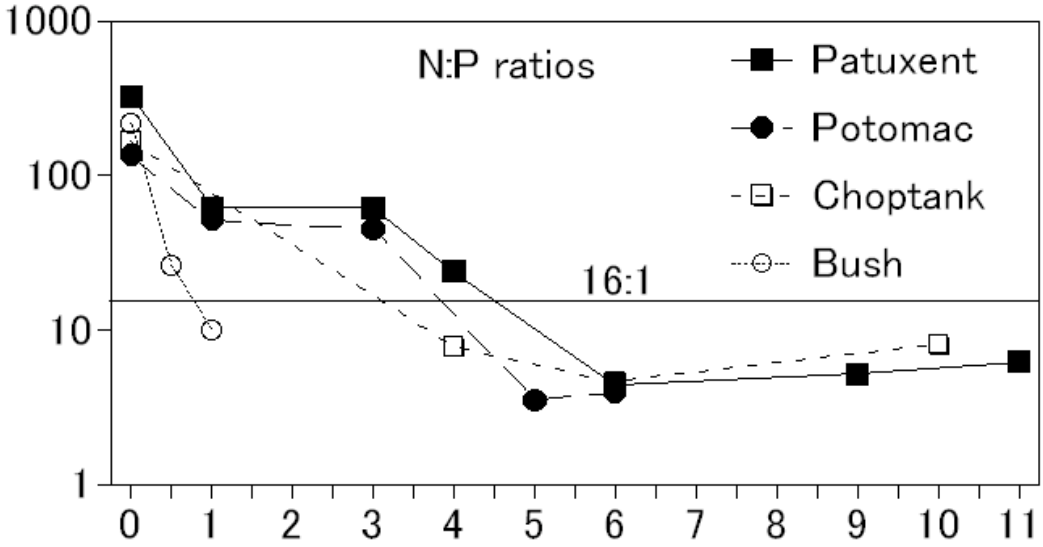

Fig. 4-4. Mean pore water N:P ratios along the salinity gradients of the four subestuaries. Ratios are mean values of all depths for the entire length of the core(s) collected at a site.

Discussion

Fe control on P availability

In all three subestuaries where we were able to sample the mesohaline regions, PP concentrations in the sediments sharply declined with increased salinity. Declines in citrate-dithionite-bicarbonate (CDB) extractable P, which we refer to as Fe-P, accounted for 90% of the decline in PP in each subestuary (Fig. 4-5).

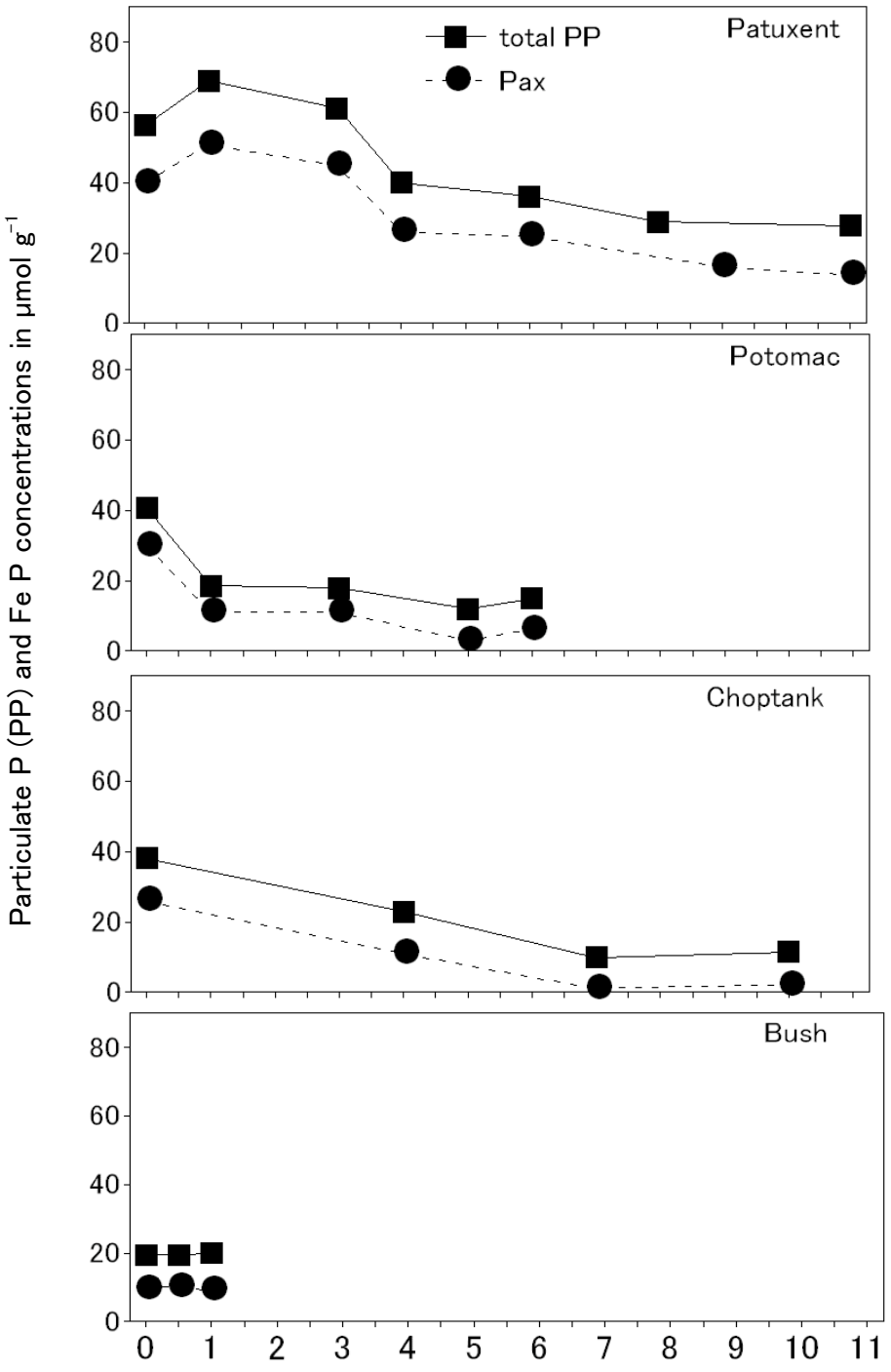

Fig. 4-5. Trends of total particulate P and Fe-P along the salinity gradient.

CDB is meant to extract PO_4^{3-} bound to metal oxides, predominantly Fe in our subestuaries (Chapters 2, 3, and 5), suggesting that Fe plays a dominant role in regulating P sequestration in the sediments along the salinity gradient. Additionally, with increased salinity, there were opposing trends of pore water Fe and PO_4^{3-} concentrations in all four subestuaries. Pore water Fe concentrations declined by 88 – 100% while pore water PO_4^{3-} concentrations increased by a similar extent (90 – 97%), suggesting a decoupling of pore water Fe and PO_4^{3-} with increased salinity, and that soluble Fe is less available to precipitate with PO_4^{3-} in saline sediments.

In both freshwater and saltwater sediments, P bound to Fe oxides can be released to the pore waters with sediment burial and the subsequent reductive dissolution of the Fe oxides. In freshwater sediments, the soluble Fe(II) can diffuse upward to the aerobic surficial sediments, become re-oxidized, and bind PO_4^{3-}, thus preventing PO_4^{3-} from being released to the water column (Caraco et al. 1990, Chambers and Odum 1990). Fe(II) can also precipitate with PO_4^{3-} in freshwater sediments, forming ferrous phosphate minerals, such as vivianite (Postma 1982, Gächter and Müller 2003). These mechanisms for Fe precipitation with PO_4^{3-} could explain the low concentrations of pore water PO_4^{3-} observed in the freshwater sediments. In contrast to freshwater sediments, anaerobic saline sediments have greater amounts of sulfides which preferentially bind to Fe(II) to form ferrous sulfides, thus Fe is less available to bind P in saline sediments. Therefore, PO_4^{3-} concentrations build up in the pore waters of saline sediments and diffuse into the overlying water.

The opposing trends of pore water Fe and PO_4^{3-} concentrations with increased salinity led to a decline in pore water Fe:P ratios with increased salinity in all four subestuaries. In all four subestuaries, pore water Fe:P ratios were >2 in the freshwater sediments. At salinities of 4 and greater, all Fe:P ratios were <2 (Fig. 4-3). A pore water Fe:P ratio of at least 2 may be required to provide sufficient Fe to block PO_4^{3-} from diffusing to the water column by forming complexes of Fe oxide-bound P in the surficial aerobic sediments (Gunnars et al. 2002, Gächter and Müller 2003). It is interesting to note that at all of the freshwater sites soluble Fe concentrations in the pore waters were abundant enough to prevent phosphate diffusion to the water column (i.e., Fe:P ratios were $\geq$2). However, in the sites with salinities greater than 1 – 3, soluble pore water Fe concentrations may have been insufficient to retain phosphates in the aerobic sediments.

Lower Fe:P ratios in the saltier sediments support the hypothesis that Fe is binding with sulfides in the saline sediments resulting in a decreased availability of Fe to sequester P. Indeed iron sulfide concentrations in the Patuxent sediments were found to increase with increased salinity (Chapter 5). Furthermore, Fe-P-S interactions appear to promote increased bioavailability of PO_4^{3-} to the water column and hence also promote a nutrient limitation switch along the salinity gradient. Other researchers have found that PO_4^{3-} is released to the water column in low salinity waters. For example, PO_4^{3-} concentrations in the water column of the Chesapeake Bay are consistently higher than water quality model predictions at salinities of approximately 3 – 4 (Cerco and Cole

1993). Additionally, in a review of 48 estuaries, PO_4^{3-} fluxes out of sediments were highest at salinities of 5 – 10 (Boynton and Kemp 2008).

Ammonium trends with salinity

Concentrations of pore water NH_4^+ declined along the salinity gradient, which contributed to the observed shift in N:P pore water ratios. Other researchers have also reported lower concentrations of dissolved NH_4^+ in sediment pore waters with increased salinity (e.g., Elderfield et al. 1981, Jordan et al. 2008). This pattern in the pore waters may be explained by that fact that concentrations of water column inorganic N tend to be highest in tidal freshwater or oligohaline regions of estuaries and decrease seaward (Boynton and Kemp 2008). Each of our study subestuaries was no exception to this pattern of higher concentrations of water column inorganic N in the fresher regions (Magnien et al. 1987, Maryland Department of Natural Resources 2005). Furthermore, in the Patuxent declines in water column dissolved inorganic nitrogen concentrations with increased salinity paralleled declines in pore water NH_4^+ concentrations indicating the coupling between water column and sediment N species (Jordan et al. 2008). Declining NH_4^+ concentrations in the water column or pore waters with increased salinity can often be related to distance from watershed N sources. For example, in two North Carolina estuaries high water column concentrations of NH_4^+ in the freshwater reaches from urban and agricultural sources declined rapidly with increased salinity as N was lost through biogeochemical processes and as N-rich freshwater mixed with N-poor seawater (Dafner et al. 2007). In another example of NH_4^+ concentrations reflecting watershed loading,

pore water NH_4^+ concentrations increased with increased salinity in the marsh sediments of the Cooper River, South Carolina, the opposite pattern of what we found, probably because the freshwater reaches of this estuary are located in a rural area and receive N poor water, whereas the more saline reaches receive N loads from the city of Charleston (Sundareshwar and Morris 1999). Other factors besides N loading from the watershed may also affect NH_4^+ patterns with salinity. For example, NH_4^+ can desorb from sediments with increased salinity because of ion pairing with salt water anions, or from displacement of loosely-sorbed NH_4^+ by saltwater cations, and the NH_4^+ desorbed from the sediments can accumulate in the pore waters (Gardner et al. 1991, Seitzinger et al. 1991). Thus in some estuaries pore water NH_4^+ concentrations can increase when exposed to increased salinity (Hopkinson et al. 1999, Andrieux-Loyer et al. 2008). However, in our subestuaries, salinity-driven desorption of NH_4^+ apparently had less influence than did the salinity-related trend in N concentrations in the water column.

Shift in the N:P ratio along the salinity gradient

The opposing trends of pore water PO_4^{3-} and NH_4^+ led to distinct shifts in N:P ratios from greater than 16 (the Redfield ratio) in the freshwater cores to less than 16 in the mesohaline cores (Fig. 4-4). Furthermore, the shift in the N:P ratios occurred at remarkably similar salinities of 1 – 4 in all four subestuaries. We found few other published reports of pore water N:P ratios in pore waters along salinity gradients from tidal fresh to mesohaline waters. A study of intertidal marsh sediments along a salinity gradient in South Carolina reported N:P ratios >16 in the freshwater sediments and <16 at

water column salinities of 0.44 and higher (Sundareshwar and Morris 1999), a slightly lower salinity than where we observed the N:P ratio switch. However, marsh sediments would be expected to undergo different biogeochemical interactions than the subtidal sediments of our study. For instance, marsh plants have a high demand for N in saltwater; therefore increased N uptake by marsh plants could affect a N deficit in sediments at lower salinities than in sediments with no vegetation (Crain 2007). There have been a few reports of a general decline in N:P ratios in pore waters of subtidal sediments with increased salinity, but determining a salinity level where the 16:1 switch occurred was complicated by very large seasonal or tidal fluctuations in salinity. For example, in a Massachusetts estuary, pore water N:P ratios generally declined with increased salinity in the subtidal sediments (Hopkinson et al. 1999); but since the salinity of the overlying water ranged from 0 to 29 due to the large tidal range, it would be difficult to locate a precise point where the ratio switched from above to below the Redfield ratio.

Studies examining the water column for nutrient ratio switches with salinity appear to be more common than pore water studies. However, our finding of a remarkably consistent location in the 16:1 ratio shift is not consistent with most water column research conducted on N:P ratios. Some researchers have found that nutrient ratios vary seasonally (D'Elia et al. 1986, Fisher et al. 1999); while other researches have found only weak seasonal effects (e.g., Tomasky et al. 1999). At least one study of coastal ponds found that salt effects and not seasonality affected a nutrient limitation

switch from P limiting at salinities of 0 to 6.5 to N limiting at salinities of 31-32 and both N and P co-limiting at the intermediate salinities of 6.8 – 30 (Caraco et al. 1987). Perhaps the differing findings can be partially attributed to the fact that seasonal changes in nutrient loading also occur with changes in freshwater inputs to estuaries. For example, in the spring the Chesapeake Bay receives higher inputs of freshwater and N. Higher inputs of N can contribute to P limitation and a seasonal change in N:P loading may explain a seasonal change in nutrient limitation (D'Elia et al. 1986, Fisher et al. 1992). However, since a higher input of freshwater also lowers the salinity of estuaries, it is possible that this seasonal nutrient limitation switch may be at least partly a salt-effect.

Other seasonal effects on nutrient uptake by phytoplankton can include changes in light levels and temperatures. For example, in temperate regions increasing light levels and temperatures in spring and summer can increase primary production, especially in nutrient-rich and previously light limited low-salinity regions of estuaries (Fisher et al. 1999). Increasing temperatures in spring can also increase benthic respiration rates, which can accelerate denitrification rates and thus deplete N relative to P. However, in eutrophied systems such as the Chesapeake Bay, low oxygen levels in the summer months can lead to marked reduction of rates of nitrification and denitrification and enhance NH_4^+ recycling to the water column (Kemp et al. 1990). On the other hand, PO_4^{3-} availability can also be enhanced during summer anoxic events with Fe oxide reduction and SO_4^{2-} reduction to sulfide and subsequent release of associated PO_4^{3-}.

Undoubtedly, all of the factors that can affect spatial and temporal nutrient limitation can be complex.

We did not specifically test for seasonality in our pore water concentrations. However, we did collect our samples over a large range of the year – spanning from April to November, and we did not find any clear trends in pore water concentrations and the month the core was collected. Perhaps since we used mean values of pore water salinities and solutes to depths of 100 cm, this allowed us to locate a more precise location for the N:P ratio switch by averaging out seasonal variations in nutrient loading, N cycling and salinity.

Which nutrient exerts greater control over the N:P switch?

Pore water NH_4^+ concentrations declined with increased salinity, and PO_4^{3-} concentrations increased with increased salinity; but which trend contributed the most to a switch in the N:P ratio along the salinity gradient? Our results indicate that increases in pore water PO_4^{3-} concentrations with increased salinity held a greater control over the N:P switch than the declines in NH_4^+ concentrations. In all four subestuaries, if NH_4^+ concentrations had remained constant at the freshwater values then the N:P ratio still would have dropped to approximately $\leq$16 with increased salinity, albeit at a slightly higher salinity level than if both nutrients changed (Fig. 4-6).

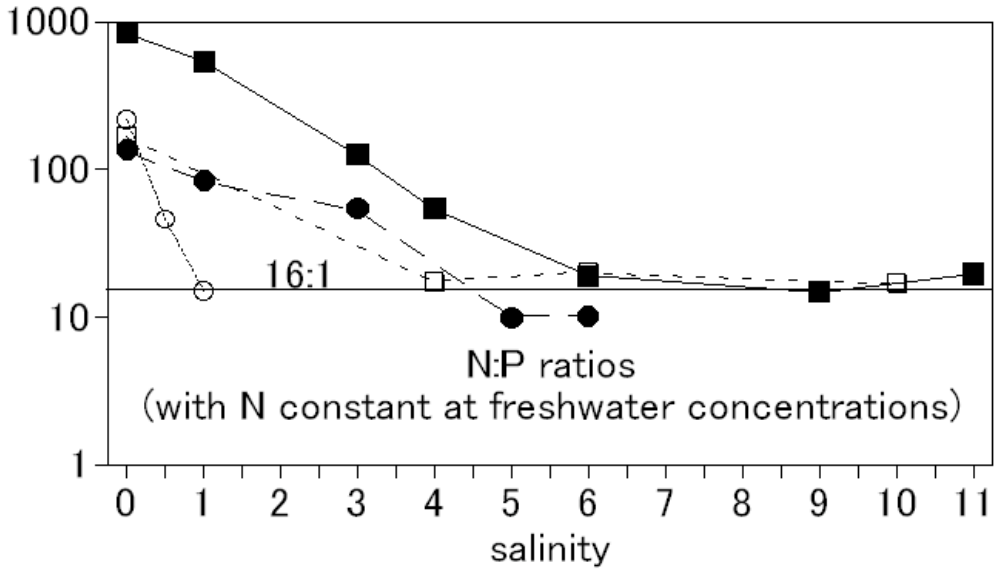

Fig. 4-6. Mean pore water N:P ratios along the salinity gradients of the four subestuaries if N remained constant at freshwater concentrations.

On the other hand, if we kept PO_4^{3-} concentrations constant at the freshwater values, the N:P ratios remained >16 at all salinities (Fig. 4-7).

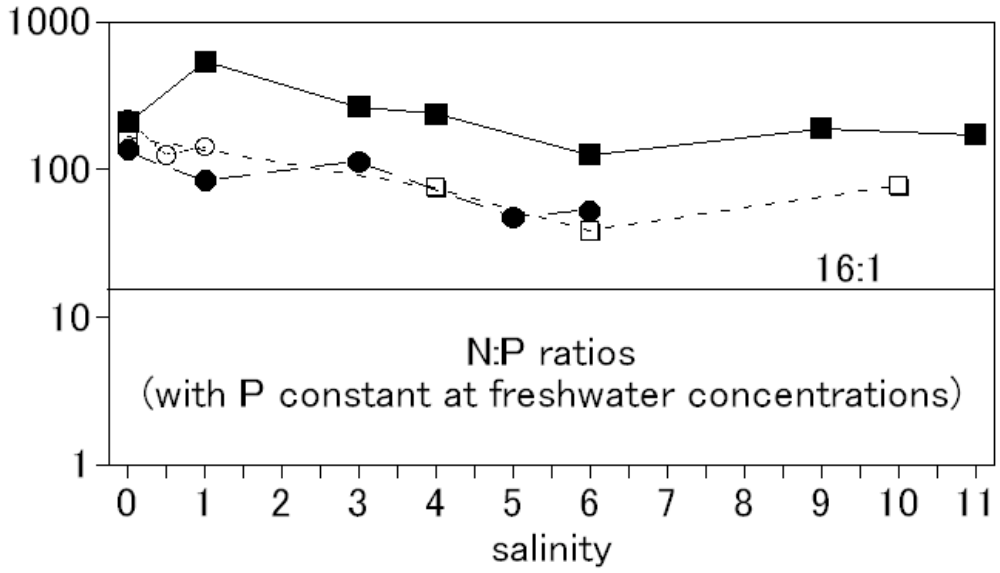

Fig. 4-7. Mean pore water N:P ratios along the salinity gradients of the four subestuaries if P remained constant at freshwater concentrations.

Thus it appears that salinity induced changes in pore water PO_4^{3-} concentrations alone could alter the pore water N:P ratios enough to promote a nutrient limitation switch. Another indication of the dominance of PO_4^{3-} concentration trends along the salinity gradient is the fact that PO_4^{3-} concentrations increased by 90 to 97%, as opposed to a 43 to 69% decline in NH_4^+ concentrations with increased salinity. This underscores the importance of P-Fe-S interactions which apparently drive the increase in pore water PO_4^{3-} concentrations with increasing salinity.

Conclusions

There are undoubtedly many complex factors that contribute toward the general pattern of P limitation in freshwater and N limitation in coastal saltwater. However, we have shown that in these four subestuaries changes in pore water chemistry of Fe, PO_4^{3-}, and NH_4^+ can lead to dramatic changes in the pore water N:P ratio along the salinity gradient. The opposing trends of pore water PO_4^{3-} and NH_4^+ led to distinct shifts in N:P ratios from greater than 16 (the Redfield ratio) in the freshwater cores to less than 16 at salinities greater than 1 – 4. This suggests that efflux of pore water PO_4^{3-} and NH_4^+ could play a major role in promoting a nutrient limitation switch along the salinity gradient. Furthermore, we found that PO_4^{3-} dynamics along the salinity gradient played a greater role than NH_4^+ dynamics in promoting the 16:1 ratio switch. Additionally, soluble Fe is less available to precipitate with PO_4^{3-} in the sediments with salinities >1 – 4, as evidenced by the distinct shift in Fe:P ratios along the salinity gradient. Thus, Fe regulation of P in the pore waters can play a major role in the switch from P limitation in

freshwater to N limitation in mesohaline waters. Additional research is required to determine if there is evidence that other estuaries around the world also have distinct shifts in N:P ratios in pore waters at salinities of 1 – 4, and whether Fe and P interactions control that shift.

Chapter 5: Evidence for ferrous phosphate mineral formation in the saline sediments of the Patuxent River

Abstract

Fe-bound P (Fe-P) is normally considered a reactive form of particulate phosphorus (PP) that can release bioavailable phosphates to the water column with burial in saline sediments. However, we found that P extracted with citrate-dithionite-bicarbonate (CDB), a supposedly Fe oxide-bound P, was the dominant sink for P at all salinities and all depths in the sediments of the Patuxent subestuary. We examined the form of CDB extractable P that is persisting in the saline sediments of the Patuxent by 1) modeling the solubility of phosphate minerals in the saline sediments, 2) analyzing acid soluble Fe(II) and Fe(III) concentrations in the sediments, 3) measuring the sulfide concentrations in the sediments, and 4) analyzing the mineralogy of the sediments. While we were unable to directly identify any Fe phosphate minerals, all of the other results indicate that the ferrous phosphate mineral vivianite ($Fe_3(PO_4)_2 \cdot 8H_2O$) may be forming in the saline sediments of the Patuxent. The solubility calculations indicated that the pore waters are supersaturated with respect to vivianite in the anoxic saline sediments. Additionally, little to no measurable Fe(III) persisted below about 20 cm in depth in the sediments, and Fe concentrations in the sediments were high relative to sulfide concentrations, indicating that excess Fe(II) may be available to precipitate vivianite after

sulfides are exhausted. Ferrous phosphate formation is normally indicative of freshwater environments; however, it appears that vivianite formation is a potentially important mechanism for sequestering P in the saline reaches of the Patuxent. Therefore P burial in estuaries may be influenced by vivianite solubility in the sediments.

Introduction

Determining the fate of P entering estuaries is key to understanding global P cycling, developing accurate global P budgets, and managing the widespread problems associated with eutrophication. Up to 95% of phosphorus carried by rivers to estuaries and coastal waters is in the form of particulates (Föllmi 1996). The form of particulate P (PP) affects whether P will become sequestered and buried in the sediments, or conversely, released to the water column as bioavailable PO_4^{3-}. Fe-bound P (Fe-P) is quantitatively one of the most important forms of PP, perhaps accounting for more than 50% of the chemically weathered-phosphorus river flux to the global oceans (Compton et al. 2000). Despite the importance of this large P fraction, the fate of Fe-P entering estuaries and coastal environments is uncertain (Compton et al. 2000), leading to uncertainties in attempts to quantify the global phosphorus cycle.

Trivalent Fe oxides have a strong capacity to sorb P, and may be an important burial sink for PP in some environments (e.g., Ruttenberg and Berner 1993). However, Fe(III) oxides can become reduced to soluble ferrous iron (Fe(II)) with burial in anoxic sediments, releasing associated P; thus Fe oxides may provide only a temporary sink for

P, especially in saltwater environments (Krom and Berner 1981, Sundby et al. 1992, Jensen et al. 1995, Föllmi 1996, Anschutz et al. 1998). In freshwater sediments, Fe(II) can diffuse upward to the aerobic surficial sediments, become re-oxidized, and bind PO_4^3, thus preventing PO_4^{3-} from being released to the water column (Caraco et al. 1990, Chambers and Odum 1990). Fe(II) can also precipitate with PO_4^{3-} in freshwater sediments, forming ferrous phosphate minerals, such as vivianite ($Fe_3(PO_4)_2 \cdot 8H_2O$) (Postma 1982, Gächter and Müller 2003). In contrast to freshwater sediments, the presence of sulfides in saline sediments effectively decouples Fe-P interactions. Fe(II) readily binds with sulfides to form ferrous sulfides, making Fe less available to bind P in saline sediments. Additionally, the presence of sulfides can result in the dissolution of vivianite, resulting in the formation of ferrous sulfides and dissolved phosphate by the pathway shown below (Gächter and Müller 2003):

$$Fe_3(PO_4)_2 \cdot 8H_2O + 3H_2S \rightarrow 3FeS + 2H_3PO_4 + 8H_2O$$

Therefore, the importance of Fe in sequestering P may be diminished in saltwater sediments (e.g., Caraco et al. 1989, Roden and Edmonds 1997). The decreased availability of Fe to sequester P in the presence of sulfides may explain why a decrease in sediment PP content with increased salinity has been found to be closely correlated to decreases in Fe-P in many estuaries (Upchurch et al. 1974, Strom and Biggs 1982, Jordan et al. 2008). Phosphate release from saline sediments due to Fe-S interactions may also

contribute to the generally observed switch from P limitation in freshwater to N limitation in coastal marine waters (Caraco et al. 1990).

Because of Fe-P-S interactions one could reasonably expect that Fe-P would not be an important long-term sink for PP in saline sediments. We found support for this hypothesis in the Potomac and Choptank subestuaries where Fe-P was the dominant fraction at most depths in the freshwater sediments (pore water salinity range of 0 to 3), but Fe-P concentrations declined to near zero at depth in the more saline sediments (pore water salinity range of 4 – 10) (Chap 3). However, in the Patuxent subestuary, Fe-P was more persistent. While there were declines in Fe-P concentrations with increased salinity in the Patuxent sediments, Fe-P persisted as the largest sink for PP at all salinities (0 – 11) and all depths ($\leq$ 1 m) in the sediments. Thus, Fe-P was more important in providing a long-term sink in the saline sediments of the Patuxent than in the Potomac and Choptank (Chapters 2 & 3).

In spite of the importance of Fe-P in regulating P bioavailability in the Chesapeake Bay, the exact chemical identity of this PP fraction remains unidentified. P extracted with citrate-dithionite-bicarbonate (CDB) is normally assumed to be associated with metal oxides such as Fe oxides (Ruttenberg 1992, Kostka and Luther 1994). Thus we have operationally defined CDB extractable P as Fe-P. It is possible that Fe oxides persist in some sediments because they are in a form that is not susceptible to reduction (Slomp et al. 1996b). For example, Fe minerals that persist in saltwater sediments can be

more crystalline, and thus less easily reducible, than iron species found in freshwater sediments (Slomp et al. 1996b, Hyacinthe and Van Cappellen 2004, Hartzell et al. 2008). Fe oxides can also be protected from reduction by a surface coating of Fe(II) either adsorbed or precipitated onto the Fe(III) oxides (Roden and Zachara 1996). Thus, a plausible hypothesis for the persistence of Fe-P in the saline sediments of the Patuxent is that Fe oxides are persisting with depth in the sediments –either in the form of refractory Fe(III) oxides, or as Fe(III) oxides coated with Fe(II).

Another hypothesis is that ferrous phosphate minerals are forming in the brackish sediments of the Patuxent. The presence of ferrous phosphate minerals is normally interpreted as evidence of a freshwater environment (Postma 1982); however, ferrous phosphate minerals have been reported in saline sediments where the concentration of Fe is high relative to sulfides. For example, solubility calculations have suggested that vivianite could be present in marine environments that are Fe-rich, such as the sediments of Long Island Sound (Martens et al. 1978) and the Amazon River Delta (Aller et al. 1986). Also, vivianite nodules have been identified in iron-rich marine deposits of Amazon River sediments, but mainly at depths greater than 10 m below the sediment surface where sulfate has been completely consumed (Burns 1997). Since Fe concentrations are high in the Patuxent sediments relative to the other rivers around the world (Chapter 3), it is possible that the formation of Fe(II) in reducing sediments exceeds the supply of sulfides in the Patuxent subestuary, leaving excess Fe(II) available for ferrous phosphate mineral precipitation.

Alternatively, a third hypothesis may be that the CDB extractable P that we have been referring to as Fe-P could be some other unidentified form of PP, not bound to ferric or ferrous Fe, and Fe-P may actually be a misnomer. For example, CDB can extract compounds such as Mn oxides (e.g., Van der Zee et al. 2005) and labile polyphosphates (Jensen and Thamdrup 1993). Thus, one cannot always assume that CDB extractable P is associated with Fe. However, there appears to be a correlation between P and Fe (Chapters 2 &3); therefore, for simplicity's sake we will continue to refer to this CDB extractable P as Fe-P.

To investigate the form of Fe-P that is so persistent in the Patuxent sediments, we used several approaches. Our methods included attempts to directly identify the Fe mineralogy, measurements of Fe(II) and Fe(III) concentrations in the sediments, analysis of Fe sulfides in the sediments, and calculating the solubility of ferrous phosphate in saline sediments using the geochemical modeling program MINTEQA2 (Allison et al. 1991).

Methods

Sediment and pore water collection

We used a piston-corer to collect 1 meter long sediment cores from 7 different sites along a salinity gradient of 0 -11 in the Patuxent subestuary (Chapter 2). We collected three replicate cores at site 2, five replicates at site 6, and two replicates at site 7

for the solid-phase analyses. We also collected six additional replicate cores from site 6 to extract pore water for the solubility calculations. Water depths ranged from 1 – 5 m in depth. Refer to Chapter 2 for details on the coring process.

The sediments were sectioned in a N_2-filled glove bag and loaded into 50 ml polyethylene centrifuge tubes that were capped while still under N_2. For the solid-phase analyses, the sediments were sectioned into 2-cm thick samples collected at 5 cm intervals (i.e., from 4-6 cm, 9-11 cm, 14-15 cm, etc.) For the solubility analyses, the sediments were sectioned into 4-cm thick samples collected from four different depths of two of the cores: 0-4 cm, 18-22 cm, 48-52 cm, and 68-72 cm, and two different depths: 18-22 cm and 68-72 cm from the remaining four cores. For brevity, we will refer to all of our samples by their median depths (i.e., we refer to 0-4 cm as 2 cm, 4-6 cm as 5 cm, 9-11 cm as 10 cm, etc.). The sediments were then centrifuged at 3000 rpm for 30 minutes to collect pore water. After decanting the pore water, the sediments were frozen. Some of the sediments from each sample were kept frozen and some were freeze-dried.

Pore water solubility analyses

For the solubility analyses, the capped sediment samples were transferred back to the N_2-filled glove bag after centrifugation where the supernatant pore water was decanted into beakers and then divided up into aliquots for analyses. To ensure that we had an adequate volume of pore water for all of the pore water analyses, we combined the pore water from two cores before dividing it up into aliquots for analyses; thus from the

six cores collected, we ended up with three sets of pore water. One aliquot of the pore water was used to measure alkalinity and pH. Alkalinity was measured by titration, and both pH and alkalinity measurements were conducted while the container of pore water was continuously flushed with N_2 to prevent oxidation effects. The remaining pore water was filtered with 0.45 μm polycarbonate Millipore syringe filters and transferred into four different containers for analysis of dissolved Fe, Al, Ca, Mn, Si and P, NH_4^+, PO_4^{3-} and SO_4^{2-} and Cl^-. Refer to chapter 2 for details on analysis of pore water solutes.

The concentrations of conservative seawater ions Sr^{2+} and Br^- were estimated based on standard ratios with measured concentrations of Cl^- in the samples. The pore water ion data were entered the geochemical software program Visual MINTEQ version 2.53 (Gustafsson 2007). Visual MINTEQ is a Visual Basic program based on the U.S. Environmental Protection Agency's MINTEQA2 version 4.0 (Allison et al. 1991) . Saturation indices for minerals were calculated as $\log_{10}$ [IAP/Ksp]. IAP = Ion Activity Coefficient (IAP is sometimes referred to as Q, or the reaction quotient); and Ksp is the solubility product of individual minerals. Saturation indices greater than 0 indicate oversaturation, meaning the mineral will tend to precipitate from solution.

Solid-phase Fe (II) and Fe (III)

Acid-soluble Fe in the sediments was extracted by adding 10 mL of 1 M HCl to approximately 1 g of frozen sediment in 50 mL centrifuge tubes. After shaking for 1

hour the sediments and HCl reagent were centrifuged at 3000 rpm for 5 minutes. Dissolved Fe(II) concentrations in the supernatant were determined colorimetrically using ferrozine (monosodium salt hydrate of 3-(2-pyridyl)-5,6-diphenyl-1,2,4-triazine-p,p'-disulfonic acid) as a complexing agent (Stookey 1970). Concentrations of total Fe (Fe(II) plus Fe(III)) were measured using ferrozine after reduction of all Fe to Fe(II) in a 0.25M hydroxylamine hydrochloride solution in 0.25 M HCl. Fe(III) concentrations were calculated by subtracting the Fe(II) concentrations from the total Fe concentrations. To prevent oxidation artifacts, all reagents were bubbled with N_2, and all sediment samples were sectioned under N_2. To assess the preservation state of the stored sediments, we compared Fe(II) and Fe(III) concentrations in freshly collected sediments, freshly frozen sediments, sediments that had been stored frozen for up to 2 years, freshly freeze-dried sediments, and sediments that had been freeze-dried and stored at room temperature and exposed to oxygen for several years.

AVS and CRS

A two-step sequential extraction scheme was used to determine sediment sulfide concentrations in frozen sediments that had been sectioned under N_2. Acid-volatile sulfides (AVS) were extracted using 1 M HCl. These AVS species were assumed to include Fe monosulfides including amorphous–FeS, mackinawite (FeS), and greigite (Fe_3S_4) (Cornwell and Morse 1987). Pyrite (FeS_2) sulfur was extracted by chromium reduction. AVS and CRS concentrations were determined spectrophotometrically against prepared sulfide standards (Chambers et al. 1994). Degree of pyritization (DOP), which

is a measure of the completeness of the reaction of reactive iron and sulfides, was calculated as:

pyrite Fe/(pyrite Fe + 1 M HCl extractable Fe) (Raiswell et al. 1988).

Mineralogy analyses

Transmission Electronic Microscopy

Sediment samples from site 2 (tidal freshwater) and site 7 (brackish water) of the Patuxent River were examined using Transmission Electronic Microscopy (TEM), model Jeol 3010, at the University of Illinois at Chicago (UIC). Sediments that had been sectioned under N_2 and preserved by freezing were prepared for TEM analysis by boiling in H_2O_2 to digest the organic matter that may interfere with mineral detection. The sediment samples were then rinsed by centrifuging with 0.1 M $MgCl_2$ followed by rinses in deionized water. One drop of the suspended sediment was then pipetted onto a glass slide and allowed to air dry. The ~3 mm diameter sample was transferred onto a carbon – copper grid for TEM analysis.

X-ray diffraction

Freeze-dried and ground sediments were examined using x-ray diffraction (XRD) at the Smithsonian Institution's Mineral Sciences Analytical Laboratory in Washington, D.C. and the U.S. Geological Survey (USGS), Reston, VA. The sediments were examined using a capillary mount at the Smithsonian, and a powder mount at the USGS. CoK α-radiation was used at both facilities. At the USGS the sediments were first

segregated by size using centrifugation, and the <2 μm fraction was analyzed for Fe minerals.

Raman spectroscopy

Sediment samples from sites 2, 3, and 6 of the Patuxent that had been sectioned under N_2 and preserved by freezing were transported under ice to the Geophysical Laboratory of the Carnegie Institute, Washington, D.C. The frozen samples were examined using Raman spectroscopy.

Results

Geochemical Solubility Calculations

The geochemical assessment model indicated the pore waters of site 6 of the Patuxent are oversaturated with the ferrous phosphate mineral vivianite in all of the reduced sediments. The only sample that was not oversaturated with vivianite was collected from the oxidized surficial sediments (Fig. 5-1). Vivianite stability in the sediments correlates with increased pore water Fe and PO_4^{3-} concentrations, and decreased SO_4^{2-} concentrations (Fig. 5-1).

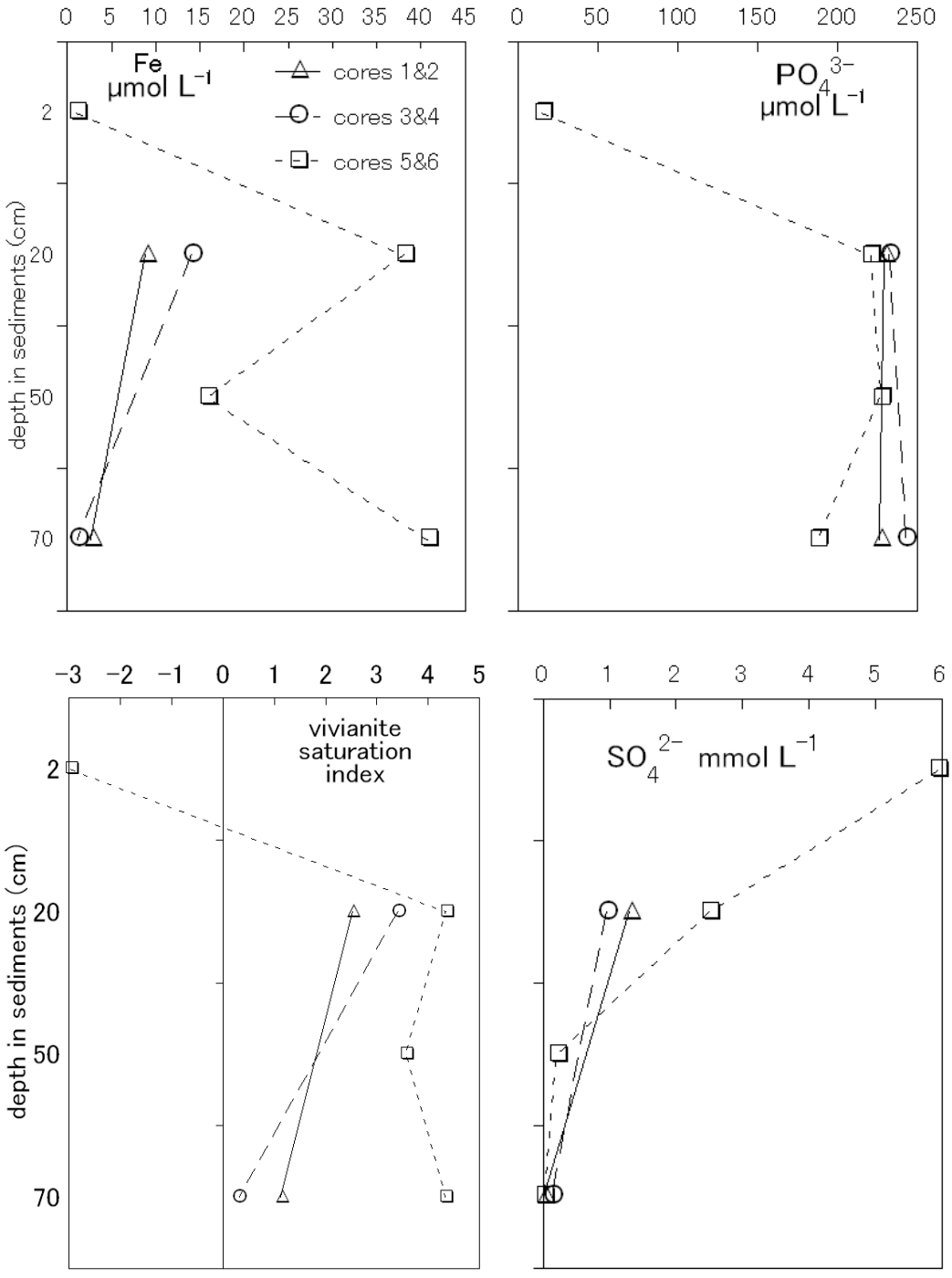

Fig 5-1. Pore water solutes Fe, PO_4^{3-} and SO_4^{2-} in μmol L^{-1}.
Vivianite saturation index = log (IAP/Ksp). IAP (Ion activity product) was calculated using Visual MINTEQ version 2.53. Ksp = solubility product of vivianite.

Table 5-1. Minerals with positive saturation indices (i.e., log IAP > log Ksp), as calculated from Visual MINTEQ. The five minerals with the highest mean saturation indices are shown in bold
--- denotes undersaturation

	cores 1&2	**cores 1&2**	**cores 3&4**	**cores 3&4**	**cores 5&6**	**cores 5&6**	**cores 5&6**	**cores 5&6**
	Sample depth:							
Mineral	**20 cm**	**70 cm**	**20 cm**	**70 cm**	**2 cm**	**20 cm**	**50 cm**	**70 cm**
Aragonite $Ca(CO_3)$	0.497	0.725	0.565	0.773	---	0.37	0.765	0.653
Boehmite AlO(OH)	---	---	0.031	---	---	0.462	---	0.07
$Ca_3(PO_4)_2$ (am2)	0.459	0.644	0.734	0.851	---	0.398	0.819	0.279
$Ca_3(PO_4)_2$ (beta)	0.883	1.232	1.151	1.449	---	0.816	1.325	0.877
$Ca_4H(PO_4)_3{:}3H_2O$	0.087	0.302	0.42	0.551	---	0.053	0.502	---
Calcite $CaCO_3$	0.639	0.868	0.707	0.916	0.136	0.511	0.907	0.796
Diaspore AlO(OH)	---	1.496	1.71	1.302	---	2.141	---	1.768
Dolomite (disordered) $CaMg(CO_3)_2$	**1.678**	**2.048**	**1.744**	**2.117**	**0.635**	**1.351**	**2.125**	**1.905**
Dolomite (ordered) $CaMg(CO_3)_2$	**2.216**	**2.594**	**2.282**	**2.664**	**1.17**	**1.889**	**2.667**	**2.451**
Gibbsite (C) $Al(OH)_3$	---	0.63	0.846	0.436	---	1.277	---	0.902
Hercynite $FeAl_2O_4$	---	3.363	4.665	2.753	---	5.679	---	4.907
Huntite $CaMg_3(CO_3)_2$	1.045	1.709	1.107	1.822	---	0.319	1.856	1.423
Hydroxyapatite $Ca_5(PO_4)_3(OH)$	**8.551**	**9.073**	**9.035**	**9.456**	**4.525**	**8.396**	**9.307**	**8.444**
Magnesite $Mg(CO_3)$	0.341	0.547	0.337	0.572	---	0.139	0.552	0.479
$MnCO_3$ (am)	1.302	1.061	1.274	1.1	1.085	1.228	1.25	1.192
$MnHPO_4$	**3.957**	**3.526**	**3.919**	**3.559**	**3.11**	**4.037**	**3.696**	**3.64**
Rhodochrosite $Mn(CO_3)$	1.805	1.562	1.778	1.6	1.59	1.731	1.752	1.693
Siderite $Fe(CO_3)$	0.314	---	0.591	---	---	0.82	0.792	1.102
Vaterite $Ca(CO_3)$	0.08	0.304	0.148	0.352	---	---	0.346	0.232
Vivianite $Fe_3(PO_4)_2 \cdot 8H_2O$	**2.518**	**1.12**	**3.416**	**0.313**	**---**	**4.355**	**3.556**	**4.332**
charge imbalance (%)	5.4	2.5	1.1	2.1	0.8	5.7	0.1	0.9

The phosphate mineral hydroxyapatite ($Ca_5(PO_4)_3OH$) had the highest saturation indices of any mineral. Another phosphate mineral, $MnHPO_4$, was also one of the five minerals with the highest mean saturation indices (Table 5-1). The pore waters were also oversaturated with respect to several carbonate minerals including ordered and disordered dolomite minerals ($CaMg(CO_3)_2$). The charge imbalance between measured cations and anions was $\leq$ 6% in all of our samples.

HCl Fe(II) and Fe (III) extractions

We found that Fe(II) was the dominant form of Fe at all salinities and all depths in the sediments of the Patuxent. Fe(II) was also the dominant form of Fe in the Potomac, Choptank and Bush subestuaries (Appendix B). Fe(III) was detected in the surficial 0 – 5 cm of all of the samples, but little to no Fe(III) persisted below 20 cm deep in most of the sediments (Fig. 5-2a). The unusual persistence of Fe(III) in the sediments at Patuxent site 1 compared to the other sites may be explained by our ^{210}Pb dating results which indicated that the sediments at this site may be young and sediment deposition was non-steady-state (Chapter 2); however, even at this site, Fe(II) was the major form of Fe at the deepest depths in the sediments (Fig. 5-2a).

Our test results also indicated that sectioning the sediments under N_2 and preserving the sediments by freezing prevents oxidation of Fe(II). When we tested replicate samples of sediments sectioned under N_2, Fe(III) was the dominant form of Fe in sediment samples that were preserved by freeze-drying; whereas Fe(II) dominated in

the samples that were frozen. Additionally, archived sediment samples that had been frozen for several years had similar depth patterns of Fe(II) and Fe(III) as freshly frozen sediment samples collected from the same study site, indicating that preservation by freezing was effective at protecting the oxidation state of the Fe in the sediments.

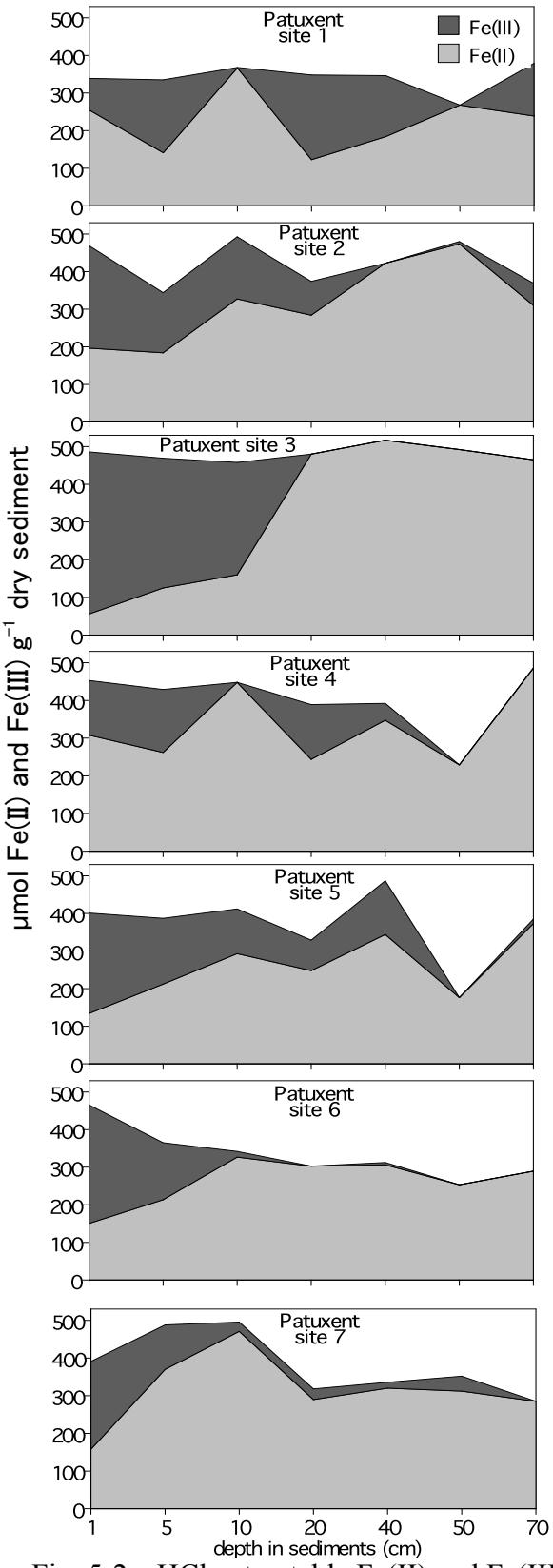

Fig. 5-2a. HCl extractable Fe(II) and Fe(III) concentrations with depth in the sediments

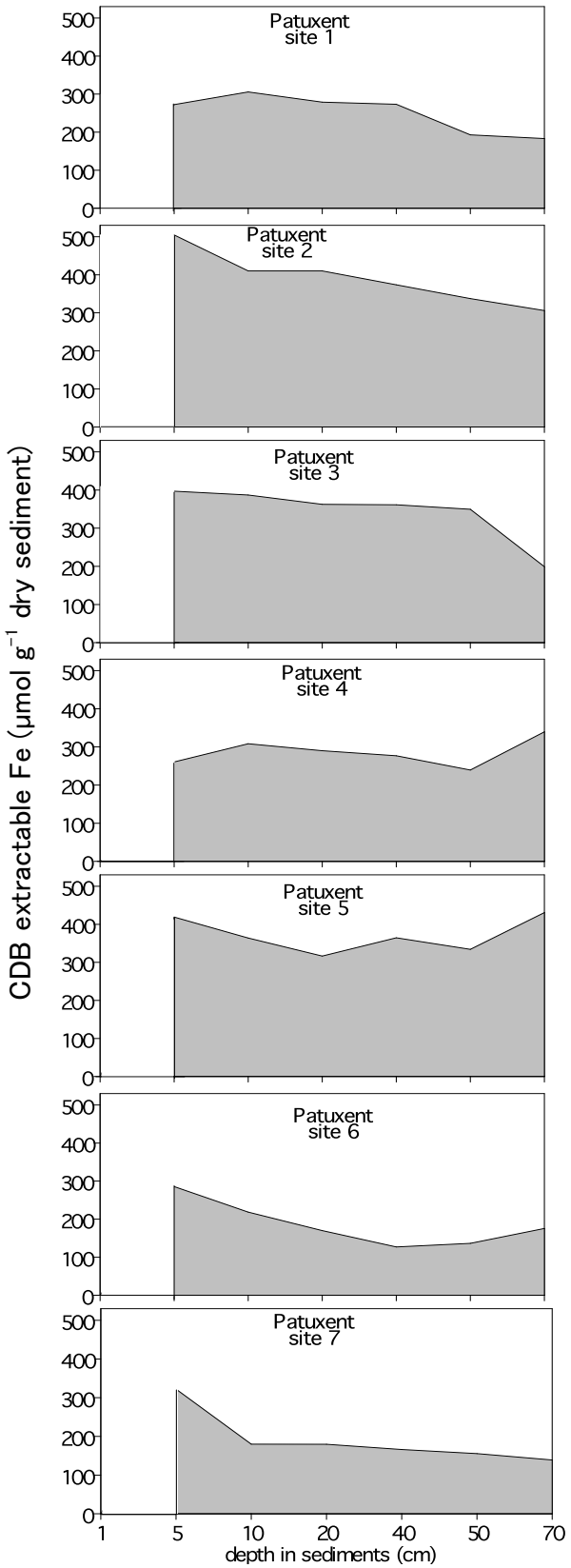

Fig. 5-2b. CDB extractable Fe concentrations with depth in the sediments

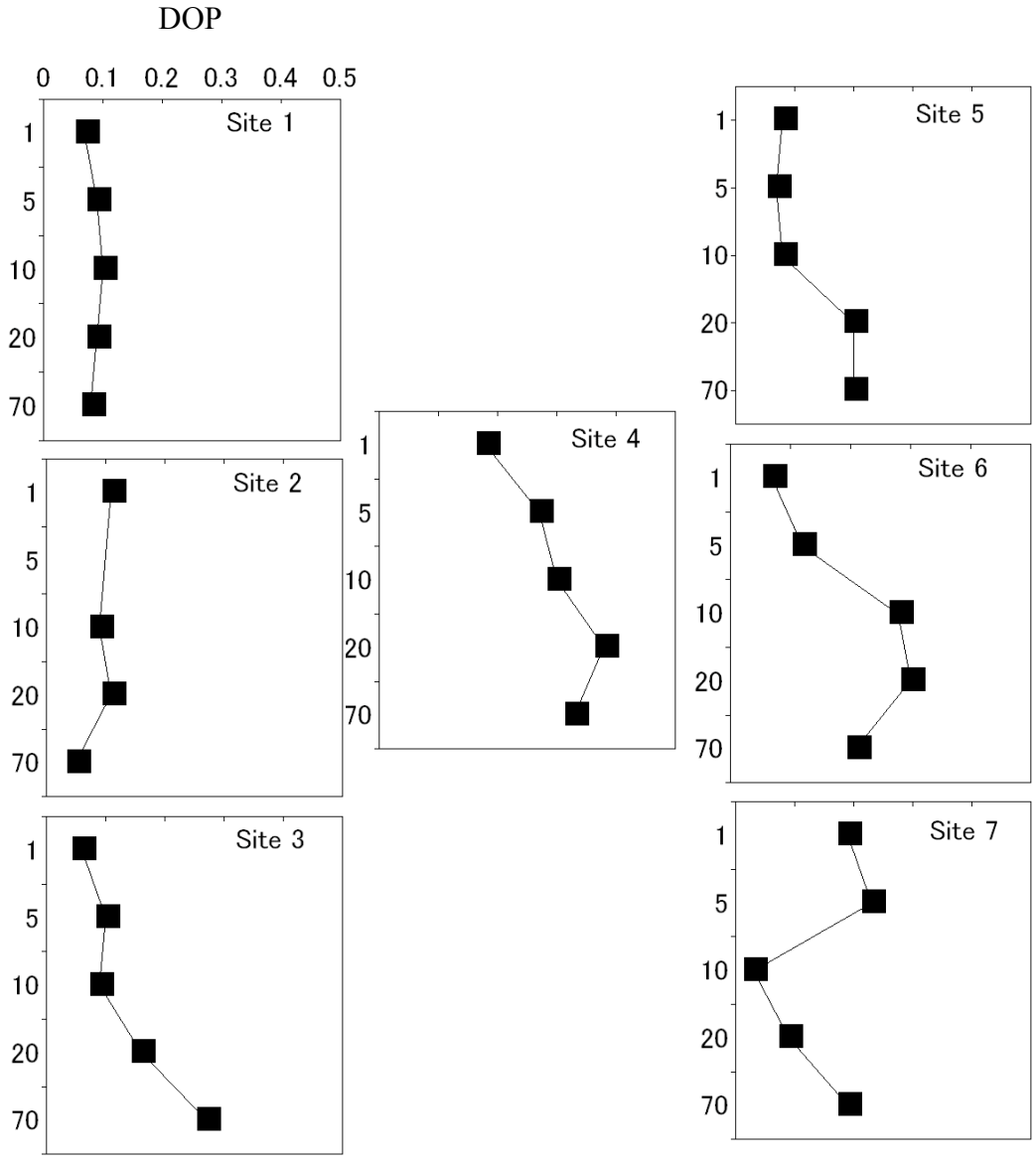

Fig. 5-3. Degree of pyritization (DOP) values with depth in the sediments of the Patuxent
[DOP = pyrite Fe/(pyrite Fe + 1 M HCl extractable Fe]

Acid Volatile Sulfide (AVS), Chromium Reducible Sulfides (CRS) and Degree of Pyritization (DOP)

There was a general trend of increased AVS and CRS concentrations with increased salinity and depth in the sediments. Therefore, DOP values also increased with increased salinity, and generally increased with increased depth in the more saline sediments (Fig. 5-3). The highest DOP values were found at site 4, with DOP values of 0.38 and 0.33 at 20 cm and 70 cm depths in the sediments respectively. All other DOP values were $\leq$0.30.

Mineral identification

Our attempts to identify the Fe minerals in our samples were largely unsuccessful. The concentrations of Fe in the sediments (<3% by weight), while high for most natural sediments, may have been too low for these analytical techniques. Additionally, the sample preparation methods used for TEM and XRD analyses allowed oxidation of Fe(II), leaving the identity of *in situ* Fe minerals in doubt. However, the TEM analyses did indicate the presence of some amorphous and low crystallinity particles containing Fe and P, as well as Al, Si, and Ca, in the surficial freshwater sediments of the Patuxent. Amorphous Fe particles were not apparent in the deeper freshwater samples (>30 cm) or in the saltwater sediments.

We did not identify any iron minerals using XRD at the Smithsonian; instead only quartz and clay minerals were apparent. Even in the <2 μm fraction examined at the

USGS, only quartz and clay minerals were identifiable. This does not indicate that Fe minerals were not present in our samples. It is difficult to determine Fe mineralogy using XRD because of the low concentrations, sometimes low levels of crystallinity, and inherent complexity (i.e., the Fe may be present as coatings on other minerals or interlayered in clays) in natural sediments. Additionally, Fe minerals can be very fine-grained, and perhaps examining a grain size of <1 μm would have yielded more success (Slomp et al. 1996b, van der Zee et al. 2003).

Using the Raman spectrometer, we were able to identify several ferrous minerals, including a framboid FeS mineral, possibly triolite, as well as marcasite (a polymorph of pyrite - FeS_2) from 10 cm depth in the sediments of site 6 of the Patuxent. However, while using the Raman spectrometer we observed greenish minerals changing color to tan or red as the sediment sample thawed and dried; thus it was apparent that oxidation was compromising the samples. Also, we did not positively identify any Fe minerals from a surficial sample from site 2 of the Patuxent, in spite of the fact that this sample has some of the highest concentrations of Fe of any of our sediments. It is possible that the abundance of the Fe minerals in our samples may be too small to be detected by Raman spectroscopy, or the Fe is interlayered within the matrixes of clay minerals. The results from the Raman spectrometer work at the Carnegie Institute indicate that oxidation artifacts are hard to avoid, but the frozen samples do preserve ferrous minerals, indicating that freezing is effective in preventing oxidation.

Discussion

Most of the PP input from the Patuxent watershed is deposited in the upper tidal section of the Patuxent subestuary where Fe-P persists at depths below where Fe(III) was depleted (Chapter 2, Jordan et al. 2008). Although we were not able to directly identify the mineralogy of any Fe phosphate minerals, all of the other evidence indicates that ferrous phosphates, such as the mineral vivianite, are likely to be present in the saline sediments of the Patuxent, and to provide the dominant sink for P.

The most compelling evidence for vivianite formation in our sediments is from the geochemical solubility calculations. IAP calculations indicate that the brackish pore waters of the Patuxent are supersaturated with respect to vivianite in all but one sample. The only sample that was not supersaturated with respect to vivianite was collected from the surficial, oxic layer which had low concentrations of pore water Fe and PO_4^{3-} and high levels of SO_4^{2-} (Fig. 5-1). Fe and PO_4^{3-} concentrations increase with depth in the sediments, resulting in supersaturation with respect to vivianite by 20 cm in depth, indicating that vivianite may be a sink for P below the redox boundary of the brackish sediments.

We did not analyze the pore waters for sulfide concentrations; thus the pore water solubility results are tentative. If sulfides are present, this could result in greater sequestration of the dissolved Fe by sulfides, thus inhibiting vivianite precipitation. However, it might be unlikely that concentrations of sulfides are detectable in the pore

waters of our sediments. Previous researchers have indicated that sulfides are not detectable in the pore waters in the region of the Patuxent we studied (J. Cornwell, personal communication). Dissolved sulfide might only accumulate in pore waters once Fe oxides have been consumed since reactions between Fe oxides and dissolved sulfide are rapid enough to remove sulfide as fast as it is produced (e.g., Raiswell 1999). Thus sulfide might only accumulate in pore waters once all of the Fe available to precipitate with S is consumed (Raiswell and Canfield 1996). High concentrations of dissolved Fe in the pore waters have been correlated with limited sulfide accumulation in pore water (Billon et al. 2001). Dissolved Fe concentrations ranging from 1.0 to 40.8 μmol L^{-1} were present in the pore waters of the sediment cores used for the solubility calculations (Fig. 5-1); thus it seems unlikely that sulfides could accumulate in the presence of this reactive Fe.

The formation of vivianite is also supported by our findings that little to no Fe(III) was present below 20 cm in the sediments (Fig. 5-2a). Thus the CDB extraction, which provided the dominant form of PP in our sediments (Chapter 2) is evidently solubilizing something other than Fe oxides, which is contrary to what is normally assumed by the standard Ruttenberg (1992) extraction analysis. For example, CDB extractable Fe in the sediments of the Mississippi Delta (Ruttenberg 1992) and the Scheldt estuary of Belgium and The Netherlands (Hyacinthe and Van Cappellen 2004) were attributed to Fe oxides. Additionally, Mössbauer spectroscopy and CDB extractions were used to conclude that high concentrations of Fe(III) oxides persist below the oxic zone in freshwater sediments

in the Scheldt estuary of Belgium and The Netherlands (Hyacinthe and Van Cappellen 2004) and in saline sediments of the Mediterranean (Van der Zee et al. 2005). However, in each of these cases freeze-dried sediments were used for the analyses, and it should be noted that freeze-drying may oxidize solid phase Fe (this study, Hjorth 2004). Moreover, it has been found that CDB can extract ferrous phosphate minerals such as vivianite (Williams et al. 1980). Therefore, even if ferrous phosphate minerals were not oxidized during sample preparation, they would be extractable by CDB and could be mistaken for ferric phosphate.

Another line of support for ferrous phosphate formation in the saline sediments of the Patuxent comes from our sulfide analyses. The AVS and CRS results do indicate that Fe monosulfides and pyrite minerals are forming in the brackish sediments of the Patuxent; however, relatively low degree of pyritization (DOP) values of <0.40 were found even in the most saline sediments (Fig. 5-3). These results concur with those of O'Keefe (2007), who found mean DOP values of up to 0.3 in the sediments of the same Patuxent sites. A DOP value of 1.0 implies that all of the HCl extractable Fe is sequestered for the formation of pyrite, whereas a DOP value of <1.0 indicates that pyrite formation is not iron-limited, and excess Fe(II) is left over after all of the sulfide is exhausted (Raiswell et al. 1988). Although DOP values do not consider the reactivity of Fe toward forming sulfides (Canfield et al. 1992), our low DOP values may indicate that Fe(II) is available to form ferrous phosphates even with depth in the most saline sediments of our study sites.

While the IAP calculations, ferrozine results, and sulfide analyses all indicate ferrous phosphate formation, we did not directly identify vivianite (or any other Fe phosphate mineral) in our sediments. Therefore, we cannot completely rule out the possibility that the CDB extractable P that is so prominent in our sediments is bound to something other than vivianite. CDB can extract compounds other than Fe minerals, such as Mn oxides (e.g., Van der Zee et al. 2005) and labile polyphosphates (Jensen and Thamdrup 1993). CDB may also extract Fe minerals that are not available to bind P, such as pyrite (Slomp et al. 1996b) and acid volatile sulfides (Kostka and Luther 1994). However, in our study, it appears that the CDB extractable P was indeed associated with Fe. CDB extractable Fe was correlated to CDB extractable P in the sediments of all four subestuaries that we studied ($r^2 > 0.72$, $p < 0.001$). Significant correlations ($p < 0.001$) were also found between CDB extractable Al and P in all four subestuaries, and between both Mn and Si and P in the Patuxent and Choptank subestuaries. However, in each subestuary the R^2 values were smaller for the correlations of P with CDB extractable Al, Mn, and Si than for correlations with CDB extractable Fe. Moreover, the concentrations of these elements were much lower than concentrations of CDB Fe (Fig. 5-4), suggesting that most of the CDB extractable P was bound to Fe.

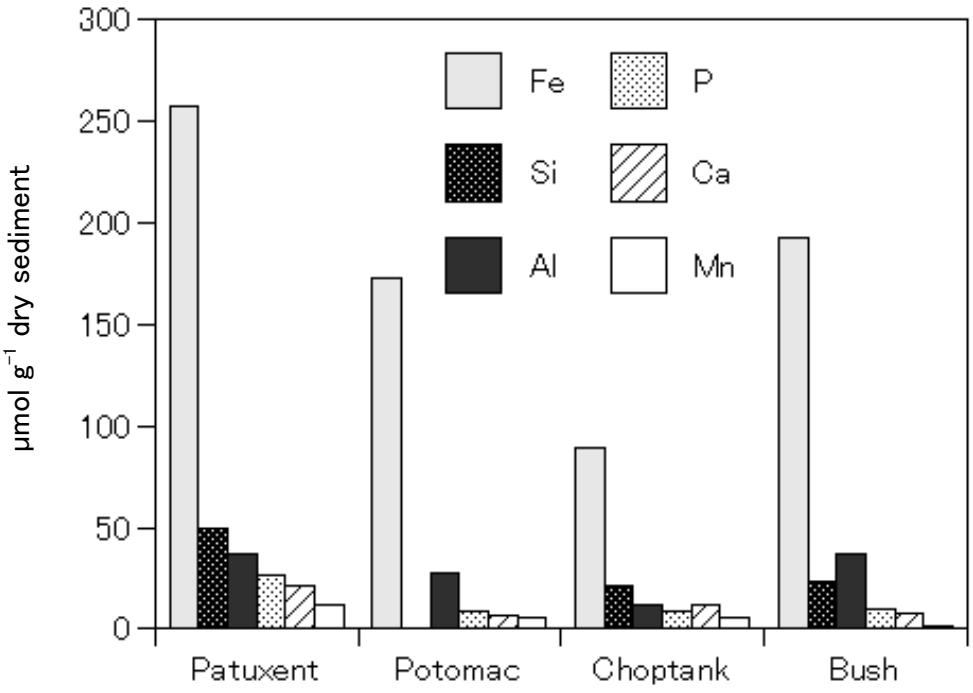

Fig 5-4. CDB extractable elements in the sediments of the four subestuaries.

While it appears that ferrous Fe may provide the dominant sink for P in the Patuxent, we cannot discount the possibility that Fe oxides do indeed persist with depth sediments in other environments. CDB is designed to specifically extract Fe oxides, and several studies have reinforced that notion. For example, a calibrated chemical extraction scheme using anoxic lab conditions was used to conclude that crystalline Fe(III) oxides were abundant to 20 cm in depth in saltmarsh sediments (Kostka and Luther 1994); positive oxidation potential produced by the roots of saltmarsh plants may their explain the finding of abundant Fe(III) oxides at sediment depths that are typically anoxic. Additionally, differential XRD was used to identify poorly crystalline Fe oxides persisting in the reduced zone of North Sea sediments that were sectioned under N_2;

however it is not clear if the sediments remained anoxic during sample preparation for XRD (Slomp et al. 1996b). On the other hand, Mössbauer spectroscopic examination of undisturbed marine sediments from the Peru Basin indicated that the Fe(III) oxides goethite and hematite were found only above the redox boundary (Drodt et al. 1997). Thus the persistence of Fe(III) oxides in sediments probably varies among different environments.

We concluded that little to no Fe(III) minerals exist in our sediments below about 20 cm based on results from our HCl extractions. There is a possibility that HCl extractable Fe is different in mineralogy than CDB extractable Fe. CDB extracts both poorly and highly crystalline Fe oxides (Mehra and Jackson 1960, Ruttenberg 1992), whereas HCl might not dissolve all of the more crystalline Fe(III) oxides, such as goethite and hematite (Chao and Zhuo 1983, Canfield 1988). Additionally, HCl can extract some forms of Fe that CDB may not target, such as ferrous Fe associated with silicate minerals and monosulfides (Chao and Zhuo 1983, Canfield 1988, Larsen and Postma 2001). Therefore, it is possible that the HCl extraction did not dissolve the more crystalline Fe(III) oxides that may actually have been present in our sediments. In at least one study of saltmarsh sediments, higher concentrations of CDB extractable Fe than 0.5 M HCl extractable Fe were attributed to the high concentrations of crystalline Fe(III) oxides (Kostka and Luther 1994). However, in our study, almost all of sediment samples actually had higher concentrations of HCl extractable Fe than CDB extractable Fe (Figs. 5-2a and 5-2b, Appendix B), suggesting that the HCl may have extracted some additional

Fe mineral phases over the CDB extractions. Perhaps our use of 1.0 M HCl was one reason we had different findings than Kostka and Luther (1994). Additionally, the presence of sulfides enhance the reduction of Fe(III) to Fe(II) in crystalline minerals such as goethite (e.g., Pyzik and Sommer 1981, Afonso and Stumm 1992). Thus while calibrated extractions using standard iron minerals show that HCl extracts only negligible amounts of crystalline Fe(III) oxides, in the naturally sulfidic sediments of the saline sediments of the Patuxent, HCl may be effective in dissolving crystalline Fe(III) oxides. Additional research would be required to determine the exact forms of Fe extracted by HCl and CDB in the Patuxent sediments.

Conclusion

Although the presence of ferrous phosphate minerals, such as vivianite, is normally interpreted as evidence of freshwater environment (Postma 1982, Hearn et al. 1983), it appears that vivianite precipitation may be occurring in the saline sediments of the Patuxent, providing an important long-term sink for P in that system.

If ferrous phosphate formation regularly occurs in saline sediments of estuaries, then commonly held assumptions about estuarine P biogeochemistry need to be revised. Fe-bound P may be a more efficient long-term sink for P than previously thought. However, whether ferrous phosphate formation is common within saline sediments of estuaries is unknown. Ferrous phosphate formation may be a function of salinity as well as the amount and form of Fe present in the sediments. The sediments of the Patuxent

may be exceptionally Fe-rich, allowing for excess Fe(II) available for binding P in the sediments even in the presence of sulfides. Indeed, the lower ratios of CDB extractable Fe and P in the Patuxent than the other subestuaries we studied (Chapter 3) indicate that Fe in the sediments of the Patuxent is more available to bind P. The persistence of Fe-P with depth in the saline sediments of the Patuxent, which is in contrast to the Potomac and Choptank, also indicates that Fe-P dynamics in the Patuxent may be different than the other subestuaries we studied (Chapter 3). Therefore, although Fe(II) was the dominant form of Fe below 20 cm depth in the sediments of all four subestuaries (Appendix B), vivianite might only be forming in the saline sediments of the Patuxent. Sulfide analyses and solubility calculations of the pore water of the other three subestuaries are needed to test whether vivianite may be forming in our other study sites. To gain more accurate knowledge about global P cycling, much broader research would be required to determine whether ferrous phosphate formation is common in estuaries around the world. The amount and form of particulate iron in estuarine sediments may be a key factor in determining the amount of PP burial in estuaries.

Appendix A: Sampling locations, GPS coordinates, mean pore water salinity, and water depths of sediment cores collected from the four subestuaries

Site	Location description		GPS coordinates	Mean pore water salinity	Water depth (m)
			Patuxent River		
1	Jug Bay		38° 46.24' N 76° 41.783' W	0.1	1.2
2	Jones Point	a	38° 41.114' N 76° 41.539' W	1.0	2.4
		b	38° 41.202' N 76° 41.840' W	0.8	2.4
		c	38° 41.593' N 76° 41.878' W	1.1	2.3
3	Cocktown Creek		38° 37.727' N 76° 41.539' W	2.8	1.7
4	Summerville Creek		38° 35.584' N 76° 40.564' W	4.3	1.7
5	Potts Point		38° 33.544' N 76° 40.278' W	6.2	2.0
6	Buena Vista	a	38° 31.159' N 76° 39.686' W	8.6	4.1
		b	38° 31.137' N 76° 39.659' W	10.6	3.0
		c	38° 31.326' N 76° 39.944' W	8.9	4.0
		d	38° 31.364' N 76° 40.032' W	8.8	2.0
		e	38° 31.607' N 76° 39.473' W	8.5	2.2
7	Trent Hall	a	38° 29.212' N 76° 39.803' W	11.5	3.5
		b	38° 29.328' N 76° 39.793' W	10.5	5.1

Appendix A: Continued.

Site	Location description	GPS coordinates	Mean pore water salinity	Water depth (m)
		Potomac River		
1	Gunston Cove	38° 40.583' N 77° 09.400' W	0.1	1.2
2	Quantico	38° 28.934' N 77° 18.416' W	1.0	4.3
3	MD Point	38° 21.596' N 77° 11.368' W	3.0	2.1
4	Port Tobacco	38° 25.605' N 77° 03.691' W	4.8	3.1
5	301 Bridge	38° 21.180' N 77° 00.585' W	6.0	2.5
		Choptank River		
1	Confluence of Tuckahoe Creek & Choptank	38° 48.368' N 75° 54.663' W	0.4	4.7
2	Windy Hill	38° 41.222' N 75° 58.442' W	3.9	4.1
3	Between Cabin Creek & Warwick River	38° 37.478' N 75° 58.858' W	6.5	3.0
4	Cambridge	38° 35.134' N 76° 03.770' W	9.6	6.8
		Bush River		
1	Otter Point Creek	39° 26.666' N 76° 16.542' W	0.45	0.5
2	Bush Point	39° 27.504' N 76° 14.246' W	0.6	1.6
3	Sud Run	39° 25.758' N 76° 14.224' W	1.2	2.1

Appendix B: HCl extractable Fe(II) and Fe(III) and CDB extractable Fe

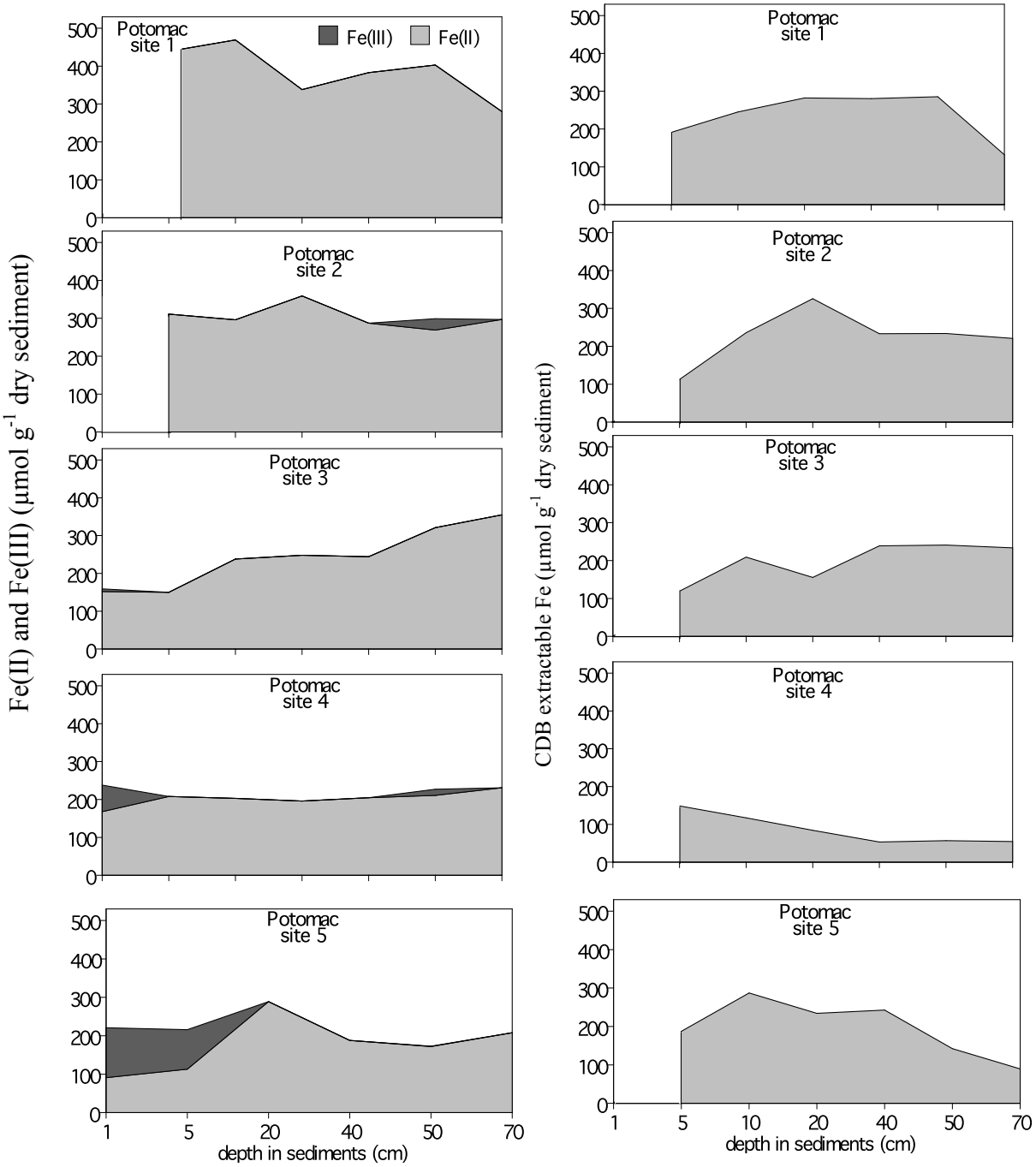

Appendix B: HCl extractable Fe(II) and Fe(III) and CDB extractable Fe (continued)

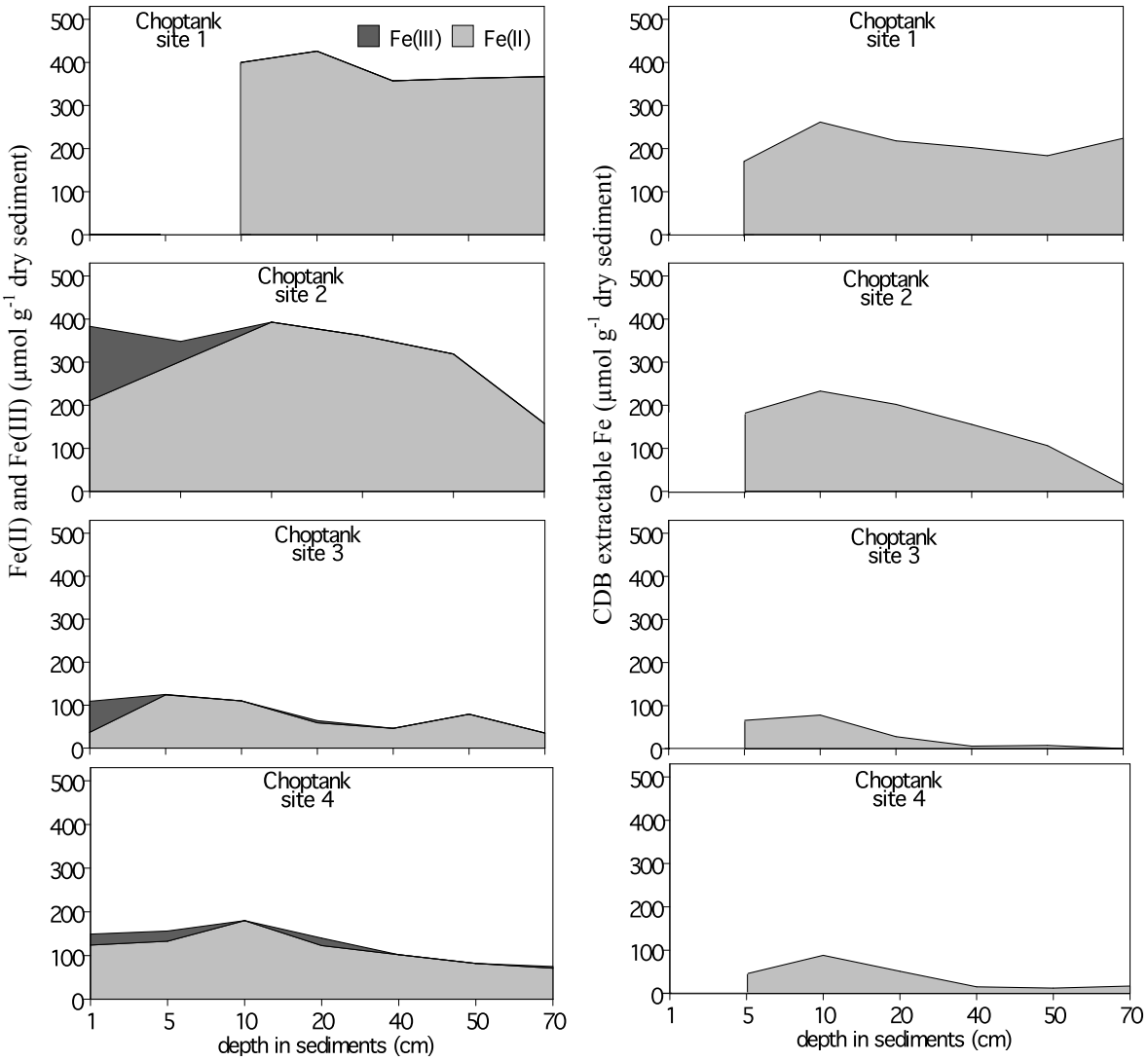

Appendix B: HCl extractable Fe(II) and Fe(III) and CDB extractable Fe (continued)

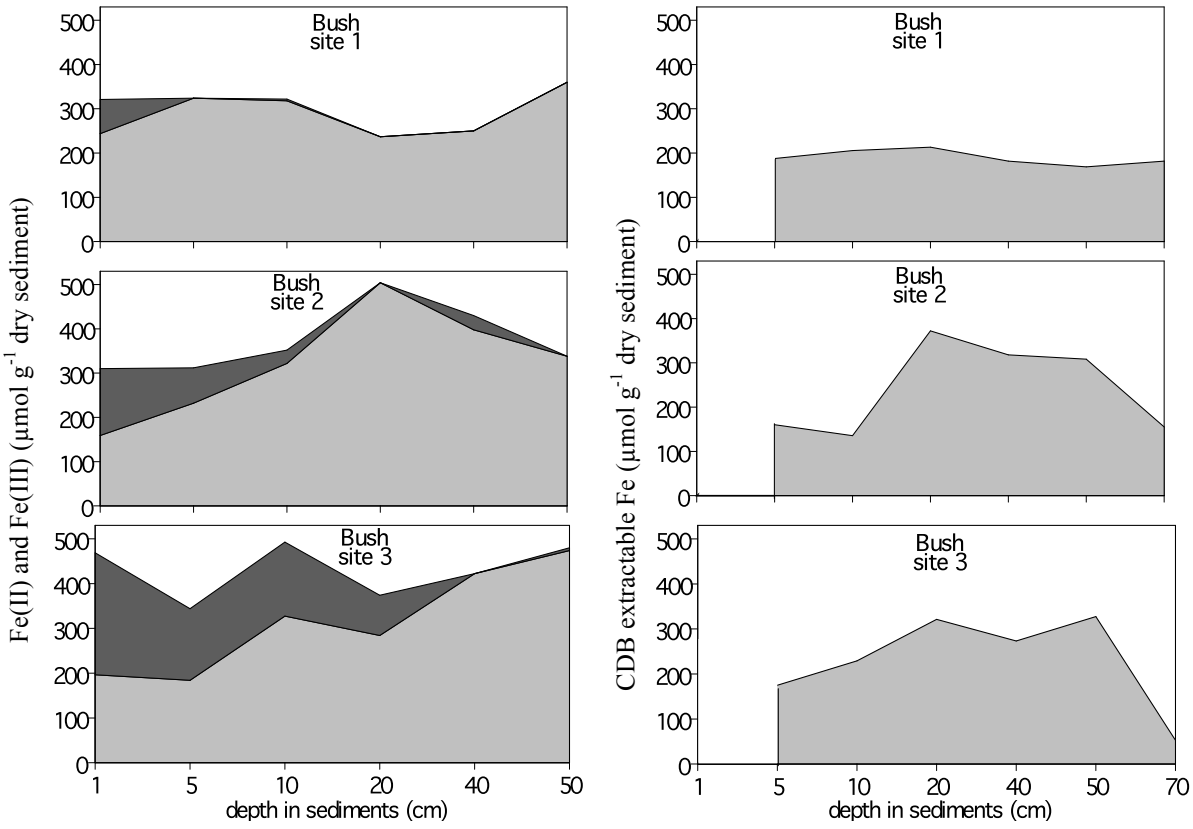

References

References

Afonso, M. d. S., and W. Stumm. 1992. Reductive Dissolution of Iron(III) (Hydr)oxides by Hydrogen Sulfide. Langmuir **8**:1671-1675.

Aller, R. C., J. E. Mackin, and R. T. Cox Jr. 1986. Diagenesis of Fe and S in Amazon inner shelf muds: apparent dominance of Fe reduction and implications for the genesis of ironstones. Continental Shelf Research **6**:263-289.

Allison, J. D., D. S. Brown, and K. J. Novo-Gradac. 1991. MINTEQA2, A geochemical assessment data base and test cases for environemtal systems: Vers. 3.0 user's manual. Report EPA/600/3-91/-21, Athens, GA.

Anderson, L. D., M. L. Delaney, and K. L. Faul. 2001. Carbon to phosphorus ratios in sediments: Implications for nutrient cycling. Global Biogeochemical Cycles **15**:65-79.

Andrieux-Loyer, F., X. Philippon, G. Bally, R. Kérouel, A. Youenou, and J. Le Grand. 2008. Phosphorus dynamics and bioavailability in sediments of the Penzé Estuary (NW France): in relation to annual P-fluxes and occurrences of *Alexandrium Minutum*. Biogeochemistry **88**:213-231.

Anschutz, P., S. Zhong, B. Sundby, A. Mucci, and C. Gobeil. 1998. Burial efficiency of phosphorus and the geochemistry of iron in continental margin sediments. Limnology and Oceanography **43**:53-64.

Benitez-Nelson, C. R. 2000. The biogeochemical cycling of phosphorus in marine systems. Earth-Science Reviews **51**:109-135.

Berner, R. A. 1982. Burial of organic carbon and pyrite sulfur in the moderns oceans: Its geochemical and environmental significance. American Journal of Science **282**:451-473.

Billon, G., B. Ouddane, and A. Boughriet. 2001. Chemical speciation of sulfur compounds in surface sediments from three bays (Fresnaye, Seine and Authie) in northern France, and identification of some factors controlling their generation. Talanta **53**:971-981.

Boesch, D. F., R. B. Brinsfield, and R. E. Magnien. 2001. Chesapeake Bay eutrophication: Scientific understanding, ecosystem restoration, and challenges for agriculture. Journal of Environmental Quality **30**:303-320.

Boynton, W. R., J. H. Garber, R. Summers, and W. M. Kemp. 1995. Inputs, transformations, and transport of nitrogen and phosphorus in Chesapeake Bay and selected tributaries. Estuaries **18**:285-314.

Boynton, W. R., J. D. Hagy, J. C. Cornwell, W. M. Kemp, S. M. Greene, M. S. Owens, J. E. Baker, and R. K. Larsen. 2008. Nutrient budgets and management actions in the Patuxent River Estuary, Maryland. Estuaries and Coasts **31**:607-813.

Boynton, W. R., and W. M. Kemp. 2008. Estuaries. *in* D. G. Capone, D. A. Bronk, M. R. Mulholland, and E. J. Carpenter, editors. Nitrogen in the Marine Environment. Elsevier Inc.

Brush, G. S., and F. W. Davis. 1984. Strategraphic evidence of human disturbance in an estuary. Quaternary Research **22**:91-108.

Brush, G. S., E. A. Martin, R. S. DeFries, and C. A. Rice. 1982. Comparisons of ^{210}Pb and Pollen Methods for Determining Rates of Estuarine Sediment Accumulation. Quaternary Research **18**:196-217.

Burns, S. J. 1997. Early Diagenesis in Amazon Fan Sediments. Pages 497-504 *in* R. D. Flood, D. J. W. Piper, A. Klaus, and L. C. Peterson, editors. Proceedings of the Ocean Drilling Program, Scientific Results. Ocean Drilling Program, College Station, TX.

Callendar, E. 1982. Benthic phosphorus regeneration in the Potomac River Estuary. Hydrobiologia **92**:431-446.

Canfield, D. E. 1988. Sulfate reduction and the diagenesis of iron in anoxic sediments. Ph.D. dissertation. Yale University, New Haven, CT.

Canfield, D. E., R. Raiswell, and S. Bottrell. 1992. The reactivity of sedimentary iron minerals toward sulfide. American Journal of Science **292**:659-683.

Caraco, N. F., J. J. Cole, and G. E. Likens. 1989. Evidence for sulphate-controlled phosphorus release from sediments of aquatic systems. Nature **341**:316-318.

Caraco, N. F., J. J. Cole, and G. E. Likens. 1990. A comparison of phosphorus immobilization in sediments of freshwater and coastal marine systems. Biogeochemistry **9**:227-290.

Caraco, N. F., A. Tamse, O. Boutros, and I. Valiela. 1987. Nutrient limitation of phytoplankton growth in brackish coastal ponds. Canadian Journal of Fisheries and Aquatic Sciences **44**:473-476.

Carman, R., G. Edlund, and C. Damberg. 2000. Distribution of organic and inorganic phosphorus compounds in marine and lacustrine sediments: a ^{31}P NMR study. Chemical Geology **163**:101-114.

Carpenter, S. R., N. F. Caraco, D. L. Correll, R. W. Howarth, A. N. Sharpley, and V. H. Smith. 1998. Nonpoint pollution of surface waters with phosphorus and nitrogen. Ecological Applications **8**:559-568.

Cerco, C. F., and T. Cole. 1993. Three-dimensional eutrophication model of Chesapeake Bay. Journal of Environmental Engineering **119**:1006-1025.

Cha, H. J., C. B. Lee, B. S. Kim, M. S. Choi, and K. C. Ruttenberg. 2005. Early diagenetic redistribution and burial of phosphorus in the sediments of the southwestern East Sea (Japan Sea). Marine Geology **216**:127-143.

Chambers, R. M., J. T. Hollibaugh, and S. M. Vink. 1994. Sulfate reduction and sediment metabolism in Tomales Bay, California. Biogeochemistry **25**:1-18.

Chambers, R. M., and W. E. Odum. 1990. Porewater oxidation, dissolved phosphate and the iron curtain: Iron-phosphorus relations in tidal freshwater marshes. Biogeochemistry **10**:37-52.

Chao, T. T., and L. Zhuo. 1983. Extraction techniques for selective dissolution of amorphous iron oxides from soils and sediments. Soil Science Society of America Journal **47**:225-232.

Cloern, J. E. 2001. Our evolving conceptual model of the coastal eutrophication problem. Marine Ecology Progress Series **210**:223-253.

Colman, A. S., and H. D. Holland. 2000. The global diagenetic flux of phosphorus from marine sediments to the oceans: redox sensitivity and the control of the atmospheric oxygen levels. Pages 53-75 *in* Marine Authigenesis: From Global to Microbial. SEPM (Society for Sedimentary Geology).

Compton, J., D. Mallinson, C. R. Glenn, G. Fillippelli, K. Follmi, G. Shields, and Y. Zanin. 2000. Variations in the Global Phosphorus Cycle. Pages 21-33 *in* Marine Authigenesis: From Global to Microbial. SEPM (Society for Sedimentary Geology).

Cooper, S. R., and G. S. Brush. 1983. A 2,500-year history of anoxia and eutrophication in Chesapeake Bay. Estuaries **16**:617-626.

Cornwell, J. C., D. J. Conley, M. Owens, and J. C. Stevenson. 1996. A sediment chronology of the eutrophication of Chesapeake Bay. Estuaries **19**:488-499.

Cornwell, J. C., and J. W. Morse. 1987. The characterization of iron sulfide minerals in anoxic marine sediments. Marine Chemistry **22**:193-206.

Correll, D. L., T. E. Jordan, and D. E. Weller. 1992. Nutrient flux in a landscape: Effects of coastal land use and terrestrial community mosaic on nutrient transport to coastal waters. Estuaries **15**:431-442.

Crain, C. M. 2007. Shifting nutrient limitation and eutrophication effects in marsh vegetation across estuarine salinity gradients. Estuaries and Coasts **30**:26-34.

D'Elia, C. F., W. R. Boynton, and J. G. Sanders. 2003. A watershed perspective on nutrient enrichment, science and policy in the Patuxent River, Maryland: 1960-2000. Estuaries **26**:171-185.

D'Elia, C. F., J. G. Sanders, and W. R. Boynton. 1986. Nutrient enrichment studies in a coastal plain estuary: phytoplankton growth in large scale, continuous cultures. Canadian Journal of Fisheries and Aquatic Sciences **43**:397-404.

Dafner, E. V., M. A. Mallin, J. J. Souza, H. A. Wells, and D. C. Parsons. 2007. Nitrogen and phosphorus species in the coastal and shelf waters of Southeastern North Carolina, Mid-Atlantic U.S. coast. Marine Chemistry **103**:289-303.

Darke, A. K., and J. P. Megonigal. 2003. Control of sediment deposition rates in two mid-Atlantic coast tidal freshwater wetlands. Estuarine, Coastal and Shelf Science **57**:259-272.

Denis, J. M., and J. D. Blomquist. 1995. Nitrate in streams in the Great Valley Carbonate subunit of the Potomac River Basin: U.S. Geological Survey Fact Sheet 161-95, 4 p. *in*.

Douglas, B. C. 1991. Global Sea Level Rise. Journal of Geophysical Research **96**:6981-6992.

Drodt, M., A. X. Trautwein, I. König, E. Suess, and C. Bender Koch. 1997. Mössbauer spectroscopic studies on the iron forms of deep-sea sediments. Physics and Chemistry of Minerals:281-293.

Eaton, A. D., L. S. Clesceri, and A. E. Greenberg. 1995. Standard methods for the examination of water and wastewater. American Public Health Association, Washington DC.

Elderfield, H., R. J. McCaffrey, N. Luedtke, M. Bender, and V. W. Tuesdale. 1981. Chemical diagenesis in Narragansett Bay sediments. American Journal of Science **281**:1021-1055.

Filippelli, G. M. 1997. Controls on phosphorus concentration and accumulation in oceanic sediments. Marine Geology **139**:231-240.

Filippelli, G. M., and M. L. Delaney. 1996. Phosphorus geochemistry of equatorial Pacific sediments. Geochimica et Cosmochimica Acta **60**:1479-1495.

Fisher, T. R., A. B. Gustafson, K. Sellner, R. Lacouture, L. W. Haas, B. Michaels, and R. Karth. 1999. Spatial and temporal variation of resource limitation in Chesapeake Bay. Marine Biology **133**:763-778.

Fisher, T. R., E. R. Peele, J. W. Ammerman, and L. W. Harding, Jr. 1992. Nutrient limitation of phytoplankton in Chesapeake Bay. Marine Ecology Progress Series **82**:51-63.

Föllmi, K. B. 1996. The phosphorus cycle, phosphogenesis and marine phosphate-rich deposits. Earth-Science Reviews **40**:55-124.

Fox, L. E. 1989. A model for inorganic control of phosphate concentrations in river waters. Geochimica et Cosmochimica Acta **53**:417-428.

Froelich, P. N. 1988. Kinetic control of dissolved phosphate in natural rivers and estuaries: A primer on the phosphate buffer mechanism. Limnology and Oceanography **33**:649-668.

Froelich, P. N., M. L. Bender, N. A. Luedtke, G. R. Heath, and T. DeVries. 1982. The marine phosphorus cycle. American Journal of Science **282**:474-511.

Gächter, R., and B. Müller. 2003. Why the phosphorus retention of lakes does not necessarily depend on the oxygen supply to their sediment surface. Limnology and Oceanography **48**:929-933.

Gardner, W. S., S. P. Seitzinger, and J. M. Malczyk. 1991. The effects of sea salts on the forms of nitrogen released from estuarine and freshwater sediments: Does ion pairing affect ammonium flux? Estuaries **14**:157-166.

Greene, S. E. 2005. Nutrient removal by tidal fresh and oligohaline marshes in a Chesapeake Bay tributary. Master's thesis. University of Maryland.

Gunnars, A., S. Blomqvist, P. Johansson, and C. Andersson. 2002. Formation of Fe(III) oxyhydroxide colloids in freshwater and brackish seawater, with incorporation of phosphate and calcium. Geochimica et Cosmochimica Acta **66**:745-758.

Gustafsson, J. P. 2007. Visual MINTEQ, version 2.53, Dept. of Land and Water Resources Engineering, Stockholm, Sweden.

Hartnett, H. E., R. G. Keil, J. I. Hedges, and A. H. Devol. 1998. Influence of oxygen exposure time on organic carbon preservation in continental margin sediments. Nature **391**:571-574.

Hartzell, J. L., F. Aunon, L. Buchanan, and G. D. Foster. 2008. Determination of inorganic phosphate sorption to iron as a function of mineral crystallinity, salinity, and depth in estuarine sediments based on an HCl extraction method. Journal of Undergraduate Chemistry Research **7**:35-39.

Hearn, P. P., D. L. Parkhurst, and E. Callender. 1983. Authigenic vivianite in Potomac River sediments: Control by ferric oxy-hydroxides. Journal of Sedimentary Petrology **53**:165-177.

Hicks, S. D., H. A. Debaugh, Jr., and L. E. Hickman, Jr. 1983. Sea level variations for the United States 1855-1980. National Ocean Service, U.S. Department of Commerce. Rockville, Maryland. 170 p.

Hjorth, T. 2004. Effects of freeze-drying on partitioning patterns of major elements and trace metals in lake sediments. Analytica Chimica Acta **526**:95-102.

Hopkinson, C. S., Jr., A. E. Giblin, J. Tucker, and R. H. Garritt. 1999. Benthic metabolism and nutrient cycling along an estuarine salinity gradient. Estuaries **22**:863-881.

Horne, A. J., and C. R. Goldman. 1994. Limnology, 2nd edition. McGraw-Hill, Inc., New York.

House, W. A. 2003. Geochemical cycling of phosphorus in rivers. Applied Geochemistry **18**:739-748.

Howarth, R. W. 1988. Nutrient limitation of net primary production in marine ecosystems. Annual Reviews of Ecology, Evolution, and Systematics **19**:89-110.

Howarth, R. W., F. Chan, and R. Marino. 1999. Do top-down and bottom-up controls interact to exclude nitrogen-fixing cyanobacteria from the plankton of estuaries? An exploration with a simulation model. Biogeochemistry **46**:203-231.

Howarth, R. W., and R. Marino. 2006. Nitrogen as the limiting nutrient for eutrophication in coastal marine ecosystems: Evolving views over three decades. Limnology and Oceanography **51**:364-376.

Howarth, R. W., R. Marino, J. Lane, and J. J. Cole. 1988. Nitrogen fixation in freshwater, estuarine, and marine ecosystems. 1. Rates and importance. Limnology and Oceanography **33**:669-687.

Hyacinthe, C., and P. Van Cappellen. 2004. An authigenic iron phosphate phase in estuarine sediments: composition, formation and chemical reactivity. Marine Chemistry **91**:227-251.

Ingall, E. D., and R. A. Jahnke. 1997. Influence of water-column anoxia on the elemental fractionation of carbon and phosphorus during sediment diagenesis. Marine Geology **139**:219-229.

Jensen, H. S., P. B. Mortensen, F. O. Andersen, and A. Jensen. 1995. Phosphorus cycling in a coastal marine sediment, Aarhus Bay, Denmark. Limnology and Oceanography **36**:908-917.

Jensen, H. S., and B. Thamdrup. 1993. Iron-bound phosphorus in marine sediments as measured by bicarbonate-dithionite extraction. Hydrobiologia **253**:47-59.

Jones, R. C., R. Kraus, and D. P. Kelso. 2007. An Ecological Study of Gunston Cove, Final Report. Submitted to the Department of Public Works, County of Fairfax, VA.

Jordan, T. E., J. C. Cornwell, W. R. Boynton, and J. T. Anderson. 2008. Changes in phosphorus biogeochemistry along an estuarine salinity gradient: The iron conveyer belt. Limnology and Oceanography **53**:172-184.

Jordan, T. E., D. L. Correll, and D. E. Weller. 1997. Relating nutrient discharges from watersheds to land use and streamflow variability. Water Resources Research **33**:2579-2590.

Jordan, T. E., J. W. Pierce, and D. L. Correll. 1986. Flux of particulate matter in the tidal marshes and subtidal shallows of the Rhode River Estuary. Estuaries **9**:310-319.

Jordan, T. E., D. E. Weller, and D. L. Correll. 2003. Sources of nutrient inputs to the Pauxent River estuary. Estuaries **26**:226-243.

Kanungo, S. B. 1994. Adsorption of cations on hydrous oxides of iron: interfacial behavior of amorphous FeOOH and ß - FeOOH (akaganeite) in different electrolyte solutions. Journal of Colloid and Interface Science **62**:86-92.

Kemp, W. M., W. R. Boynton, J. E. Adolf, D. F. Boesch, W. C. Boicourt, G. S. Brush, J. C. Cornwell, T. R. Fisher, P. M. Glibert, J. D. Hagy, L. W. Harding, E. D. Houde, D. G. Kimmel, W. D. Miller, R. I. E. Newell, M. R. Roman, E. M. Smith, and J.

C. Stevenson. 2005. Eutrophication of Chesapeake Bay: historical trends and ecological interactions. Marine Ecology Progress Series **303**:1-29.

Kemp, W. M., P. Sampou, J. Caffrey, M. Mayer, K. Henriksen, and W. R. Boynton. 1990. Ammonium recycling versus denitrification in Chesapeake Bay sediments. Limnology and Oceanography **35**:1545-1563.

Khan, H., and G. S. Brush. 1994. Nutrient and metal accumulation in a freshwater tidal marsh. Estuaries **17**:345-360.

Khoshmanesh, A., B. T. Hart, A. Duncan, and R. Beckett. 2002. Luxury uptake of phosphorus by sediment bacteria. Water Research **36**:774-778.

Kostka, J. E., and G. W. Luther. 1994. Partitioning and speciation of solid phase iron in saltmarsh sediments. Geochimica et Cosmochimica Acta **58**:1701-1710.

Krom, M. D., and R. A. Berner. 1981. The diagenesis of phosphorus in a nearshore marine sediment. Geochimica et Cosmochimica **45**:207-216.

Larsen, O., and D. Postma. 2001. Kinetics of reductive bulk dissolution of lepidocrocite, ferrihydrite, and goethite. Geochimica et Cosmochimica Acta **65**:1367-1379.

Lebo, M. E. 1991. Particle-bound phosphorus along an urbanized coastal plain estuary. Marine Chemistry **34**:225-246.

Lebo, M. E., and J. H. Sharp. 1993. Distribution of phosphorus along the Delaware, an urbanized coastal plain estuary. Estuaries **16**:290-301.

Louchouarn, P., M. Lucotte, E. Duchemin, and A. d. Vernal. 1997. Early diagenetic processes in recent sediments of the Gulf of St-Lawrence: phosphorus, carbon and iron burial rates. Marine Geology **139**:181-200.

Lung, W.-S., and S. Bai. 2003. A water quality model for the Patuxent Estuary: Current conditions and predictions under changing land-use scenarios. Estuaries **26**:267-279.

Mackenzie, F. T., L. M. Ver, C. Sabine, M. Lane, and A. Lerman. 1993. C, N, P, S, Global Biogeochemical Cycles and Modeling of Global Change. Pages 1-61 *in* R. Wollast, F. T. Mackenzie, and L. Chou, editors. Interactions of C, N, P and S Biogeochemical Cycles and Global Change. Springer-Verlag, Berlin.

Magnien, R. E., R. M. Summers, M. S. Haire, W. R. Boynton, D. C. Brownlee, A. F. Holland, W. M. Kemp, K. Sellner, G. D. Foster, and D. A. Wright. 1987. Chesapeake Bay Monitoring: Monitoring for Management Actions. Maryland Department of Natural Resources.

Marino, R., F. Chan, R. W. Howarth, M. Pace, and G. E. Likens. 2002. Ecological and biogeochemical interactions constrain planktonic nitrogen fixation in estuaries. Ecosystems **5**:719-725.

Martens, C. S., R. A. Berner, and J. K. Rosenfield. 1978. Interstitial water chemistry of anoxic Long Island Sound sediments. 2. Nutrient regeneration and phosphate removal. Limnology and Oceanography **23**:605-617.

Maryland Department of Natural Resources. 2005. Maryland Biological Stream Survey 2000 - 2004, Volume VIII, Chesapeake Bay Watershed Programs Monitoring and Non-Tidal Assessment - EA-05-5

McGlathery, K. J., R. Marino, and R. W. Howarth. 1994. Variable rates of phosphate uptake by shallow marine carbonate sediments: mechanisms and ecological significance. Biogeochemistry **25**:127-146.

Mehra, O. P., and M. L. Jackson. 1960. Iron oxide removal from soils and clays by a dithionite-citrate system buffered with sodium bicarbonate. Pages 317-327 *in* E. Ingerson, editor. Clays and Clay Minerals Monograph no. 5, Earth Science Series. Pergamon Press, London.

Merrill, J. Z. 1999. Tidal freshwater marshes as nutrient sinks: Particulate nutrient burial and denitrification. Ph.D. dissertation. University of Maryland.

Mitsch, W. J., and J. G. Gosselink. 2000. Wetlands, 3rd edition. John Wiley & Sons, Inc., New York, NY.

Nixon, S. W. 1995. Coastal Marine Eutrophication: A definition, social causes, and future consequences. Ophelia **41**:199-219.

Nixon, S. W., J. W. Ammerman, L. P. Atkinson, V. M. Berounsky, G. Billen, W. C. Boicourt, W. R. Boynton, T. M. Church, D. M. Ditoro, R. Elmgren, J. H. Garber, A. E. Giblin, R. A. Jahnke, N. J. P. Owens, M. E. Q. Pilson, and S. P. Seitzinger. 1996. The fate of nitrogen and phosphorus at the land-sea margin of the North Atlantic Ocean. Biogeochemistry **35**:141-180.

NRC. 2000. Clean coastal waters: Understanding and reducing the effects of nutrient pollution. National Academies Press.

O'Keefe, J. A. 2007. Sediment Biogeochemistry across the Patuxent River estuarine gradient: Geochronology and Fe-S-P interactions. Master's thesis. University of Maryland.

Paludan, C., and J. T. Morris. 1999. Distribution and speciation of phosphorus along a salinity gradient in intertidal marsh sediments. Biogeochemistry **45**:197-221.

Pasternack, G. B., G. S. Brush, and W. B. Hilgartner. 2001. Impact of historic land-use change on sediment delivery to a Chesapeake Bay subestuarine delta. Earth Surface Processes and Landforms **26**:409-427.

Postma, D. 1982. Pyrite and siderite formation in brackish and freshwater swamp sediments. American Journal of Science **282**:1151-1183.

Pyzik, A. J., and S. E. Sommer. 1981. Sedimentary iron monosulfides: kinetics and mechanism of formation. Geochimica et Cosmochimica Acta **45**:687-698.

Raiswell, R. 1999. Pore water dissolved sulfide profiles: chemical controls of thickness and magnitude. *in* H. Armannsson, editor. Geochemistry of the Earth's Surface: Proceedings of the 5th International Symposium on the Geochemistry of the Earth's Surface. Taylor and Francis, Reykjavik, Iceland.

Raiswell, R., F. Buckley, R. A. Berner, and T. A. Anderson. 1988. Degree of pyritization of iron as a paleoenvironmental indicator of bottom water oxygenation. Journal of Sedimentary Petrology **58**:812-819.

Raiswell, R., and D. E. Canfield. 1996. Rates of reaction between silicate iron and dissolved sulfide in Peru Margin sediments. Geochimica et Cosmochimica Acta **60**:2777-2787.

Reitzel, K., J. Ahlgren, H. DeBrabandere, M. Waldebäck, A. Gogoll, L. Tranvik, and E. Rydin. 2007. Degradation rates of organic phosphorus in lake sediment. Biogeochemistry **82**:15-28.

Roden, E. E., and J. W. Edmonds. 1997. Phosphate mobilization in iron-rich anaerobic sediments: microbial Fe (III) oxide reduction versus iron-sulfide formation. Archiv für Hydrobiologie **139**:347-378.

Roden, E. E., and J. M. Zachara. 1996. Microbial reduction of crystalline iron(III) oxides: Influence of oxide surface area and potential for cell growth. Environmental Science and Technology **30**:1618-1628.

Rozan, T. F., M. Taillefert, R. E. Trouwborst, B. T. Glazer, S. Ma, J. Herszage, L. M. Valdes, K. S. Price, and G. W. Luther III. 2002. Iron-sulfur-phosphorus cycling in the sediments of a shallow coastal bay: Implications for sediment nutrient release and benthic macroalgal blooms. Limnology and Oceanography **47**:1346-1354.

Ruttenberg, K. C. 1992. Development of a sequential extraction method for different forms of phosphorus in marine sediments. Limnology and Oceanography **37**:1460-1482.

Ruttenberg, K. C., and R. A. Berner. 1993. Authigenic apatite formation and burial in sediments from non-upwelling continental margin environments. Geochimica et Cosmochimica Acta **57**:991-1007.

Scatena, F. N. 1987. Sediment budgets and delivery in a suburban watershed: Anacostia watershed. Ph.D. dissertation. Johns Hopkins University.

Schindler, D. W. 1977. Evolution of phosphorus limitation in lakes. Science **195**:260-262.

Seitzinger, S. P. 1988. Denitrification in freshwater and coastal marine ecosystems: Ecological and geochemical significance. Limnology and Oceanography **33**:702-724.

Seitzinger, S. P., W. S. Gardner, and A. K. Spratt. 1991. The effect of salinity on ammonium sorption in aquatic sediments: Implications for benthic nutrient recycling. Estuaries **14**:167-174.

Slomp, C. P., E. H. G. Epping, W. Helder, and W. V. Raaphorst. 1996a. A key role for iron-bound phosphorus in authigenic apatite formation in North Atlantic continental platform sediments. Journal of Marine Research **54**:1179-1205.

Slomp, C. P., S. J. V. d. Gaast, and W. V. Raaphorst. 1996b. Phosphorus binding by poorly crystalline iron oxides in North Sea sediments. Marine Chemistry **52**:55-73.

Smith, V. H. 1983. Low nitrogen to phosphorus ratios favor dominance by blue-green algae in lake phytoplankton. Science **221**:669-671.

Stookey, L. L. 1970. Ferrozine: a new spectrophotometric reagent for iron. Analytical Chemistry **42**:779-781.

Strom, R. N., and R. B. Biggs. 1982. Phosphorus distribution in sediments of the Delaware River Estuary. Estuaries **5**:95-101.

Sundareshwar, P. V., and J. T. Morris. 1999. Phosphorus sorption characteristics of intertidal marsh sediments along an estuarine salinity gradient. Limnology and Oceanography **44**:1693-1701.

Sundby, B., C. Gobeil, N. Silverberg, and A. Mucci. 1992. The phosphorus cycle in coastal marine sediments. Limnology and Oceanography **37**:1129-1145.

Tomasky, G., J. Barak, I. Valiela, P. Behr, L. Soucy, and K. Foreman. 1999. Nutrient limitation of phytoplankton growth in Waquoit Bay, Massachusetts, USA: a nutrient enrichment study. Aquatic Ecology **33**:147-155.

Tyrrell, T. 1999. The relative influences of nitrogen and phosphorus on oceanic primary production. Nature **400**:525-531.

U.S. Environmental Protection Agency. 1994. Chesapeake Bay watershed pilot project, EPA/620/R94/020. Research Triangle Park, North Carolina.

Upchurch, J. B., J. K. Edzwald, and C. R. O'Melia. 1974. Phosphates in sediments of Pamlico Estuary. Environmental Science & Technology **8**:56-63.

Van Cappellen, P., and E. D. Ingall. 1996. Redox Stabilization of the Atmosphere and Oceans by Phosphorus-Limited Marine Productivity. Science **271**:493-496.

Van Cappellen, P., and E. D. Ingall. 1997. Benthic phosphorus regeneration, net primary production, and ocean anoxia: A model of the coupled marine biogeochemical cycles of carbon and phosphorus. Paleoceanography **9**:677-692.

van der Zee, C., D. D. Roberts, D. G. Rancourt, and C. P. Slomp. 2003. Nanogoethite is the dominant reactive oxydyroxide phase in lake and marine sediments. Geology **31**:993-996.

Van der Zee, C., C. P. Slomp, D. G. Rancourt, G. J. de Lange, and W. van Raaphorst. 2005. A Mössbauer spectroscopic study of the iron redox transition in eastern Mediterranean sediments. Geochimica et Cosmochimica Acta **69**:441-453.

van der Zee, C., C. P. Slomp, and W. van Raaphorst. 2002. Authigenic P formation and reactive P burial in sediments of the Nazaré canyon on the Iberian margin (NE Atlantic). Marine Geology **185**:379-392.

Virtasalo, J. J., T. Kohonen, I. Vuorinen, and T. Huttula. 2005. Sea bottom anoxia in the Archipelago Sea, northern Baltic Sea - Implications for phosphorus remineralization at the sediment surface. Marine Geology **224**:103-122.

Williams, J. D. H., T. Mayer, and J. O. Nriagu. 1980. Extractability of phosphorus from phosphate minerals common in soils and sediments. Soil Science Society of America Journal **44**:462-465.

Zimmerman, A. R., and E. A. Canuel. 2000. A geochemical record of eutrophication and anoxia in Chesapeake Bay sediments: anthropogenic influence on organic matter composition. Marine Chemistry **69**:117-137.

Curriculum Vitae

Jeanne L. Hartzell grew up in Vermont, where it is almost impossible not to develop a reverence for the natural environment. She received an Associate's Degree in Management from the University of Maryland's Okinawa Japan campus in 1989, and a Bachelor's Degree in Geology from Georgia Southwestern State University in 1991. In between going to school and taking time off to be a stay-at-home mom, she has worked as a hydrogeologist for the State of North Carolina and a research scientist for Battelle Memorial Institute. She lives in Stafford, Virginia with her husband, Will, and two sons, Steven and Kyle.